# Contention resolution in optical packet-switched cross-connects

*Please check the document version of this publication:*

• A submitted manuscript is the version of the article upon submission and before peer-review. There can be important differences between the submitted version and the official published version of record. People interested in the research are advised to contact the author for the final version of the publication, or visit the DOI to the publisher's website.
• The final author version and the galley proof are versions of the publication after peer review.
• The final published version features the final layout of the paper including the volume, issue and page numbers.

[Link to publication](#)

# Contention Resolution in Optical Packet-Switched Cross-Connects

PROEFSCHRIFT

ter verkrijging van de graad van doctor aan de
Technische Universiteit Eindhoven, op gezag van de
Rector Magnificus, prof.dr.ir. C.J. van Duijn, voor een
commissie aangewezen door het College voor
Promoties in het openbaar te verdedigen
op maandag 5 maart 2007 om 16.00 uur

door

Ronelle Geldenhuys

geboren te Bellville, Zuid Afrika

Dit proefschrift is goedgekeurd door de promotoren:

prof.ir. G.D. Khoe

en

prof.ir. A.M.J. Koonen

Copromotor:

dr. H.J.S. Dorren

Typeset using Microsoft Word, printed in the Netherlands.

**SUMMARY**

This thesis considers optical contention resolution in both all-optical and electro-optic implementations. After an introduction to the relevant all-optical technology developed within the COBRA research group in Chapter 2, the unique contributions of this thesis are the following:

1.  In Chapter 3 various all-optical cross-connect architectures are analysed with respect to contention resolution in terms of a buffering architecture. Because an *all-optical* implementation is considered, this implies various necessary assumptions due to the limitations of the available technology, such as very limited signal processing, simplified header processing, and the utilisation of very simple algorithms for contention resolution. In order to obtain a realistic picture of the technology required and implementation limitations of an all-optical approach, a realistic bursty traffic model was used, the wavelength dimension was exploited in the cross-connect, and the physical amount of fibre required for the fibre delay lines was analysed.

2.  The buffer requirements for the all-optical approach as outlined in Chapter 3 are compared to estimated buffer requirements based on Transmission Control Protocol (TCP) dynamics in Chapter 4.

3.  A novel design for an optical threshold function based on nonlinear polarisation rotation in a single semiconductor optical amplifier (SOA) is introduced in Chapter 5. Optical threshold functions provide an all-optical way of implementing simple decisions in various applications. The method investigated in this research has the advantage of being reliant on a single active element, and being able to switch with a relatively low power optical control signal. The experimental results are supported by simulation results based on the SOA rate equations.

4.  Due to the implementation challenges associated with all-optical contention resolution schemes, hybrid electro-optic solutions currently still seem to be

more feasible. The second part of this thesis describes optical buffer implementations using a novel ultra-fast electro-optic switch, the CrossPoint switch. The CrossPoint switch improves on other electro-optic switches such as LiNbO$_3$ switches, and was used to investigate implementation challenges of a recirculating buffer, which is the buffering configuration requiring the least amount of physical fibre, and providing the most flexibility. The CrossPoint facilitates a recirculating buffer architecture with electronic control that results in a very small processing delay, and in Chapter 6 it is shown that signal integrity can be maintained due to the low crosstalk of the CrossPoint switch.

5.   Exploiting the low crosstalk characteristics and flexible control of the CrossPoint switch, the first demonstrations of Time Slot Interchange (TSI) and contention resolution using this switch are described in Chapter 7. The first implementation of the CrossPoint for asynchronous switching of variable length packets is also shown, and very low bit error rates are achieved by using Differential Phase Shift Keying (DPSK).

**CONTENTS**

**CHAPTER 1 INTRODUCTION**

## 1.1 Background

The proliferation of optical technology in telecommunications networks over the past decade has been as a direct result of the development of the Erbium-Doped Fibre Amplifier (EDFA) that is an optical amplifier capable of amplifying multiple channels simultaneously in the optical domain. This also led to the widespread deployment of Wavelength Division Multiplexing (WDM) because the multiplexed optical channels can now all be amplified together, and do not need to be separated and amplified individually [1]. This marked the start of intense research and development in the field of optical technology in order to support high bandwidth communications applications. Using EDFAs and other similar amplifiers together with transmission line optimization and spectral efficiency enhancement (through e.g. polarisation-division multiplexing or vestigial sideband filtering), transmission speeds of up to 10Tbit/s have been shown transmitting multiple 40Gbit/s channels [2], [3], [4]. Initial experiments investigated such high-speed transmission over short distances, but recently up to 6Tbit/s transmission has been shown over a 6120km distance using a newer type of long-haul amplification, Raman amplifiers, together with DPSK modulation [5].

The limitation of the speed of optical communication does not lie in transmission though. The problem is in the electronic bottleneck of the network nodes. If signal processing is required at intermediate transmission nodes, e.g. to analyse a header in order to route traffic, optical-to-electrical (O/E) conversion is required, after which the signal processing is performed in the optical domain, and electrical-to-optical (E/O) conversion is performed at the output of the node. Not only does this slow down the speed of the network, but it also increases the cost of the nodes as each O/E/O conversion requires optical transmitters and receivers. This problem has been bypassed

to an extent using circuit switching in optical networks, whereby end-to-end lightpaths are set up that have the added benefit of providing a guaranteed amount of bandwidth. This type of network is referred to as a wavelength routing network (WRN). The disadvantage of circuit switching, however, is that bursty traffic is handled inefficiently as network resources end up being either congested or underutilised. Packet switching provides a solution to this, whereby the data stream is divided into data packets, each with its own header and routed along its own path [6]. This kind of statistical multiplexing, however, requires various functions that are quite complex to implement in the optical domain, such as header recognition and processing, and buffering. Optical burst switching has been suggested as an intermediate solution between circuit switching and packet switching, providing a way of handling bursty traffic without relying on undeveloped optical technology [7]. This is done through the separation between the control and data planes, which results in increased network manageability and flexibility [8]. Another alternative is described in the STOLAS project [9] where a hybrid circuit/packet-switched network is proposed, and while the payload is kept in the optical domain the label processing is performed in the electrical domain. The next step from such hybrid solutions is the development of an all-optical packet-switched node that will be able to facilitate fast and transparent operation with high transmission efficiency, as addressed by the IST-LASAGNE project [10]. This thesis deals with some of the relevant technology issues, in particular optical buffering, and the design of an all-optical cross-connect architecture.

## 1.2 Technology

To achieve the higher processing speeds required by future-proof networks, all-optical switching technology provides a superior solution to the hybrid electro-optic approach. Often the term "all-optical" is used for implementations where the packet payload is kept in the optical domain. In this thesis, however, we will use "all-optical" to refer to a completely optical implementation: not even the control or signal processing will be done in the electronic domain. The all-optical solution provides a

much higher processing speed, provides transparency, and mitigates the optoelectronic conversion bottleneck. In order to make optical packet switching possible, the supporting optical technology must be developed. Figure 1.1 shows a schematic diagram of a generic packet switched node structure.
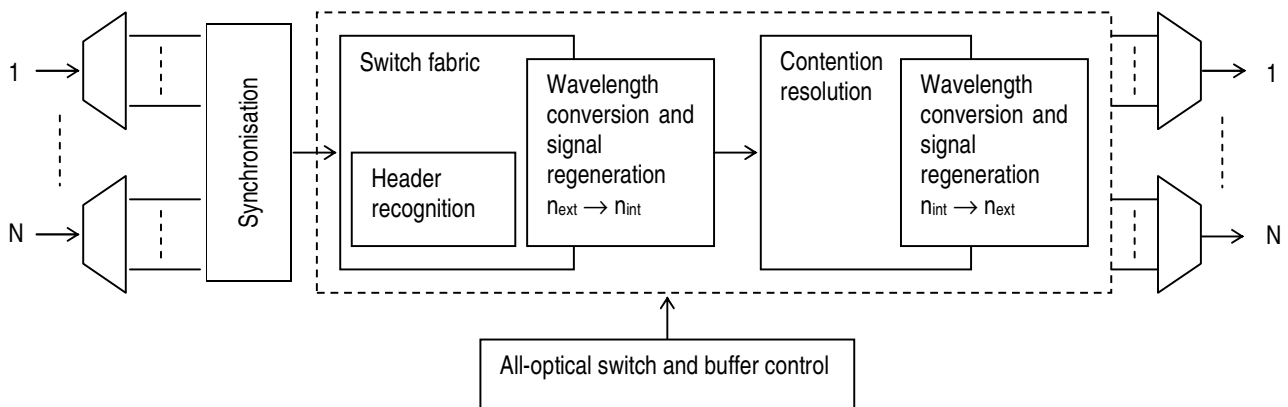


**Figure 1.1. Generic packet switched node structure. The three most important sections are synchronisation, switching and buffering. Wavelength conversion is used to facilitate some of these functions.**

The three most important functional blocks of the cross-connect are synchronisation, switching (including header processing) and buffering. Synchronisation of optical packets can be done with switchable delay lines for coarse synchronisation and with wavelength conversion with dispersive fibre for fine synchronisation [1]. Header recognition is required to make a routing decision, as the destination of a packet is determined by the address contained in the header. Exactly what the content of this header is, and whether the header needs to be deleted and reinserted, or will be handled in a different way, depends on both the technology used to implement the routing functionality as well as the protocols defined for the network. The following sections provide a brief background to relevant optical technologies.

## 1.3 Switching

The main optical switching technologies rely on a combination of optical technology and electronics, so that some kind of electronic control signal is always necessary [11]:

- Optomechanical switches rely on mechanical switching by means of prisms, mirrors or couplers.

- Microelectromechanical system devices (MEMS) are a kind of optomechanical switch reliant on moving miniature two or three dimensional mirrors.

- Electrooptic switches, such as $LiNbO_3$ switches, use directional couplers with a coupling ratio dependent on a variable refractive index.

- Thermooptic switches also rely on a change of the refractive index, but based on temperature variation.

- Liquid-crystal switches operate together with polarisation selective beam splitters in order to route light depending on its polarisation characteristics.

- Bubble switches are similar to thermooptic switches as they are controlled by temperature, but are based on the formation of bubbles in a liquid that will determine whether is passed through or deflected.

- Arrayed waveguide gratings can be used as a passive wavelength router together with tunable wavelength converters that are controlled according to a routing table [9].

- Semiconductor optical amplifiers (SOAs) can be used for switching by exploiting nonlinearities due to carrier density changes, such as cross gain modulation (XGM) [12]. Interferometric configurations can also be used, most commonly with a Mach-Zehnder Interferometer (MZI), with the advantage of being suitable for optoelectronic integration.

All these basic technologies can be used to comprise larger switch fabrics that are used to construct cross-connects, such as a Switch with Large Optical Buffers (SLOB),

WaveMux or Staggering switch, several of them described in Ramaswami et al. [1] and compared in Chia et al. [13].

In this thesis, however, the eventual aim is to investigate a packet-switched cross-connect that is not reliant on any electronic control whatsoever. In order to realise switching in this way, the wavelength domain is very important, and the basic element that enables all-optical switching is a threshold function (THF) that outputs different wavelengths depending on whether a specific input packet is detected or not [14]. The concept is described in further detail in Chapter 6.

## 1.4 Header Processing

### 1.4.1 Feasibility of Optical Header Processing

In optical packet-switched networks all-optical processing has become necessary to support high speed transparent transmission. To complete an all-optical transmission path, signals should remain in optical form during switching, signal processing, and address recognition. Optical networks up to now have typically employed methods where the payload remains an optical signal, but the header is converted to an electronic signal to be processed. One reason to consider optical header processing is because the payload needs to be buffered during header processing. Because of the problems associated with optical buffering, it would be preferable to increase the header processing speed by using an optical implementation so that less buffering is required. Alternatively a method such as wavelength routing can be used where a routing path is selected depending on the wavelength used to transfer the data. In this method the control is still electronic, the routing information is the selected wavelength, and the payload is switched transparently. Other packet-routing methods include broadcast-and-select, and space-switch based routing. In order to have optical control, however, a method must be found to read the header optically and generate optical control signals.

In regarding the various proposed methods for optical address recognition, there are several issues that influence the feasibility of these methods. These relate to the 5 low-level packet switch functions [15]:

- Routing (header processing and switching)

- Flow control and contention resolution

- Synchronisation

- Header regeneration/reinsertion at the switch output

- Scalability and cascadability

Very briefly, feasibility is influenced by the effects of crosstalk, noise, fibre dispersion, switching time, contrast ratios, power saturation and polarisation dependence [16]. Another factor that is important is contention resolution, specifically with reference to internal blocking in a switch. Buffering is typically done with delay lines, which does not provide an optimal solution as it involves kilometres of fibres per switch, and introduces noise and crosstalk - specifically Amplified Spontaneous Emission (ASE) from repeated circulations through optical amplifiers.

The maximum number of cascaded stages in a multistage network is furthermore influenced by any spontaneous emission in the switch, switching efficiency, coupling loss, splitting-and-recombining loss, and BER requirements. A BER of between $10^{-9}$ and $10^{-12}$ is aimed for in optical switches, but there are various parameters that degrade the Q value, in particular the sources of noise in the header processors: amplitude fluctuations in the laser sources, amplifiers, timing jitter, inter-symbol interference (ISI), and incomplete switching and pump leakage in certain types of switches [17].

Another issue relevant to the switching technology is whether the packet length is fixed or not. In most of the proposed solutions the packet length is fixed to accommodate the method of synchronisation. A fixed packet length simplifies the implementation of packet contention resolution and buffering, packet routing and packet synchronisation, but limits the flexibility of bandwidth utilisation. If, however,

synchronisation is not required, it would be possible to accommodate variable-length packets, although more buffering would be required, which is not desirable in an all-optical implementation.

Furthermore, the photonic hardware complexity is important, as this influences the viability and cost. The number of header bits in these first experiments is an indication of the scalability of the method. The use of a key word or specific frame format will necessarily influence the flexibility of the header processing technique. Header recognition time is important, because the point of optical address recognition is to have the processing fast enough to accommodate the potential data rate of an all-optical network. And finally, of course, all the functions must preferably be implemented optically, such as optical thresholding and optical correlation in order to perform routing and synchronisation in real-time for high bit rates [18]. Of course in an optical implementation dispersion and nonlinearities must be taken into account. Specifically, a common problem encountered is that dispersion causes pulse walkoff between the data signal containing the header to be processed, and the control pulses used to extract the header.

It is important to realise that although these factors affect the limitations to scaling multihop networks, they are not fundamental limitations of the network but rely on device technology, which will improve with time.

The following section provides a brief background to optical technology used for header processing. The exact implementation of the header processing (e.g. the processing steps) depends on the technology and switch architecture, but could typically include header extraction from the packet, header recognition, generation of a new header (by e.g. consulting a look-up table), and header reinsertion.

### 1.4.2 Optical Header Processing Methods

Nonlinear-Optical Loop Mirrors (NOLMs) are used for ultrafast switching, and the switching threshold is determined by the product of the loop length and the pulse power [19]. The loop must, however, have sufficient length for dispersion to take

place, and must often be implemented in a soliton regime to obtain optimal switching characteristics. NOLM's are very versatile optical devices, and Park et al. [20], [21] describe a system that does synchronising and address extraction utilising NOLM's. A control pulse is generated using an interferometer that aligns two start pulses, and the resulting control pulse is then wavelength converted using a NOLM as a switch. This pulse is converted to a pulse stream by a splitter that is then input into a second NOLM switch where the address bits are then extracted, and this NOLM outputs the data bits on one port and the address bit on the other. Because the fibre in a NOLM is long, and there is a long interaction length, nonlinearities become a problem.
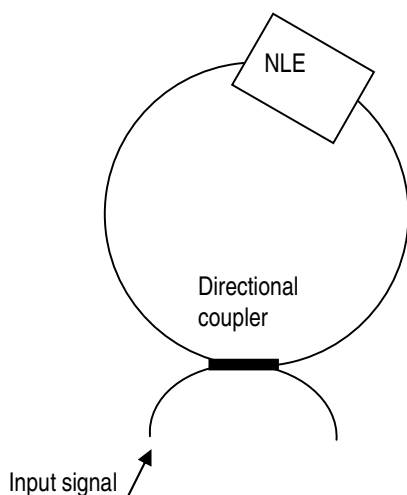


**Figure 1.2. Nonlinear Optical Loop Mirror (NOLM). NLE: nonlinear element, e.g. a semiconductor optical amplifier (SOA).**

Logic gates have been used for header processing in [19],[22] and [23]. The gates rely on a synchronised input, and can be realised using a NOLM.

Glesk et al. [24], [25] demonstrate all-optical multi-bit address recognition at 250-Gb/s using a self-routing scheme that uses Terahertz Optical Asymmetric Demultiplexers (TOADs) to demultiplex packet headers. A TOAD is a demultiplexer that consists of a short fibre loop with an optical nonlinear element (SOA) placed asymmetrically in the loop, an intraloop 2×2 coupler for injecting the control pulses into the SOA, and an adjustable fibre delay line [26]. It exploits nonlinearities that

other demultiplexers seek to avoid, and does not require the long lengths of fibre necessary in a NOLM. The pulses that enter a TOAD split equally into a clockwise and a counter clockwise component. These pulses arrive at the SOA at different times, and a control pulse is injected between the two. Data pulses that do not straddle the control pulse are reflected and exit the header processor. It is shown that one TOAD can be used as the routing controller that sets the switch, but also that a second TOAD can be used as an all-optically controlled routing switch [27].
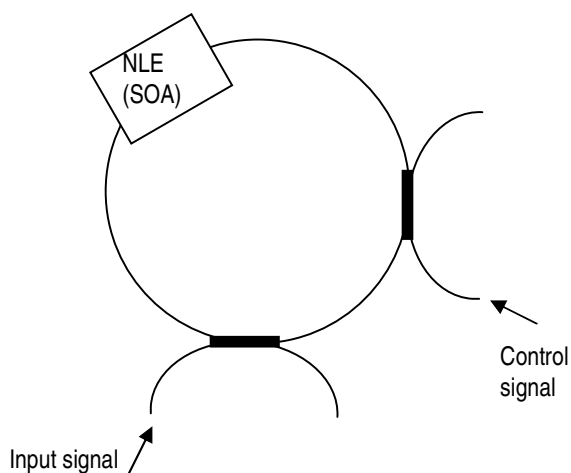


**Figure 1.3.Terahertz Optical Asymmetric Demultiplexer (TOAD).**

All-optical header recognition can be done optically by using a SLALOM structure [28], [29], [30], [31]. In SLALOM, semiconductor laser amplifiers are used in a loop configuration either in nonlinear single pulse switching or two-pulse switching at different speeds [32]. These modes determine which application the SLALOM configuration can be used for: pulse shaping in a fibre ring buffer, decoding for pulse-interval coded signals, retiming gates for an optical regenerator, or time division multiplexing. A SLALOM configuration for 2-pulse correlation can be used for optical header recognition. The header is selected to produce a specific correlation pulse. The header is at a lower bit rate than the payload, and the payload is Manchester encoded to distinguish the payload from the header. This is important because the header and payload are not separated: the payload is suppressed and sent through the switch together with the header. The packet's optical power is split in two: one part is

wavelength converted and delayed (the payload that will be forwarded), while the other part is used for the header processing. This second part is correlated in the SLALOM and then sent through a threshold function where the power is split in two again. One part is used to set the output wavelength of the flip-flop, and the other part is delayed and used to reset the flip-flop wavelength after a delay equal to the packet length. Figure 1.4 shows an experimental setup for a 1×2 all-optical packet switch. The header processor in the figure is used to identify one particular header. The correlation pulse output by the SLALOM is filtered with the threshold function so that the contrast between the payload and correlation pulse is 25dB. Different headers result in different correlation pulses, and these can be recognised by the optical flip-flop that is used as a threshold function. The header data rate for this experiment was low, but the payload data rate was 2,5Gbit/s. This was limited by the wavelength converter and could potentially reach 100Gbit/s.
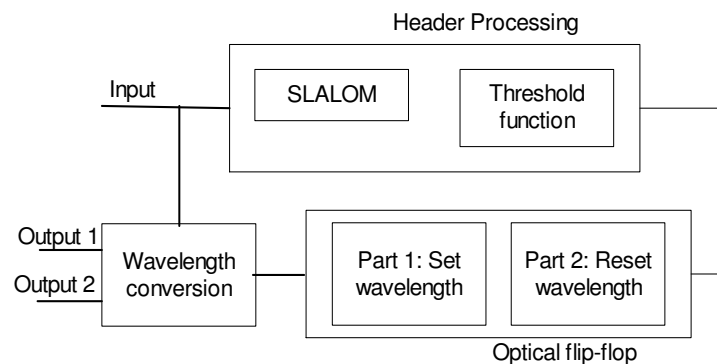
**Figure 1.4 Diagram of the 1×2 All-Optical Packet Switch Demonstration**

Most all-optical header processing methods make use of some form of correlation to be able to match a header with a lookup table [33]. In [34] bipolar phase-shift keyed (PSK) optical pulse sequences are used for the headers. Routing control is done by attaching an optical code (OC) label to the packet. The photonic label selection is based on the optical correlation between the optical bipolar code of the arriving packet and the assigned code of the node. In [35] cross-gain compression in a semiconductor optical amplifier for time-to-wavelength mapping is used, and two fibre Bragg grating

arrays are used for tuneable correlation decoding. The operation is accomplished by shifting each bit of a header packet onto a different wavelength, introducing different time delays for each wavelength, and then using an optical decoder to determine if the series of header bits match the header code of a tuneable optically-encoded look-up table. The wavelength shifting is accomplished by time-gated cross-gain compression in a semiconductor optical amplifier. Other methods include the one described in [36] where all-optical header processing using multi-mode injection locking in a single Fabry-Perot laser diode (FP-LD) is demonstrated. Using injection-locking in FP-LDs has the added benefit of providing 2R regeneration. Yet another method is described in [37] where header processing is shown using two ultrafast nonlinear interferometers where cross-gain and cross-phase modulation in a SOA provide the gate functionality. It is clear from most of these methods that SOAs are a vital building block for the majority of signal processing methods required for header processing.

## 1.5 Buffering

One of the most important technological limitations of all-optical cross-connects is the implementation of optical buffering. Hybrid optical packet switches have used electronic RAMs that have limited access speed, and use optical-to-electronic (O/E) and electronic-to-optical (E/O) conversions that add to the system complexity. Eliminating E/O and O/E conversions will also decrease the system cost provided that the alternative optical processing is more cost-effective than the electrical processing.

Buffering is required when more than one input packet is destined for the same output port during the same time slot. Variable delays are required as multiple packets need to be delayed and processed one at a time. Both wavelength and time multiplexing are used to address the congestion. Optical buffering is done using fibre delay lines (FDLs), which are long lengths of fibre used to buffer packets of known lengths for specific times. A 512 byte packet (the average IP packet size) being transmitted at 10 Gbit/s, for example, requires 82 m of fibre per packet in the buffer. These FDLs cannot be accessed at any point in time, but comprise a FIFO system as

the packets have to traverse the entire length of the FDL that they are buffered in. In section 2 of this paper the buffering requirements of a packet-switched OXC are analysed by investigating the performance of a hypothetical all-optical cross-connect.

FDLs can be implemented in either travelling or recirculating configurations [33], as shown in Figure 1.5. The travelling buffers can be either input or output buffers, and each delay line is traversed only once by a buffered packet. In recirculating buffers packets can be returned to the delay line, and thus buffered for multiple time slots at the cost of signal degradation due to the attenuation in the switch and fibre, but especially due to the crosstalk that results from traversing the switch fabric multiple times.
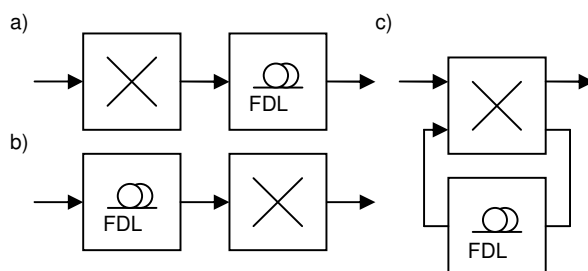


**Figure 1.5 Travelling buffers can be either a) output buffers or b) input buffers. c) Recirculating buffers provide more flexibility and more buffering for less physical fibre.**

Implementations of optical buffers typically depend on wavelength conversion, for example in a NOLM [39], together with add/drop functionality such as a multiplexer [40],[41] or decision-making with an optical threshold function (OTF) [42]. Space domain contention resolution (deflection routing) cannot be used in an all-optical implementation due to the complexity of the dynamic routing decisions required in the network [43].

An all-optical travelling buffer is shown in Figure 1.6. The packets used are fixed length packets. The buffering necessary when two optical packets are simultaneously routed to the same output is done with a fibre delay line. If both packets have the same wavelength they cannot be output on the same line. Assuming that packet 1 has

priority, it is split into two parts: one part passes the node directly to the egress node while the other part is used in the signal processing part of the switch to place packet 2 in the buffer. When it is injected into the threshold function (which is based on coupled ring lasers) the wavelength converter outputs light at $\lambda_2$ and the wavelength of packet 2 is converted to $\lambda_2$. If packet 1 is not present, then packet 2 is converted to $\lambda_1$ and directed to the pass-port. A spatial demultiplexer routes the two wavelengths into different ports, which means that packet 2 will go through the delay line only if packet 1 is present. Interferometric wavelength converters are used to convert the packet back to its original wavelength. This means that the path of packet 2 is determined by packet 1.
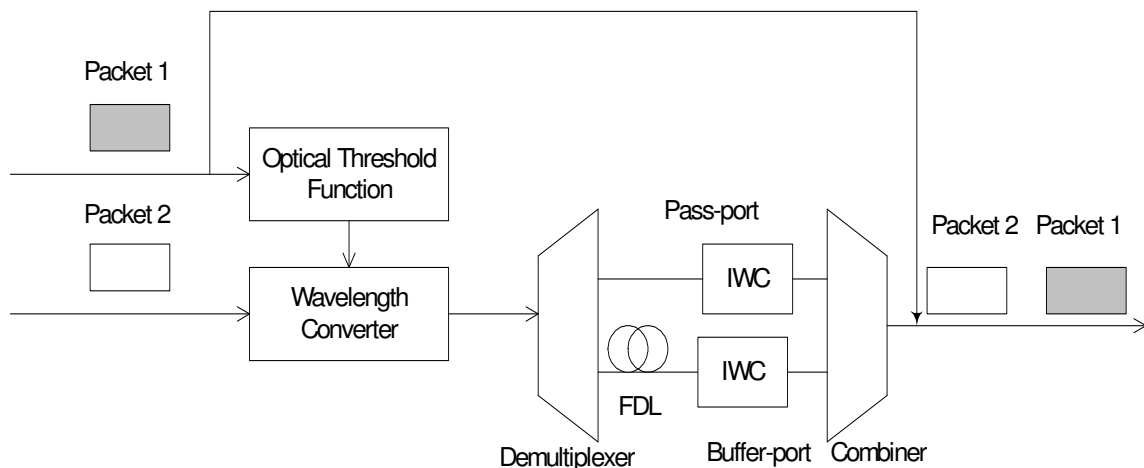
**Fig 1.6 All-optical switching and buffering. IWC: Interferometric wavelength converter Adapted from Liu et al.** [31]

It is interesting to note that exactly the same buffering principle is described in [43], only this time the optical threshold function does not rely on coupled ring lasers. The same functionality is provided using dual wavelength injection locking (DWIL) of Fabry-Perot laser diodes (FP-LD). The setup shown in Figure 1.7 has the same building blocks as that shown in Figure 1.6, except that the technologies to realise the building blocks are different.

The packet at input 1 has priority over the packet at input 2. When there is no contention, one of the following two scenarios take place:

1. Packet 1 is present, and is output on $\lambda_s$.

2. Packet 2 is present, and is output on $\lambda_1$. The reason for this is because the optical threshold function outputs $\lambda_1$. This happens because the first part of the OTF is a FP-LD locked to $\lambda_1$ from the DFB laser, DFB$_1$. The output of this first part, then also locks the second part of the OTF to $\lambda_1$, resulting in an OTF output of $\lambda_1$, which in turns drives the wavelength converter. The wavelength converter is also a DWIL FP-LD that is now locked to the output of the OTF: $\lambda_1$.
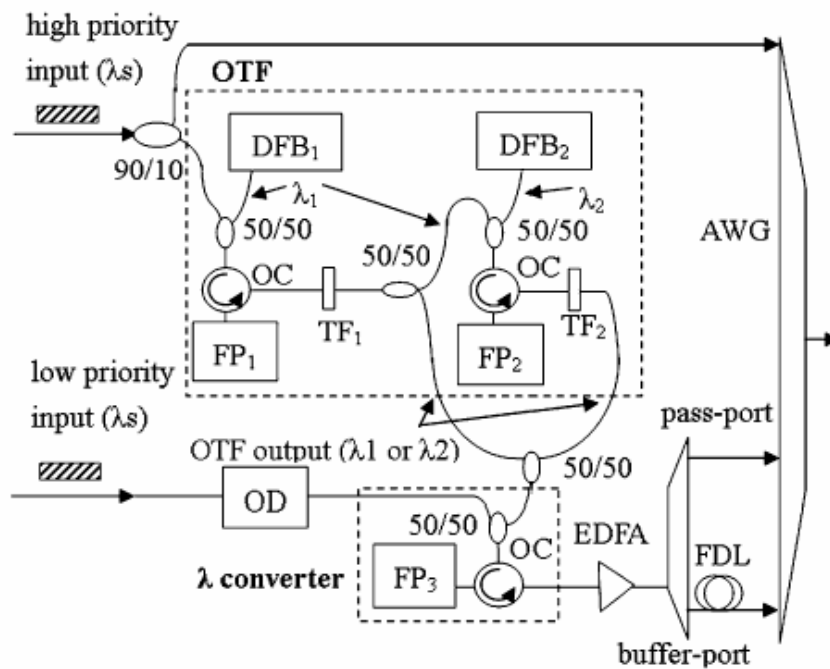


**Figure 1.7 Experimental setup of the all-optical buffer using DWIL in FP-LDs. EDFA: erbium-doped fiber amplifier, OTF: optical threshold function, AWG: array-waveguide grating, FDL: fiber delay line, OC: optical circulator, TF: tunable filter, OD: optical delay, DFP: dual feedback laser. (From [43])**

When there is contention, packet 1 causes the first part of the OTF to lock to $\lambda_s$, the wavelength of the input packet. The output of this first part of the OTF is filtered at $\lambda_1$,

however, which means that no output is observed after the first part of the OTF if packet 1 is present. This means that the second part of the OTF remains locked to $\lambda_2$, resulting in the locking of the wavelength converter FP-LD to $\lambda_2$ as well.

## 1.6 Wavelength Conversion

All-optical wavelength converters based on nonlinearities in SOAs are considered important building blocks for wavelength division multiplexed (WDM) networks [44],[45],[46].

- FWM: Wavelength conversion utilising four-wave mixing in an SOA is independent of the modulation format but it has low conversion efficiency and also the input light needs to be polarisation matched [46].

- XGM: Inverted wavelength conversion based on cross gain modulation in a single SOA has been demonstrated at 100 Gbit/s, but this approach also leads to a degradation of the extinction ratio [45].

- XPM: Interferometric wavelength converters based on cross phase modulation in combination with XGM in SOAs lead to an improved extinction ratio and can also be used to realize inverted and noninverted conversion. Furthermore, this concept can be utilized for signal reshaping [46].

- BLD: Wavelength conversion has also been achieved using bistable laser diodes (BLDs) [47]. BLDs can also be used for optical signal regeneration and optical demultiplexing, and are promising devices for optical signal processing.

## 1.7 Scope and Structure of Thesis

Optical packet switching technology is researched in order to realise higher capacities and to improve the bandwidth utilisation of the optical layer. Most of the basic building blocks required to realise these packet-switched cross-connects suffer from technological challenges, and two of the most challenging aspects are regarded in

this research: contention resolution, and the signal processing required to implement a contention resolution scheme.

Chapter 2 discusses various all-optical building blocks that could be used to implement an all-optical contention resolution scheme as described in Chapter 3. An overview is provided of several functions developed within the COBRA research group: all-optical header processing, all-optical buffering using a laser neural network, and a three-state all-optical memory based on coupled ring lasers. In this chapter, the concept of a threshold function is introduced, which is a simple yet effective optical signal processor that is shown to be invaluable in all-optical implementations of contention resolution schemes. It is important to note that there is a significant difference between simply buffering optical data (i.e. sending packets through a delay line), and implementing contention resolution, which includes, to a certain degree, decision making and switching; this is where an optical threshold function is required.

Chapter 3 analyses different buffering strategies for an all-optical cross-connect architecture. Because an all-optical implementation is considered, this implies various necessary assumptions due to the limitations of the available technology, such as very limited signal processing, simplified header processing, and the utilisation of very simple algorithms for contention resolution. In order to obtain a realistic picture of the technology required and implementation limitations of an all-optical approach, a realistic bursty traffic model was used, the wavelength dimension was exploited in the cross-connect, and the physical amount of fibre required for the fibre delay lines was analysed. It is shown that self-similar traffic requires a lot of buffer space, and that this can be partially addressed by utilising various wavelengths in each fibre delay line of the buffer. It is also shown that recirculating buffers provide a preferable solution not only because less fibre is used, but also because the fibre is utilised more effectively and because the contention resolution algorithm used is simpler as it is not necessary to keep track of the buffer content. A finer buffer granularity and more flexibility is also possible with a recirculating buffer. The all-optical approach to a packet switched

cross-connect is unique, as the technologically more feasible solution of hybrid electro-optic systems have been focused on thus far [48],[49],[50],[51],[52],[53].

Chapter 4 compares the buffer requirements for the all-optical approach as outlined in Chapter 3 to estimated buffer requirements based on Transmission Control Protocol (TCP) dynamics. It is emphasised that the metrics selected to analyse buffering architectures should suit the critical performance parameters relevant to where in the network the optical node is used.

A novel design for an optical threshold function based on nonlinear polarisation rotation in a single semiconductor optical amplifier (SOA) is introduced in Chapter 5. The threshold function uses the transverse electric (TE) and the transverse magnetic (TM) components of the optical field to determine the two states of the threshold function. This method has the advantage of being reliant on a single active element, and being able to switch with a relatively low power optical control signal. An extinction ratio of approximately 20dB is achieved, with a typical control signal of around 0dBm. The experimental results are supported by simulation results based on a model that decomposes the optical field into its TE and TM components, assuming independent propagation with indirect interaction via the gain saturation.

The first part of this thesis describes the challenges associated with all-optical implementations of contention resolution schemes, and it is clear that there are several limitations due to the current state of all-optical technology. In Chapter 3 it was shown that a *recirculating* optical buffer is a desirable scheme to try to implement. Chapter 5 described the development of a threshold function that can be used for all-optical contention resolution and switching. A significant motivation for all of this work in the *optical* domain is because of the signal degradation encountered in hybrid electro-optic implementations of recirculating buffers. Apart from the added noise due to amplification in the recirculating buffer, the biggest contribution of signal degradation is crosstalk caused by the switch fabric itself. In Chapter 6 a hybrid electro-optic solution is considered with a novel ultra-fast electro-optic switch, the CrossPoint

switch, which is unique in that it displays very low switching crosstalk. The CrossPoint facilitates a recirculating buffer architecture with electronic control that results in a very small processing delay, and in Chapter 6 it is shown that signal integrity can be maintained due to the low crosstalk of the CrossPoint switch.

Multiple recirculations were possible with little signal degradation; the performance was so promising that the implementation of the switch was also investigated for an alternative application requiring this type of functionality, not just routing and contention resolution: using the CrossPoint switch in a time slot interchange application is described in Chapter 7. Time slot interchangers are important devices in time-division multiplexed (TDM) systems, but generally suffer severely from crosstalk, which was significantly improved upon by using the CrossPoint switch. With regards to packet switching, Chapter 7 also described the development of an electronic control interface for the CrossPoint so that header recognition can be used in order to implement contention resolution, once again using a recirculating buffer. The control flexibility of the CrossPoint also made it possible to demonstrate asynchronous variable length switching. Finally the use of Differential Phase Shift Keying (DPSK) is shown to significantly improve the signal quality for applications that use the CrossPoint switch and recirculating fibre delay lines.

# CHAPTER 2 ALL-OPTICAL SIGNAL PROCESSING

## 2.1 Introduction

The bandwidth mismatch between optical transmission and electronic routers has led to the development of various optical signal processing techniques and an investigation into optical packet switching [55], [49], [50]. Figure 1.1 in Chapter 1 shows a schematic diagram of a generic node. The main functions are synchronisation, switching and buffering. The synchronisation of optical packets can be done using switchable delay lines for the coarse synchronisation, and wavelength converters with dispersive fibre for the fine synchronisation. This chapter provides a summary of the all-optical functional blocks developed within the COBRA research group which will be used as the all-optical technology context of the research described in Chapter 5.

Figure 2.1 shows an all-optical packet switch that allows routing of data packets without electronic control [28]. This packet switch utilizes several optical functionalities such as an optical header processor, an optical threshold function, and an optical flip-flop memory with a wavelength-routing switch.

All-optical header processing has been investigated using several different methods. In Cardakli et al.[56], an all-optical method for processing packet headers is presented that uses tuneable fibre Bragg gratings. Ultrafast all-optical header recognition has been reported in Cotter et al. [23] and Nesset et al. [57] by using four-wave mixing in a Semiconductor Optical Amplifier (SOA) and in Glesk et al. [24] by using Terahertz Optical Asymmetric Demultiplexers (TOADs). The TOAD configuration has also been used to demonstrate all-optical ultra-fast switching [27]. Hybrid electro-optical buffering concepts used for contention resolution are demonstrated in [4],[58],[51].

This chapter is based on the results published in [54]                    19

Performance analyses of optical buffers are presented in Zhong and Tucker, [52],[53]. In Sakamoto et al. [48], an all-optical buffering concept is demonstrated that allows a variable optical delay. In Hill et al. [28] 1×2 all-optical switching (based on two-pulse correlation in a semiconductor laser amplifier in a loop mirror (SLALOM) configuration [32]) was presented and in Liu et al. [31] an all-optical buffering concept (showing 2×1 buffering using wavelength routing) was presented.
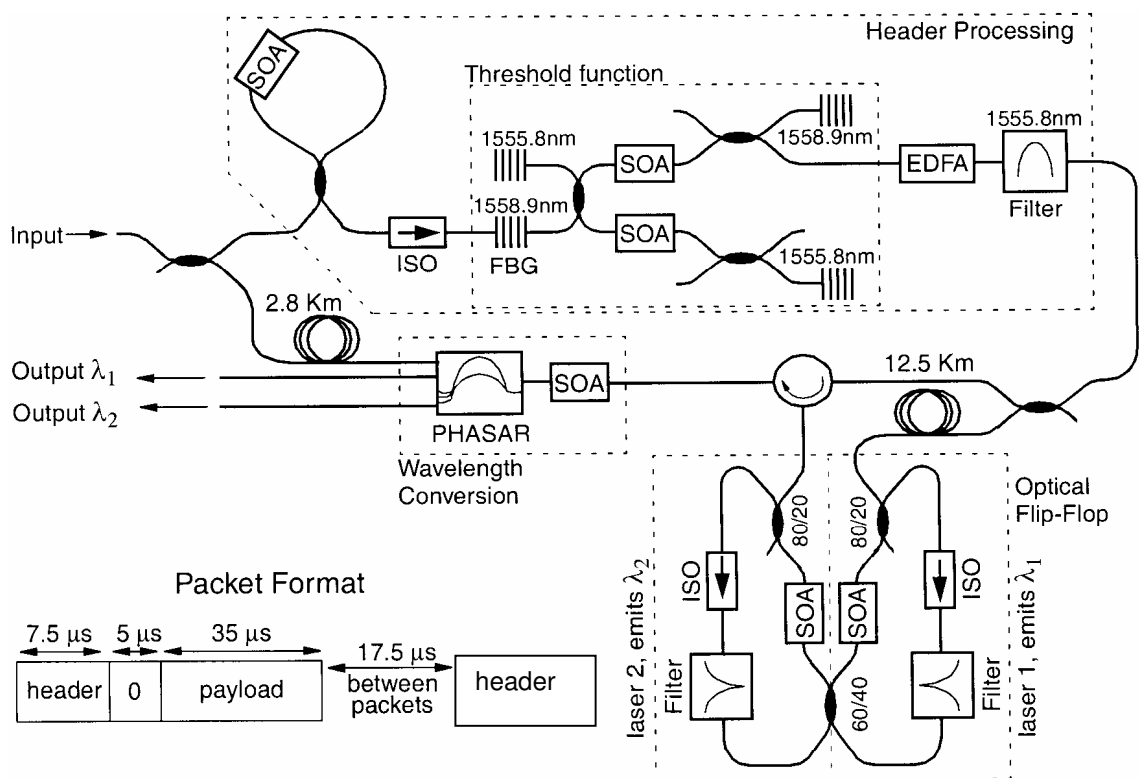


**Figure 2.1 Experimental setup to demonstrate the 1×2 all-optical packet switch. Traffic from the network is coupled in the packet switch at the input. The packet format is given. SOA, semiconductor optical amplifier; FBG: fibre Bragg grating; EDFA, erbium-doped fibre amplifier; ISO, isolator; PHASAR, phased array demultiplexer.**

In this chapter two advanced header processing concepts are described: the first one is an ultra fast TOAD in combination with a header pre-processor [60], and the second one is a header processor based on self-induced polarisation rotation [61]. Both header

processing concepts allow the 1×2 optical packet switch that was described in Hill et al. [28] and Dorren et al. [59] to be extended to a larger dimension. A 3×1 buffer using a laser neural network is also described [100], as well as a variable optical delay that can be used for recirculating buffering [65]. Finally, a three-state all-optical memory based on coupled ring lasers [42], which facilitates more output ports in an all-optical node, is described.

In advanced lightwave systems, several optical elements are required to function together. Monolithic photonic integrated circuits provide the photonic functionality as well as the inexpensive, robust on-chip interconnection of devices necessary to build integrated subsystems on a chip. The all-optical functions discussed in this section all share the advantage that they have the potential to be photonically integrated.

## 2.2 All-Optical Header Processing

The ultrafast all-optical header recognition methods reported in Cotter et al. [23] and Nesset et al. [57] require a form of optical clock recovery that introduces additional complexity in the switching system. In Dorren et al. [59] a header recognition method is described that does not require optical clock recovery but it needs a Manchester encoded packet payload. In this section we describe two methods of header recognition, both of which function asynchronously and operate at low power.

### 2.2.1 Ultra-fast Asynchronous Multi-output All-optical Header Processor

Using a TOAD-based header processing technique together with a header pre-processor, results in a system that can distinguish a large number of header patterns and allows asynchronous operation and photonic integration. Another advantage is that TOAD operation guarantees ultra-fast header processing at low power. Although the system described here was demonstrated at 10 Gbit/s [60], optical switching has been demonstrated using a TOAD at 250 Gbit/s [24],[27]. Furthermore, the header processing system as a whole operates asynchronously and the system can be extended to have multiple output ports.
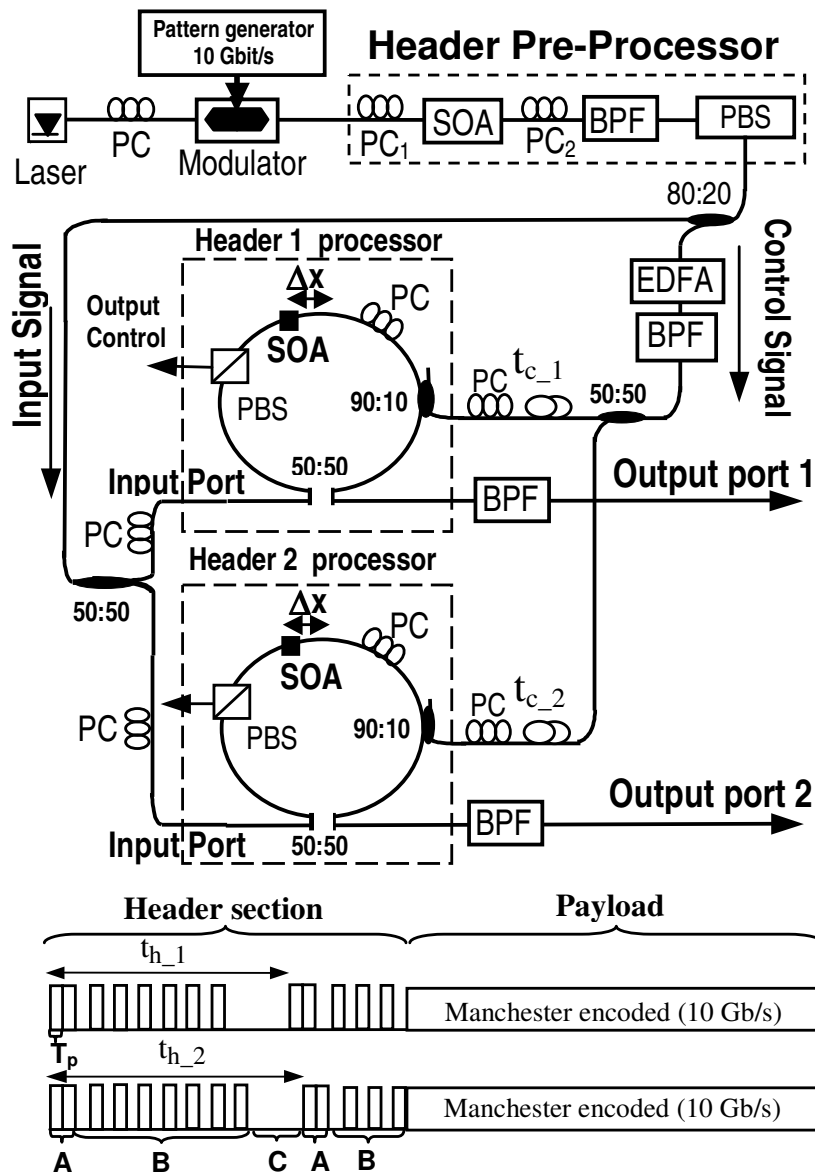
**Figure 2.2 Experimental setup to demonstrate the header processing system and packet structure. PC: polarisation controller, EDFA: erbium doped fibre amplifier, BPF: band pass filter, PBS: polarisation beam splitter.**

The optical header processing system is schematically presented in Figure 2.2. It consists of a header pre-processor (HPP) based on the principle of self-induced polarisation rotation in an SOA [61], and two TOADs that are placed in parallel. The function of the HPP is twofold: it separates the packet header from the packet payload,

and it also creates the control signal that is required for TOAD operation. Each of the TOADs is designed to recognise a specific header pattern.

An essential point of the header-processing concept is that the address information is encoded by the difference in time between the leading edges of two header pulses. The space in between the header pulses is filled with a sequence of alternating NRZ 0 and 1 bits at the same bit rate as the data payload, which ensures that the SOA remains saturated while the packet header passes through [60],[61]. A series of 0's with a duration that is longer than the SOA recovery time $\tau_r$ is placed before the second header bit, to allow the amplifier to recover before the second header pulse arrives at the SOA. Similarly, the guard time in between the header section and the payload section is filled with a sequence of alternating 0 and 1 bits to keep the amplifier saturated when the packet passes by. Finally, the packet payload (at 10 Gbit/s) is Manchester encoded to avoid repetition of the header pattern (at 2.5 Gbit/s) in the packet payload.

The operation of the TOAD has been described in Sokoloff et al. [26]. The TOAD can function as a header processor as follows. The HPP output pulses form the TOAD input signal and are split by an 80:20 coupler in a low power clockwise (CW) and counter clockwise (CCW) propagating data signal, and a high power control signal. The CCW propagating pulses arrive at the SOA after the CW propagating pulses. If no control is present the data signal is reflected back to the TOAD input. The first pulse of the high power control signal is used to saturate the SOA. Header recognition can be implemented by accurate timing of the control pulses. A pulse is only output from the TOAD if the time between the two header pulses matches with the timing of the control pulse. In contrast to header recognition based on two-pulse correlation in a SLALOM configuration, this header recognition concept does not critically depend on the SOA recovery time. Hence, the offset of the SOA with respect to the centre of the loop and the delays for the control pulses can be made sufficiently small so that this header processing concept allows photonic integration.

## *2.2.2 All-optical header processor based on self-induced polarisation rotation*

Self-induced effects in nonlinear optical mediums can be employed to realise all-optical signal processing functions. These effects occur when an optical signal introduces a change in a nonlinear medium through which the signal propagates while the medium reacts back on the signal itself.

The header processing system described here is based on self-induced polarisation rotation, and also consists of an HPP followed by the header processor. An all-optical correlator is a fundamental building block to realise all-optical header recognition. In this section an optical correlator based on a nonlinear polarisation switch is described [61].
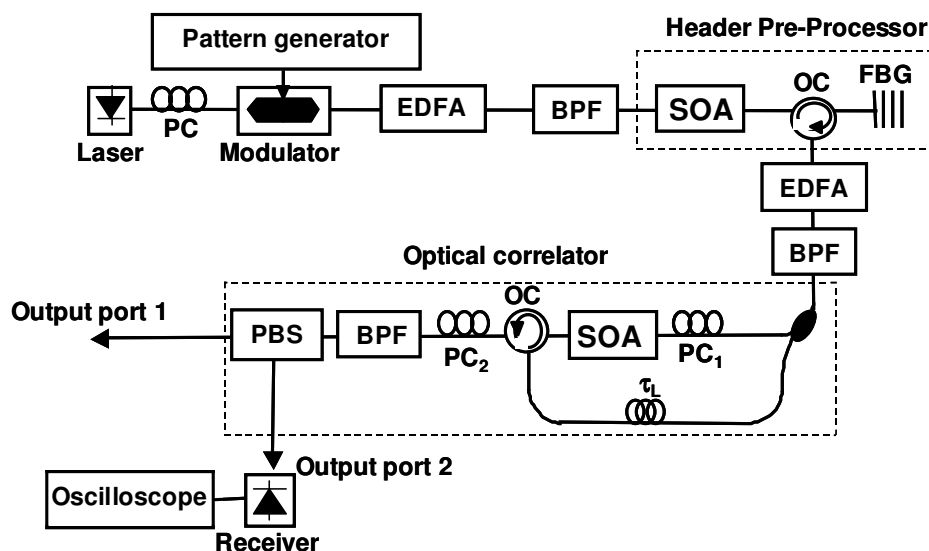


**Figure 2.3 Experimental set-up of the header processing system. BPF: band pass filter, PC: polarisation controller, OC: cptical circulator, FBG: fibre Bragg grating,$\tau_L$: delay of the counter propagating signal.**

The optical correlator used for the header processor is presented schematically in the second dashed box of Figure 2.3. The optical power of the data signal is split by a coupler into one data signal that enters the SOA on the right side (left propagating data signal) and one data signal that enters the SOA on the left side (right propagating data

signal). The right propagating data signal is first delayed by a time $\tau_L$ and then fed into the SOA of the optical correlator. PC2 is set to switch the light to output port 1 of the polarisation beam splitter (PBS), only if the left propagating data signal passes through the SOA. When the right propagating data signal also enters the SOA, and the optical power is sufficient to saturate the SOA, a correlation between the left propagating and the delayed right propagating data signal is formed since the left propagating data signal experiences polarisation rotation. As a result, the left propagating data signal is switched to output port 2.

The experimental results indicate that the header processing system can distinguish between two different header patterns. A limitation of this approach is that a packet header only contains two bits of information. The length of the packet header can be extended by creating larger packet headers that are built up out of combinations of two bits. The minimum interval between different header bits is determined by the SOA recovery time (~1ns). This means that the duration of the packet is proportional to the number of header bits times the SOA recovery time. It should be noted however that the SOA recovery time can be reduced artificially [62] – [64]. This implies that the length of header patterns can be reduced as well.

## 2.3 Optical Buffering

In an optical packet switching node as shown in Figure 1.1 in Chapter 1, a key issue is packet contention [4]. Contention takes place when packets arriving at a node simultaneously have to be routed to the same destination. All-optical buffers that use fibre delay lines are employed to solve this packet contention. In general, two types of buffers are used: travelling buffers and recirculating buffers [33]. In travelling buffers, the delay time is determined by the length of the optical delay line. Such configurations are investigated in Guillemot et al. [50], where optical travelling buffering is realised by using electronically controlled wavelength routing switches, and in Dorren et al. [59], where an all-optical travelling buffer concept is realised by using an optical threshold function (OTF) in combination with a wavelength routing switch. This

travelling buffer concept is extended in the next section to handle multipacket contention [100].

Travelling buffers have a disadvantage since a large number of delay lines are required to avoid packet loss under a heavy traffic load. This makes travelling buffers bulky. In recirculating buffers, however, the delay time is determined by the length of the loop and the circulation number. Hence, a single delay line can be used to realise a large delay by increasing the number of circulations. An important advantage of recirculating buffers over travelling buffers is that the physical size of the buffer is reduced.

### 2.3.1 Buffering Using Laser Neural Networks

In this section we describe an all-optical buffering concept that can handle multi-packet contention by using an all-optical arbiter that is based on a Laser Neural Network (LNN) [100],[14]. The LNN replaces the role of the optical threshold function in [59]. A configuration that employs an LNN for packet buffering is shown in Figure 2.4.

Assume that a maximum of three synchronised optical packets arrive simultaneously at the packet switch, and assume that the priority of the packet to pass the node decreases from packet 1 to packet 3. An optical threshold function that is driven by packet 1, controls a wavelength routing switch, so that (in the presence of packet 1) packet 2 is delayed for one packet period. Similarly, the routing of packet 3 is determined by the presence of packets 1 and 2. An optical arbiter that drives a wavelength routing switch is employed to decide whether packet contention takes place. The wavelength routing switch is operated by wavelength conversion in combination with a demultiplexer.
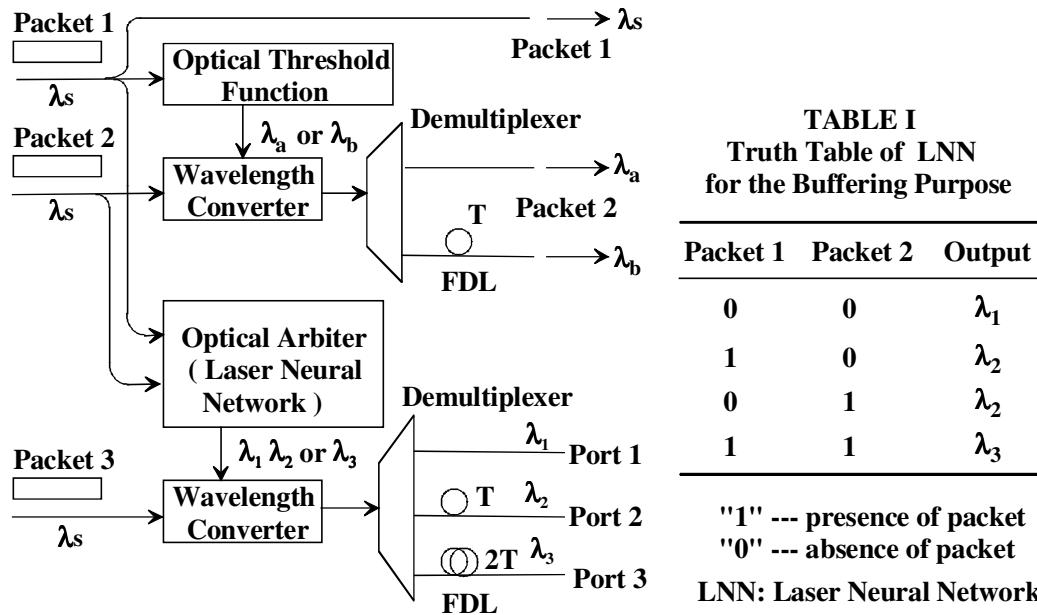
**Figure 2.4 Functional scheme of the all-optical buffer concept and the truth table of the optical arbiter (LNN) that is required for handling three packets contention. FDL: fibre delay line; T: the delay time equal to one packet length.**

Since wavelength conversion requires continuous wave light to be injected into the wavelength converter simultaneously with the data packet, the first function of the LNN is to generate continuous wave light at a specific wavelength. For this, there are 3 cases depending on how many packets enter the switch:

1. Assume that only packet 3 arrives at the buffer and that packets 1 and 2 are absent. Thus no packets are input to the LNN. The LNN should be trained in such a way that continuous wave light at wavelength $\lambda_1$ is output from the arbiter. Therefore, the wavelength of packet 3 is converted to $\lambda_1$, and packet 3 is routed into port 1, passing the buffer without any delay.

2. Only one data packet (either packet 1 or packet 2) is input to the LNN. The LNN has to output continuous wave light at wavelength $\lambda_2$ if only one packet is injected. Hence, packet 3 is routed into port 2, undergoing one packet period of delay.

3. Both packet 1 and packet 2 arrive simultaneously at the LNN. In this case the LNN has to output continuous wave light at wavelength $\lambda_3$. Hence, packet 3 is routed into port 3, undergoing two packet periods of delay.

The LNN consists of two parts. In the first part, the optical inputs are weighted. Weighting of the LNN inputs is carried out by a system of variable optical attenuators and couplers. The second part of the LNN consists of three coupled ring lasers, in which SOAs act as laser gain media. The choices of the input weights determine the truth table of the LNN; i.e. different weights lead to different logic operations. Injection of external light changes the states of the arbiter. In principle the LNN can be extended further, so that it could be employed in a system that is capable of handling the contention of more than three packets.

### 2.3.2 Variable Optical Delay for a Recirculating Buffer

In this subsection we show that an OTF in combination with a single optical wavelength converter based on nonlinear polarisation rotation in a SOA can be used to realise a variable optical delay. The variable delay time is achieved by altering the number of circulations of the packet in the loop.

The variable optical delay concept is presented schematically in Figure 2.5. The packets arrive in a synchronised fashion and the packets in Channel 2 (CH2) have a lower priority to pass the node than the packets in Channel 1 (CH1). The packets in CH2 can only pass through the node if there is no packet in CH1 that causes packet contention in a specific timeslot. The packets in CH1 are injected into an OTF that acts as an optical arbiter to decide if packet contention occurs.

The first essential building block of this concept is an OTF. The OTF is made out of two coupled lasers and is described in Dorren et al. [59]. The second essential building block is a wavelength converter that is based on nonlinear polarisation rotation in a single SOA, as described in Liu et al. [44]. It has been demonstrated in Liu et al. [44]

that this wavelength converter can realise noninverted conversion with reshaping ability, and also can convert the signal into the same wavelength.
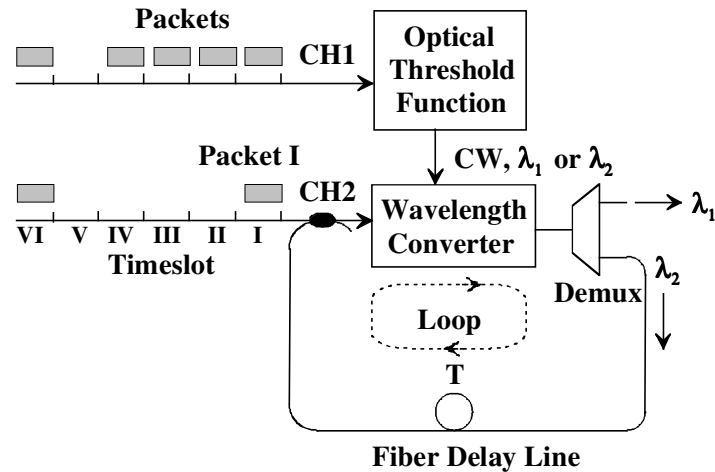


**Figure 2.5 Functional diagram of the variable optical delay concept. T: the delay time equal to one timeslot, Demux: demultiplexer.**

The system shown in Figure 2.5 can function as a variable optical delay in a recirculating loop as follows. First, it is assumed that the synchronised data packets arrive at the node in distinct timeslots. The delay time introduced by the fibre delay line is one timeslot. The continuous wave light output from the OTF controls a wavelength converter that in turn converts the wavelength of packets that arrive in CH2. The optical demultiplexer is used to route packets into a specific port, depending on the wavelength of the packets. Suppose that in Timeslot I packets in CH1 and CH2 are present, so that packet contention takes place. The packet in CH1 is injected in the OTF, thus the OTF switches its state to output continuous wave light at wavelength $\lambda_2$. Hence, the wavelength of packet I is converted to $\lambda_2$ so that packet I is routed into an optical loop which delays the packet for the duration of one timeslot. In timeslot II, the OTF also outputs continuous wave light at wavelength $\lambda_2$ due to the presence of a packet in CH1. Thus packet I, which was already converted to wavelength $\lambda_2$ and delayed by one timeslot, is reconverted to wavelength $\lambda_2$ and delayed for another

timeslot in the delay loop. A similar situation takes place in timeslots III and IV, but in timeslot V, the OTF outputs $\lambda_1$ due to the absence of a packet in CH1. Hence, packet I is reconverted from wavelength $\lambda_2$ into $\lambda_1$ and is routed out of the loop.

The maximum circulation number is determined by the quality of the OTF, the reshaping ability of the wavelength converter, the noise figure of the EDFA in the recirculating loop (not shown in the functional diagram, but necessary to compensate for recirculating loss), the packet length, and the polarisation state of the light in the loop. It is believed that at least several tens of circulations can be achieved by using integrated versions of the OTF and reducing the packet length to in the range of hundreds of nanoseconds.

## 2.4 Multistate Memory

In Dorren et al. [59], a 1×2 all-optical packet switch was presented. A key component of this packet switch is a two-state all-optical memory. In principle, the number of states of the memory determines the number of output states of the packet switch. Therefore, all-optical memories with more states are crucial for extending the 1×2 all-optical packet switch of Dorren et al. [59] to a larger dimension (1×N). In this section, we describe an all-optical memory that has three states, shown in Figure 2.6. This three-state memory concept can be extended to create an all-optical memory with an arbitrary number of states.

Two identical lasers can be coupled to make a two-state all optical memory [59]. The concept in Dorren et al. [59] can be extended to a three-state optical memory. In Figure 2.6, three identical ring lasers are coupled to one another to construct a three-state optical memory. The output of each ring laser has to be coupled into the other two lasers, but not into its own cavity. To realise this, the outputs of each ring laser are first combined by use of a multiplexer. Ten percent of the combined light is coupled out of the system with a 90/10 coupler. This is the memory output. The other 90% of the combined light is first fed into SOA4 to be amplified and then fed back into each ring

laser through a system of fibre Bragg gratings (FBGs). The output of each laser is coupled into the other lasers, but not into its own cavity because of the FBGs.

The amplification by SOA4 ensures that the light injected into each laser is sufficient to suppress the lasing mode. Since the system is symmetric, all the lasers can suppress lasing in the other lasers, and thus each laser can become dominant. The state of the memory is determined by the wavelength of the memory's output light. In each state, only one laser lases and the other lasers are suppressed; thus only one wavelength is dominant. For example, in state 1, laser 1 dominates and suppresses the lasing in the other lasers; thus $\lambda_1$ is dominant.
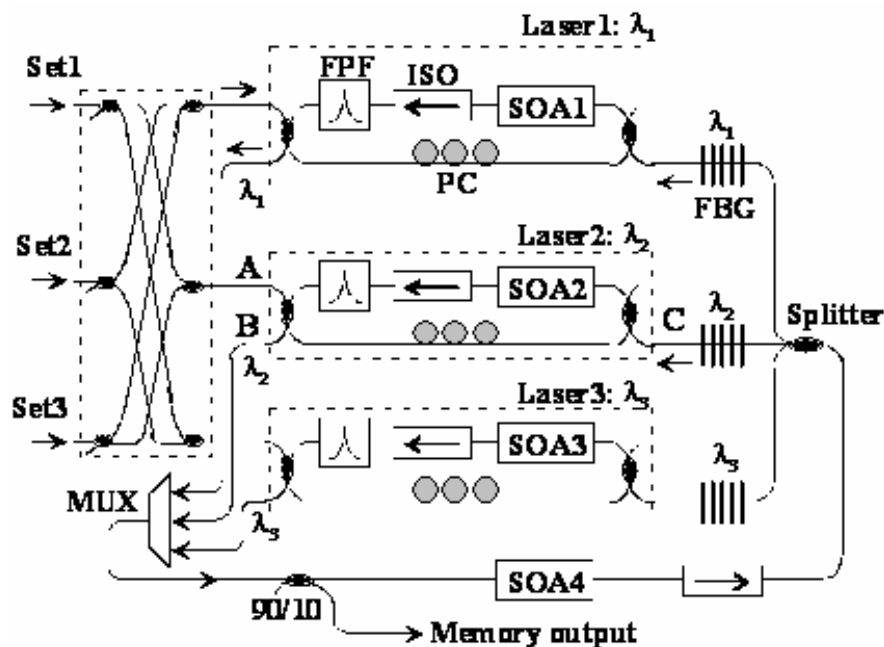


**Figure 2.6 Configuration of the three-state all-optical memory based on coupled ring lasers. ISO, isolator; FPF, Fabry–Perot filter; PC, polarisation controller; MUX: optical multiplexer; FBG, fibre Bragg grating.**

To select the state of the memory, external light is injected via one of the set ports. The external light, which is used to change the state of the memory, is first sent through a small network that is made from 3-dB couplers. The function of this network

is to dispense the external light into specific lasers, depending which input port is used. For example, if external light is injected into the set 1 port, the memory is set to state 1 (laser 1 dominates). In this case, the external light suppresses lasers 2 and 3. The saturating external light stops or reduces the light exiting from the lasers in which the external light is injected, no matter whether these lasers are dominant or suppressed. As a consequence, laser 1, into which no external light is injected, can increase its output light and thus become the dominant laser. This state remains after the external light is removed.

The speed of this memory is determined by the cavity length of the ring laser and the propagation distance between each laser. (The cavity length determines the switching time of the multistate memory, influencing the guard time between header and payload. It does not influence the data rate; data rate is dependent on the bandwidth of the wavelength converter). The experimental setup was constructed from standard commercially available fibre pigtailed components; thus each laser has a cavity length of ~16 m, and ~13 m of fibre is used between each laser, which implies that several microseconds are required for changing the state of the memory. However, in integrated versions of the memory, the laser would have a cavity length of a couple millimetres and the distance between each laser would be reduced to within the order of millimetres, indicating that integrated versions of the memory could attain speeds in the gigahertz range. The concept of this three-state memory can be extended to create all-optical memories with a larger number of states. However, the operating speed of the extended multistate memory will slow down, since the distance between the coupled lasers will increase. Furthermore, more optical switching power and more amplification of the combined light (the role of SOA4 in Figure 2.6) are required, owing to the increasing coupling loss in the extended multistate all-optical memory.

## 2.5 Conclusions

This chapter has presented some functionalities, such as an all-optical header recogniser, an all-optical packet buffer, and a multistate optical flip-flop memory, that

form essential building blocks for all-optical packet switches. These functionalities enable all-optical switching of data packets. It should be noted, however, that in fully optically controlled packet-switched cross-connects, buffering and packet synchronisation functionalities are also required. Moreover, it is desired that all these signal processing functions allow photonic integration so that eventually monolithically integrated optical packet-switched cross-connects emerge.

The TOAD-based header recogniser that was discussed in this chapter allows photonic integration. To avoid the use of polarisation beam splitters and polarisation controllers (which introduce an additional complication for photonic integration), it should be noted that it is desirable to operate the TOAD with a control signal at a different wavelength instead of a different polarisation. A control signal at a different wavelength requires an additional wavelength conversion stage in the header recogniser. Alternatively, one could use an optical correlator based on nonlinear polarisation rotation in a SOA for header recognition. From the point of view of photonic integration, such technology is challenging, since it requires functionalities such as integrated polarisation controllers and an integrated polarisation beam splitter. One should realise, however, that the concept of nonlinear cross polarisation rotation shows many similarities with the concept of cross phase modulation [66] so that the optical correlation can be implemented by use of a Mach–Zehnder interferometer.

One of the largest challenges on the road toward the application of optical packet-switched technology in optical networks is undoubtedly related to the realisation of optical packet buffers and packet synchronisers. The optical packet buffers discussed in this chapter are based on all-optically controlled fibre buffers. The buffer control was implemented by use of an all-optical threshold function or a laser neural network, both implemented with coupled lasers. Photonic integration of such a laser neural network is a challenge on its own, but the fact that all available packet buffers are based on fibre delay lines creates a more serious issue. Using optical delay lines as a packet buffer is interesting from a research point of view, but it is unlikely that optical packet-switched

cross-connects will emerge that contain many kilometres of fibre to allow optical buffering. A similar argument holds for the synchronisation issue.

Monolithically integrated delay lines might be obtained by employing a semiconductor quantum dot waveguide as a delay medium [67],[68]. The group velocity of a signal in the waveguide will slow down when a strong pump light is launched simultaneously into the waveguide, owing to the electromagnetically induced transparency effect. Simulation results indicate that this approach can slow down the group velocity of light by a factor of 55. The use of delay lines could be avoided in synchronisation and buffer functionalities, if integrated optical shift registers were available. All-optical flip-flops could act as a fundamental building block for an optical shift register. Such optical flip-flop memories should have fast (optical) set and reset times, operate at low power, have a high contrast ratio, and should have sufficiently small dimensions. An integrated optical flip-flop memory based on laser operation is presented in Takenaka et al. [69], but the power consumption, the size, and the switching speed of these devices remain an issue, which makes it difficult to couple them in large quantities as required in optical shift registers. Flip-flop concepts that address the issues of power consumption, size, and switching speed are now being investigated. Ideally, a flip-flop concept should have the potential to achieve dimensions of the order of the wavelength of light, a switching speed of a picosecond, and a switching energy below a femtojoule. If one succeeds at interconnecting these flip-flops, densely integrated digital optical logic operating at high speed and low power can be realised.

# CHAPTER 3 ARCHITECTURES AND BUFFERING FOR ALL-OPTICAL PACKET SWITCHED CROSS-CONNECTS

## 3.1 Introduction

This chapter considers the performance of an all-optical packet switched cross-connect. All-optical header processing and all-optical routing are implemented in the cross-connect architectures. The main metric considered to measure the performance is the packet loss ratio for the buffering. This is influenced primarily by three factors. The first is the cross-connect architecture: feedback or feed-forward buffering, incorporating wavelength domain contention resolution. The second is the selection of the fibre delay line distribution: degenerate or nondegenerate distributions. And the third is the traffic load together with the traffic model used for the performance analysis: a Poisson distribution or a self-similar model. It is shown that the optimal implementation of a feedback buffer requires a technique such as overflow buffering as well as the superior performance of an all-optical switch in order to maintain signal quality through multiple recirculations.

Optical cross-connects (OXCs) are the basic network elements for routing optical signals. Currently two of the most important technological limitations of all-optical cross-connects are the implementation of optical buffering and optical signal processing. Hybrid optical packet switches have used electronic RAMs that have limited access speed, and use optical-to-electronic (O/E) and electronic-to-optical (E/O) conversions that add to the system complexity. Eliminating E/O and O/E conversions will also decrease the system cost.

This chapter is based on the results published in [70]:

Buffering is required when more than one input packet is destined for the same output port during the same time slot. Variable delays are required as multiple packets need to be delayed and processed one at a time. Both wavelength and time multiplexing are used to address the congestion. Optical buffering is done using fibre delay lines (FDLs), which are long lengths of fibre used to buffer packets of known lengths for specific times. A 512 byte packet (the average IP packet size) being transmitted at 10Gbit/s, for example, requires 82m of fibre per packet in the buffer. These FDLs cannot be accessed at any point in time, but comprise a FIFO system as the packets have to traverse the entire length of the FDL that they are buffered in. Space domain contention resolution (deflection routing) cannot be used in an all-optical implementation due to the complexity of the routing decision required in the routing node [15]. Although it can be used for low overall network loads, the performance depends on the network topology and routing matrix, and poor performance results from the excess consumption of network resources or the lack of alternate paths [71]. The use of FDLs together with the wavelength domain is considered in this thesis.

This chapter discusses the relevant issues for an *all-optical* implementation. Considering the rudimentary state of all-optical technology, several implementation assumptions had to be made for the simulations in order to minimise the required optical signal processing. Various architectures are considered utilizing all-optical concepts. The performance (measured in terms of packet loss ratio, PLR) of these architectures is analysed by looking at an all-optical buffering implementation. To facilitate the simulations, and in order to gain a clear perspective of the differences in performance, the architectures and the influence of various parameters were analysed using a Poisson traffic model. It is however necessary to take the self-similarity of Internet traffic into account, so to obtain realistic values of how much buffering will be required, the final buffer sizes are analysed using a Pareto distribution to model the traffic. It is shown that the best performance is achieved using a feedback buffer

architecture. Although this is often not feasible in an electro-optic implementation due to the adverse effects of crosstalk [4], the all-optical switches maintain signal quality through the recirculations, facilitating multiple recirculations required for a low packet loss ratio.

The original contributions of this work are a new all-optical packet switch design based on all-optical switching and buffering as described in [59] (no electronic signal processing or control is assumed), fully shared buffers incorporating a buffer overflow algorithm in the wavelength domain is introduced, and these buffer architectures are investigated varying the following parameters: traffic load and models, the number of FDLs and FDL distributions, and the number of switch and buffer ports.

The chapter is organised as follows. In section 2, optical switching is discussed. In section 3 the influence and selection of the appropriate traffic model is explained. Section 4 discusses the options for all-optical cross-connect architectures, while these architectures are evaluated according to the buffer implementations as analysed in section 5.

## 3.2 Optical Switching

All-optical technology is aimed at application in routing nodes that require high bandwidth, fast switching, and transparency. Packet switching is required to handle the burstiness of Internet traffic because of its fine granularity and effective utilization of link capacity.

Processing complexity must be kept to a minimum in the all-optical routing nodes, which means that there are several networking functions that must be implemented in the edge routers, such as maintaining packet sequence integrity. In optical packet switching, the route that a packet will follow through the network can be specified in the packet header, or the packet may specify the destination and the routing nodes will select the path. In the all-optical implementation used as the context for this discussion, the processing overhead is minimised in the routing nodes thus it is assumed that the

path (that is, the output port of a packet from a node) will be specified in the packet header. For this reason it is assumed that one of the $N \times n_{ext}$ output channels (N is the number of input and output fibres, $n_{ext}$ is the number of transmission wavelengths used on each of the N fibres outside the switch) is defined in the header, and each of the buffers thus outputs to one of these channels.

[72] describes how either fixed length packets (FLP) or slotted variable length packets (SVLP) can be handled successfully depending on the scheduling algorithm used. In this chapter, a slotted architecture is assumed, with a fixed packet length. Although in practice this requires complex synchronisation, a slotted network performs better than an unslotted network, facilitating traffic shaping, load balancing, flow control, and most importantly queuing. Although variable length packets can be handled in an asynchronous manner through techniques such as void filling described in [73], these techniques are very complex to implement, especially within the context of an all-optical implementation as assumed in this work. Because IP packets are variable length packets, this means that the edge routers will have to segment and reassemble packets, and perform grooming. To select the length of the packets, in other words the units used to dimension the buffers with, there is a trade off between the time resolution and the amount of delay provided by the buffer as discussed in [74].

## 3.3 Traffic Models

Because of the self-similar nature of Internet traffic, a Poisson traffic model is not appropriate to model the network traffic [75]. The heavy-tailed file size distribution of application layer files is transformed by the transport and network layer. This manifests as self-similar traffic at the link layer. This means that when viewed at different scales the correlational structure of the traffic remains unchanged. When using a self-similar model to describe long-range dependence, a single parameter is required: self-similarity is characterised by the Hurst parameter, H, which relates linearly to the shape parameter, $\alpha$, of the heavy-tailed file size distribution in the application layer [76],

[77]. 0.5<H<1.0, and as H approaches 1, both self-similarity and long-range dependence increases. 0<α<2, and if α<2 then the distribution has infinite variance, and if α≤1 then the distribution has infinite mean. According to [76] a typical value for α is 1.2.

It has been shown that buffers cannot deliver desirable performance when accommodating self-similar traffic [78],[79]. Traffic shaping at the edge router is one possible solution to mitigate the adverse effects of self-similar traffic in optical packet-switched networks. It is important to note that with self-similarity, traffic aggregation is not a solution because the burstiness of a multiplexed stream is not less than that of its constituent individual streams. Traffic shaping can be done either through the use of an optical packet assembly mechanism that groups packets thus reducing the burstiness [80], or using flow control [81]. Flow control through a protocol such as TCP (Transmission Control Protocol) is able to reduce the degree of self-similarity of network traffic, but is not able to eliminate the self-similar nature of the traffic. This means that it will only decrease the Hurst parameter, H. It is however interesting to note that TCP can also contribute to the self-similarity of network traffic. It is possible to decrease the self-similarity in these cases by using queue management [82], but once again, self-similarity is not eliminated. It is mentioned in [73] that strategies such as multiserver queues, reducing the link load, and implementing multiple-path routing schemes can be used to reduce the degree of self-similarity.

In the following simulations, the simplest heavy-tailed distribution to use is the Pareto distribution. Alleviated self-similarity in a TCP environment with applicable queue management is assumed, where the ON times are more heavy-tailed than the OFF times: $\alpha_{ON} = 1.5$, $\alpha_{OFF} = 1.7$. The Pareto distribution is continuous, and to use this in the discrete simulations, the values obtained are simply rounded up to the next integer.

## 3.4 Architecture

The performance of optical packet switches strongly depends on the architecture and device technology. Important switch parameters include switching time, insertion loss (and loss uniformity), crosstalk, extinction ratio, and polarisation-dependent loss (PDL) [11]. The main limitations in the implementation of electro-optic switches in optical cross-connect architectures are optical loss, noise and crosstalk [13],[83]. The all-optical architectures proposed in this chapter are based on the 1×N all-optical switches and N×1 all-optical buffers as described in [59]. The 1×N switches are implemented in parallel planes, each element handling one packet per timeslot, which means that crosstalk is minimized. The all-optical wavelength converters used in these devices contribute to the regeneration of the signal, thus enhancing the signal quality by improving the extinction ratio as in other interferometric wavelength converters [44],[45]. Hunter et al. [4] show that signal regeneration is imperative for cascading optical cross-connects, and the electro-optic architectures discussed in [4] cannot be cascaded without including additional optical regeneration in the network. This problem is addressed in an architecture employing all-optical switching and buffering devices, both of which have been demonstrated to output packets with high output powers and high contrast ratios.

Single-stage feed-forward and feedback switch architectures are considered in this chapter. All-optical header recognition and all-optical routing is used, and all-optical signal processing is assumed. Because it is an all-optical implementation, the functionality implemented in the cross-connect is limited, and functions such as packet priority or packet sequence integrity are not catered for. Multiple wavelengths for transmission between nodes are assumed, and the internal use of wavelengths is imperative [84].

In [50] a generic node structure was presented for hybrid electro-optic packet-switches that consists of an input interface with synchronisation and header recovery, the switching fabric with the switch control, and an output interface with header

updating and signal regeneration. All three sections consist of both an optical and an electrical part. The all-optical implementation of the generic structure (shown in Figure 1.1 in Chapter 1) differs in that there is only optical signal processing and control, which means that the functional blocks differ slightly. The synchronisation of optical packets can be done using switchable delay lines for the coarse synchronisation, and wavelength converters with dispersive fibre for the fine synchronisation. This complex functionality has not been demonstrated without electronic control [1], [50].
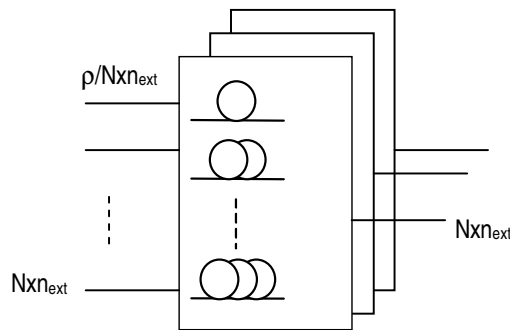


**Figure 3.1 The simulated optical buffers have $Nxn_{ext}$ input channels and 1 output channel. The traffic load on each of the input channels is $\rho/(N{\times}n_{ext})$ for an output buffer because of the uniform distribution to each output from each of the cross-connect inputs. The cross-connect has $N{\times}n_{ext}$ parallel buffers feeding each of the $N{\times}n_{ext}$ output channels. Each buffer has B fibre delay lines and the lengths of these fibres depend on the selected (degenerate or nondegenerate) distribution.**

Each of the $Nxn_{ext}$ output channels in the proposed architecture receives its packets from one of the $Nxn_{ext}$ buffers, but these buffers can all be implemented on a single set of fibres, realised on $n_{int}$ different wavelengths. The implementation of FDLs is bulky and expensive. The other disadvantages of using FDLs for buffering is that they do not have random access capability (except in a specific implementation of a feedback buffer with single packet length FDLs), there is signal degradation in the FDLs from traversing the switch in a feedback architecture, more FDLs are required for a higher

traffic load, and the FDL lengths are dependent on the specific lengths of the packets. In this analysis, the biggest consideration is minimizing the amount of buffering fibre required.

## 3.5 Travelling and Recirculating Buffers

The two architectures that can be used in an optical implementation are a travelling buffer architecture and a recirculating buffer architecture. The results shown in this section were obtained using event-driven simulations of $1 \times (N \times n_{ext})$ buffers as shown in Figure 3.1, with parameters as shown in Table 3.1 (unless otherwise specified). For both architectures, the FDLs support multiple internal wavelengths ($n_{int}$), thereby decreasing the amount of fibre required for contention resolution.

| Symbol | Parameter | Amount |
|---|---|---|
| | Number of events | $10^7$ |
| $n_{ext}$ | Number of transmission wavelengths in the network | 32 |
| $n_{int}$ | Number of internal buffer wavelengths | $N \times n_{ext}$ |
| $N$ | Number of input and output ports (fibres) | 8 |
| | Packet length | 128 Bytes |
| $B$ | Number of FDLs in the buffer | Varies: 8-35 |
| | Traffic type | Poisson and Pareto |
| $\rho$ | Input channel traffic load, $0<\rho<1$ | 0.7 |
| $\alpha_{ON}$ | Pareto ON-burst shape parameter | 1.5 |
| $\alpha_{OFF}$ | Pareto OFF-burst shape parameter | 1.7 |

**Table 3.1: Simulation Parameters**

The assumption is made that there is a uniform distribution of the traffic from all of the $N{\times}n_{ext}$ input channels to each of the $N{\times}n_{ext}$ output channels. This means that each of the $n_{int}$ parallel buffer planes has $N{\times}n_{ext}$ inputs, and only 1 output. The assumption of a uniform traffic distribution in the cross-connect improves the performance considerably, increasing throughput and limiting the buffering required. To obtain a uniform traffic distribution, load balancing would be required, resulting in a very complex switch structure [85]. The details of load balancing are beyond the scope of this dissertation.

When comparing architectures and buffer compositions, a Poisson traffic model was used to simplify the simulation. When obtaining realistic performance values to calculate, for example, the amount of fibre required for an optical buffer, a Pareto distribution was used to take the self-similar nature of network traffic into account.
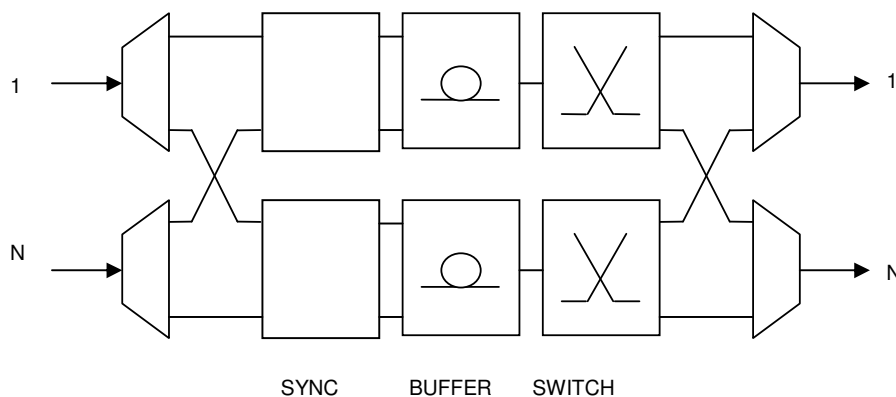


**Figure 3.2 Input travelling buffer architecture with N ($N{\times}n_{ext}$)$\times$1 input buffers and N 1$\times$($N{\times}n_{ext}$) switches. The bottleneck between the buffers and switches cannot be successfully alleviated using wavelengths because no header (destination address) information is available in the buffer.**

## 3.6 Travelling Buffers

In the travelling buffer there are $N \times n_{ext}$ total buffers, which means that at most, $n_{int} = N \times n_{ext}$ to exploit the wavelength domain and not replicate the buffer fibres. For $n_{ext}$ large, as is the case in a WDM implementation, this may be difficult to implement due to the dispersive quality of the fibre over such a wide bandwidth. There are $N \times n_{ext}$ switches, switching the packets from each of the input signals, and these are $1 \times (N \times n_{ext})$ switches, providing an input to each of the $N \times n_{ext}$ buffers. There is a wavelength conversion interface between the switching and buffering functions, placing each of the $N \times n_{ext}$ channels on one of the $n_{int}$ buffer wavelengths.

The $(N \times n_{ext}) \times 1$ all-optical buffer simulated in this chapter differs from an electrical or electro-optic implementation [86] because the header is only analysed in the switch, which means that no header information is known to the buffer. For an output travelling buffer this makes no difference, but for an input travelling buffer as shown in Figure 3.2 this means that there is no intelligent way to distribute the input traffic in the queues (for example, distributing the input traffic on different buffer wavelengths). This also means that head-of-line (HOL) blocking is not relevant [4], as the destinations of the packets are unknown to the buffering function. The reason for the poor input buffer performance in this implementation is because the input traffic load on each of the $N \times n_{ext}$ inputs to the buffer is $\rho$ (not $\rho/(N \times n_{ext})$ as is the case for an output buffer), which means that a traffic load of only $\rho < 1/(N \times n_{ext})$ can be accommodated on a single wavelength. To try and alleviate the bottleneck between the buffer and the switch as shown in Figure 2.2, header information would be required to manage the wavelength dimension.
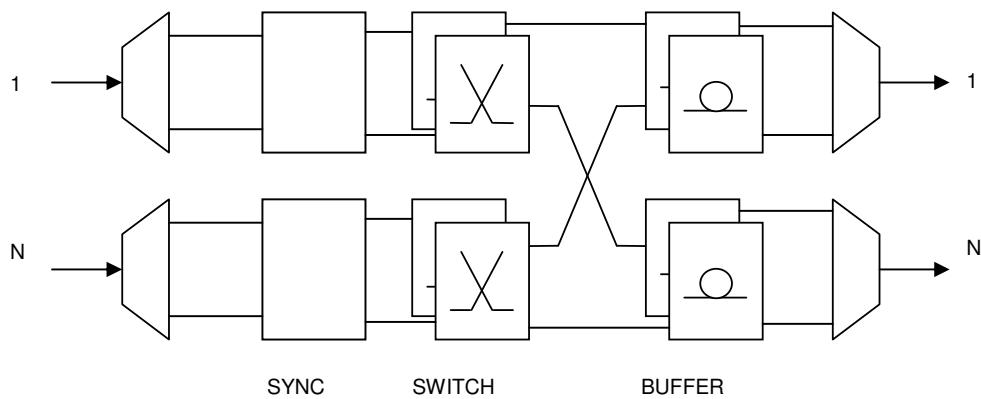
**Figure 3.3 Output travelling buffer architecture with N input and output ports and $n_{ext}$ transmission wavelengths. The cross-connect consists of $N \times n_{ext}$ parallel switching and buffering planes. With the ideal $n_{int} = N \times n_{ext}$ internal buffer wavelengths, the amount of buffer fibre is minimised.**

For this reason, only an output travelling buffer architecture is considered, as shown in Figure 3.3.

In the proposed travelling buffer, the fibre delay line that a packet will be routed to is selected according to the following:

1. Assuming a specific delay line has a duration of $\tau$ [packet lengths], a packet cannot be routed to this FDL if there is already another packet in the buffer scheduled to be output in $\tau$ timeslots on the same output port.

2. Of the available delay lines, the shortest one is chosen.

This means that fixed length delay lines cannot be used as 1. then determines that only 1 packet can enter the buffer during any given timeslot to prevent packet contention at the output of the buffer. The selection of the number and the length of the fibre delay lines is equivalent to defining the entry points to a single buffer. The length of this single buffer is the length of the longest FDL in the buffer, and is referred to as the *buffer depth*.

Travelling buffers have two main drawbacks. One is that the PLR performance is far inferior to recirculating buffers for the same amount of fibre used for the FDLs, and the other, perhaps more important, problem is that the algorithm to write packets to the buffer is very complex to implement in an all-optical approach. This is because the entire content of the buffer needs to be considered to prevent contention at each output of the buffers.

To show the effect of the selection of the fibre distribution, the travelling buffer has been simulated with two different distributions:

1. <u>Degenerate</u>: increasing uniformly

2. <u>Nondegenerate</u>: increasing nonuniformly, often implemented with an exponential increase in fibre lengths [87].

## 3.7 Recirculating Buffers

The feedback architecture is shown in Figure 3.4. Depending on the selected FDL lengths, these buffers can provide the capability of random access, whereas the travelling buffer storage times are predetermined. A larger switch fabric is required as B switch input and output ports are required for the buffering. The number of wavelengths implemented in the buffer is $n_{int}$, and the number of parallel physical buffers is denoted by $F_{buf}$. When $n_{int} = N \times n_{ext}$, $F_{buf} = 1$ and the amount of fibre used is minimised. The implementation requires wavelength converters at each of the interfaces between the switch fabric and the buffering.

Apart from the reuse of the buffering fibre, recirculating buffers provide two distinct advantages:

*1. Simple Algorithm*

First, for the recirculating buffer, the algorithm to select a FDL in the buffer is much simpler than for a travelling buffer where the entire content of the buffer needs to be known. Only the positions at the end of each FDL need to be considered

in order to see if there will be an open position at the beginning of the FDL in the next time slot. It is necessary to be able to discern the amount of delay that a packet has experienced if maximum delay is used as the output packet selection criteria. It is however not necessary to know what the entire content of the buffer is thus decreasing the required optical signal processing for the buffer algorithm. In terms of the all-optical implementation, recirculating buffers provide a more feasible algorithm that can be implemented using, for example, a laser neural network [14], and the discrimination of packet delays in the FDLs could, for example, be done using wavelength conversion and demultiplexers as illustrated by the all-optical variable optical delay circuits described in [48] and [41].
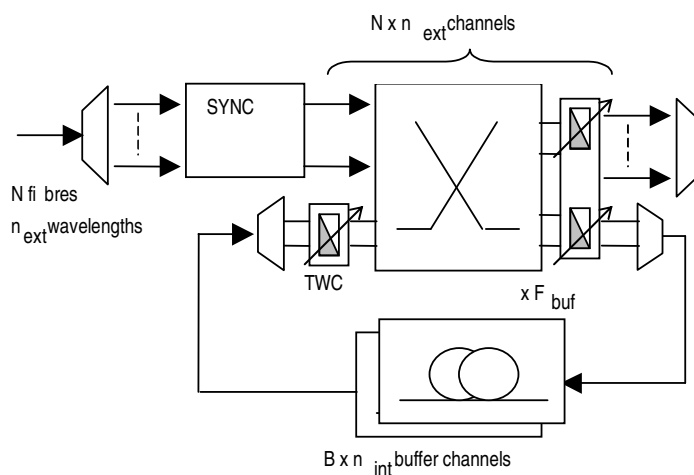


**Figure 3.4 Recirculating buffer where the cross-connect consists of ($N \times n_{ext}$+B) switches with tunable wavelength converters (TWC) on each of the N output ports as well as on the B buffer ports.**

## *2. Fibre Utilisation*

Secondly, all of the fibre in the recirculating buffer FDLs can be used at any given time, in contrast to the inefficient fibre utilisation in travelling buffers, because the condition of not writing a packet to a FDL of length $\tau$ [packet lengths] if there is already another packet in the buffer scheduled to exit in $\tau$ time slots, is not applicable.

A Poisson traffic model can be used to facilitate the comparison between, for example, different buffer configurations. Figure 3.5 shows the performance difference between different FDL configurations for both an output travelling buffer configuration, and a recirculating buffer configuration. In both travelling and recirculating buffer architectures, the nondegenerate distributions have superior performance relative to the total amount of fibre as well as the total number of FDLs, but this is also at the cost of an increased average delay as the buffer depths are, for example, *degenerate*: 20, *nondegenerate3*: 31 and *nondegenerate5*: 41.

Of course the maximum delays experienced in the recirculating buffer far exceed these as packets experience delays equal to integer multiples of the FDL lengths, with an average packet delay of 300 time slots for a degenerate or nondegenerate feedback architecture with an average of 110 packet positions in the fibre, versus only about 5 time slots for a travelling buffer. This is shown in Figure 3.6. In electro-optical applications, the maximum buffering time in recirculating buffering is limited because of the amplified spontaneous emission (ASE) noise, crosstalk and signal-fluctuation. But in the all-optical switch and buffer there is not significant loss or crosstalk in the switch or in the buffering implementation, and considerably less amplification is required, resulting in a superior signal quality.

**a) Travelling Buffer Configurations**



**b) Recirculating Buffer Configurations**



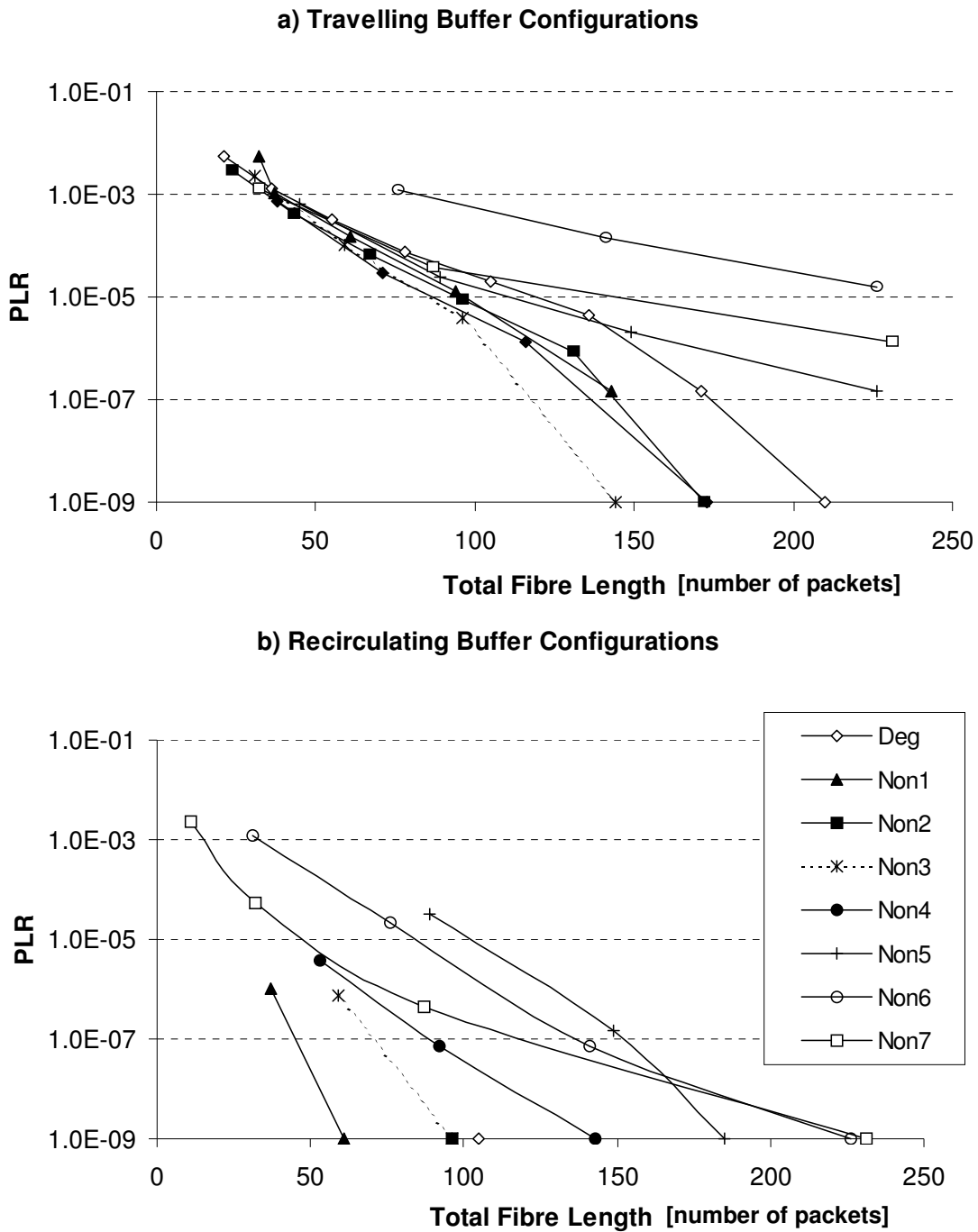**Figure 3.5 Figures a) and b) show the packet loss ratio for an output travelling buffer and a recirculating buffer, respectively. The performance is measured versus the total amount of fibre required for buffering, measured in the number of packets buffered in the fibre. It is clear that recirculating buffers outperform travelling buffers. For both, nondegenerate configurations outperform a degenerate buffer configuration.**
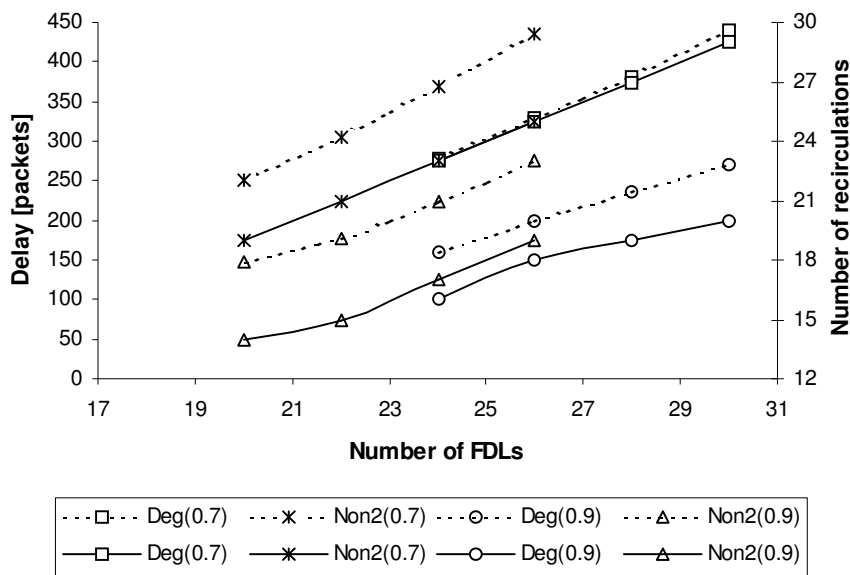
**Figure 3.6** **The dotted lines show the average delay per packet in the different FDL distributions. On the second axis, the solid lines show the average number of recirculations.**

## 3.8 Buffer Performance Under Self-Similar Traffic

Figure 3.7 c) shows the performance of two different recirculating buffer distributions, but using a realistic self-similar traffic model. Low PLRs are not attainable. The dilemma of buffering self-similar traffic satisfactorily is not limited to an optical implementation, and the probability of ATM cell loss does not decrease as the electronic buffer size increases either, due to the nature of the burstiness of self-similar traffic where the bursts have infinite variance [88]. For the queuing in ATM switches, it has been shown that there is a lower bound on the buffer overflow probability, with the overflow probability being around $10^{-4}$ for an electronic buffer of size $10^4$ [89]. In a shared-buffer improving switch throughput, the loss probability with a high traffic load ($\rho = 0.9$) is between $10^{-1}$ and $10^{-2}$, with acceptably low loss probabilities only achievable with $\rho < 0.5$ [90].
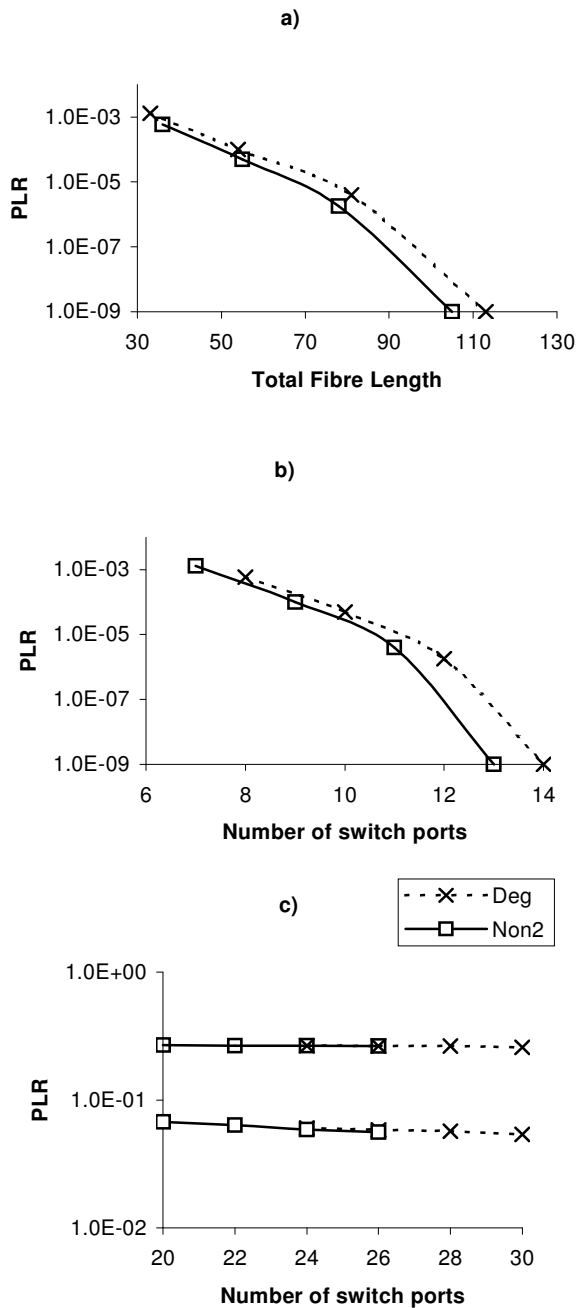
**Figure 3.7 In recirculating buffers an important performance measurement is the number of switch ports required for buffering. Each FDL requires the use of a port. The performance of the optical buffer with self-similar traffic c) is distinctly worse than the buffers simulated using Poisson traffic a) and b), even at a lower load. Figure c) shows results with both ρ = 0.7 and ρ = 0.9. It is also clear that buffer performance when analysed using a self-similar traffic model is not significantly influenced by the buffer configuration.**

The architecture used in the recirculating simulations is similar to the one described in Yao et al. [91], which provides an extensive analysis of contention resolution through various combinations of space, wavelength and time domain contention resolution. In Yao et al. [91] it is shown that a load threshold is observed under self-similar traffic conditions, and once the threshold is reached, neither deflection in the time nor the space domain is effective. A PLR of only 0.01 is attainable, even when the wavelength domain is also exploited (by providing wavelength conversion to any of the 16 output wavelengths), with a traffic load of 0.6.

## 3.9 Overflow buffering

The use of a self-similar traffic model results in unacceptably high PLRs. This can be addressed by implementing an overflow algorithm in the buffer, by routing overflow packets to available wavelengths within the buffer. Figure 2.8 compares the performance of a degenerate recirculating configuration with and without internal cross-connect overflow buffering ($n_{int} = N \times n_{ext} = 16$).
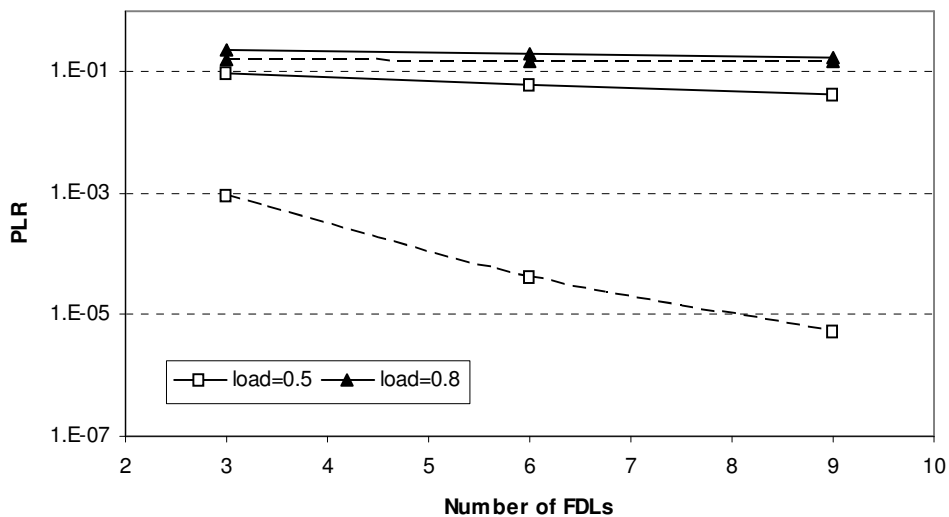


**Figure 3.8: Buffer performance can be significantly improved using overflow buffering. Solid line: without overflow, dotted line: with overflow.**

To achieve, for example, a PLR of 0.01 with ρ=0.6 with the degenerate distribution used to obtain the results in Figure 2.8, $\Sigma_i^{35}i = 630$ packet positions are required in the buffer. This translates to 12.9km of fibre at a data rate of 10Gbit/s and using a packet length of 128 Bytes. When buffer overflow is implemented with this buffer, the PLR can be brought down to $10^{-4}$.

## 3.10 Conclusion

Hybrid electro-optical cross-connect architectures are not applicable to all-optical implementations for two reasons. In all-optical routing nodes, the functionality is kept very simple as the signal processing is done in the optical domain, and thus functions such as packet priorities and packet sequence integrity are addressed at edge nodes. Furthermore, the all-optical switching and buffering devices differ from the electro-optical approach in that the control (packet routing) is in the optical domain, the header recognition is all-optical, and signal regeneration results from the implementation of wavelength conversion in the all-optical devices [44].

Of the two architectural approaches to an all-optical cross-connect, recirculating buffering provides a superior solution to travelling buffers when using the packet loss ratio as the metric. The main drawback of recirculating buffering in an electro-optic implementation is the loss resulting from traversing the switch multiple times. To compensate for this loss, amplifiers are used in the feedback loop resulting in ASE noise in the signal as it traverses the buffer multiple times. Furthermore, switch crosstalk can accumulate with multiple traversals of the signal. In electro-optic switches, feed-forward switches are preferred because of the limited attenuation in the switch fabric thus reducing the dynamic range of the signals that must be handled [1].

Utilising an all-optical switch fabric that consists of parallel 1×N all-optical switches, however, alleviates the influence of crosstalk as each individual switch has a single independent output packet per timeslot. Furthermore, implementing wavelength conversion within the switching and buffering functional units results in very good

signal quality because of the signal regeneration inherent in the all-optical architecture's building blocks [59]. An all-optical implementation of optical buffering could result in good signal quality with a feedback architecture that will minimise the required buffer fibre.

The simulations described in this chapter show that the performance of the selected architecture depends mostly on the buffer configuration and the traffic load. The self-similar nature of realistic traffic makes it very challenging to buffer efficiently, and the use of a technique such as overflow buffering is required to exploit the wavelength domain properly.

For a realistically over-provisioned network with, for example, a 50% traffic load, a total amount of fibre of around 10km would be required to keep the PLR low depending on:

- The length of the packets: IP packets can exceed 1kB, whereas the lengths in this chapter were calculated with packets of 128B lengths, and

- The implementation of an algorithm to fully utilise the available buffer space in the wavelength domain, such as overflow buffering described in this chapter.

# CHAPTER 4 SIZING ROUTER BUFFERS: TRANSMISSION CONTROL PROTOCOL (TCP) DYNAMICS AND THROUGHPUT OF CONGESTED LINKS

## 4.1 Introduction

The buffering described up to now has been only for congestion resolution related to switching in the cross-connect. It has been assumed that the capacity of the incoming and outgoing links are the same, and that this does not contribute to the congestion at the cross-connect's output ports. Buffer dimensioning is however generally related to congested links in the network. Generally core router buffers are dimensioned according to the dependence of TCP's congestion control algorithm on buffer sizes [92].

This chapter is aimed at relating buffer sizing claims based on TCP dynamics to actually physical sizes of fibre delay lines. Furthermore, it is confirmed that small buffers are required when dimensioning for throughput. The question, however, remains whether throughput is the best metric to use in a typically over-provisioned network.

## 4.2 TCP Congestion Control and Buffer Dimensioning

TCP works with a feedback system: after sending packets, the sender waits for an acknowledgement from the receiver. TCP relies on a specific window size, which defines how many acknowledgements can be outstanding at a specific time. When congestion occurs and packets are lost, the result is that TCP reacts to the lost packets by reducing the window size and adapting the speed at which data is sent accordingly. What this effectively means is that TCP is designed to fill up any buffer, as the buffers in the network play an integral part in the dynamics of TCP's congestion control algorithm.

According to this scenario, buffers are usually dimensioned in order to keep congested links busy 100% of the time. As traffic is bursty, the buffers are used to keep feeding the output link in times when there are no input packets. For applications dependent on TCP (and 95% of Internet traffic comes from TCP sources), latency has a more adverse effect than packet loss. For this reason it is important to analyse buffer performance in terms of throughput instead of packet loss ratio.

Jitter refers to a variation in latency which complicates matters because consistent latency could be compensated for. Jitter depends on traffic characteristics, the number of nodes in the network and the speed of the nodes [93]. Jitter buffers can be used to smooth out changes in arrival times, but are usually only able to compensate for small changes in latency. Clock recovery and synchronisation are required for this type of functionality [94] and are beyond the scope of this dissertation.

Because buffer dimensioning relates to the dynamics of TCP, the general rule of thumb has been to size buffers according to the product of the average roundtrip time $\overline{RTT}$ (typically 50 – 200ms) and the link capacity $C$ of the congested link [1]. This dimensioning has been based on the saw tooth shape of transmitted traffic from a TCP source that responds to dropped packets by slowing down transmission.

This rule has recently been challenged [93], and it has been argued that the required buffer size to optimise throughput to the congested link also relates to the number of TCP flows, $n$, transmitted through the node as follows:

$$B = \frac{\overline{RTT}C}{\sqrt{n}}$$

With thousands of TCP links transmitted concurrently this brings down the required buffer sizes considerably. With an average $\overline{RTT}$ of 100ms, a link capacity of 10Gb/s and 10 000 TCP flows, this approximation still translates to around 200km of optical fibre required for buffering (more, considering that neither recirculating nor travelling buffers consist of a single fibre delay line).

## 4.3 Buffer Dimensioning According to Throughput

In the context of optical networks it is important to note that the core network is typically over-provisioned carrying loads in the range of 30%, and dimensioning buffers to optimise throughput does not necessarily make sense. Furthermore, the access links also typically have smaller capacities than the core links, making congestion at the output of the core nodes unlikely. Figure 4.1 shows how throughput will always be low if the access links have much smaller capacities than the core link.
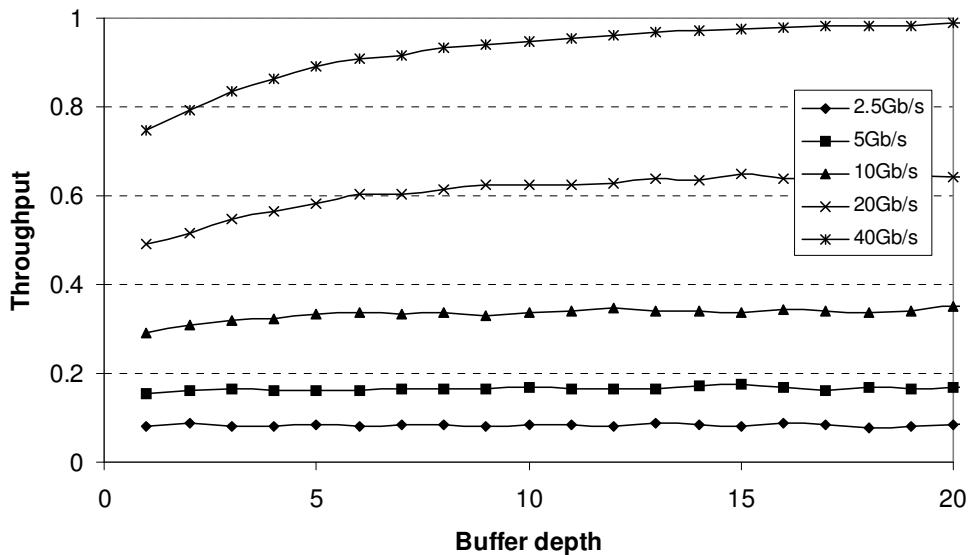


**Figure 4.1. Throughput with varying access link capacities. The core link in this case has a capacity of 40Gb/s.**

For these over-provisioned networks the question arises whether packet-switching is necessary at all, or whether a circuit-switched technology such as TDM which also provides the added benefit of QoS may be more suitable. This emphasises that different technologies may be better suited to different networks or to different parts of a network, and there is no simple, clear answer to this question. However, TDM and optical packet-switching are not necessarily mutually exclusive, but can be used as complimentary technologies under certain circumstances [96]. The fact remains though that TDM is unable to efficiently accommodate bursty data applications, and that QoS

can be facilitated in an optical packet-switched network through protocols such as MPLS.

In the case of congestion dimensioning buffers for throughput does start to become an issue. Taking this into account, together with the traffic characteristics of multiple TCP flows, it has been argued that quite small buffers are required, and that the buffer dimensioning is in fact not dependent on TCP dynamics [96],[98]. In [93] the heavy-tailed characteristics of TCP traffic are described but in [98] it is shown that limited capacity on the access network has the effect of smoothing out the traffic. Either way, Figure 4.2 shows that acceptable throughput on a congested network ($\rho \approx 1$) can be achieved with small buffers, irrespective of how much the access network manages to smooth out the traffic.

In [98], the number of TCP flows in the link are increased to describe the effect of congestion on the networks. Once again assuming an average $\overline{RTT}$ of 100ms, a maximum window size of 32 packets and that these are 1000 byte packets, each flow contributes approximately 2.5Mb/s of traffic to a link.
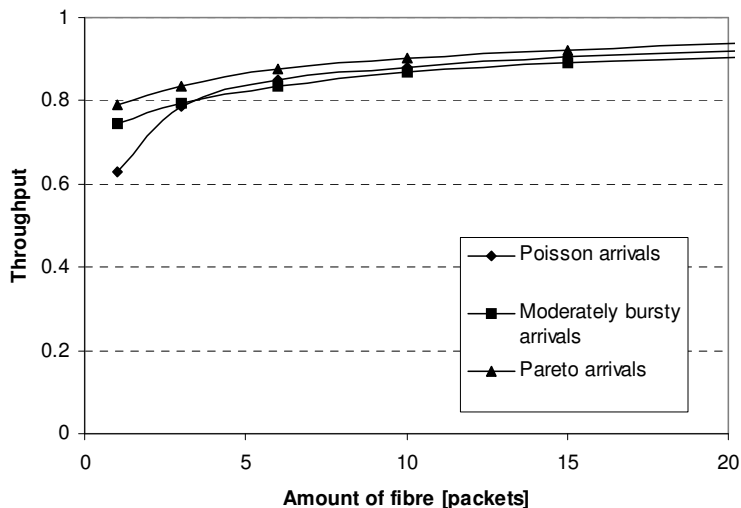


**Figure 4.2. Throughput of different traffic types assuming a congested link with $\rho \approx 1$. Slow access links display smoothed out traffic characteristics in comparison to normal TCP which is heavy-tailed.**

In a similar simulation as the one performed in [98], but not taking into account TCP dynamics, only using an event-driven simulation of an optical cross-connect, comparable results are shown in Figure 3.3 where the throughput of the bottleneck link is shown as a function of the buffer size for various numbers of flows.
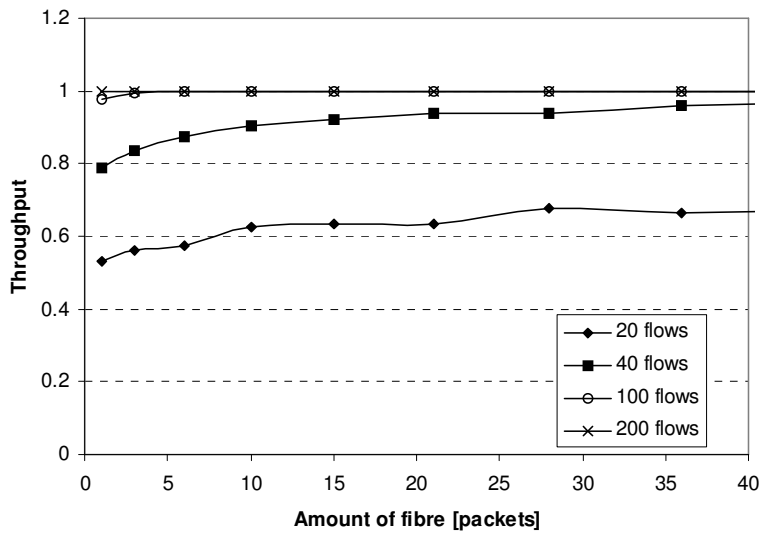


**Figure 4.3. Bottleneck link utilisation as a function of the amount of fibre required for buffering.**

One important issue to note is that the space needed for buffering cannot simply be translated into "packets" from the required memory computed in, for example, MB. Note that the X-axis in Figure 4.3 refers to the amount of fibre required for the buffering, not the number of packets that the buffer needs to accommodate. This is because a travelling buffer was simulated, consisting of multiple fibres according to a degenerate distribution. I.e., a required buffer space of 10 packets translates into 10 fibres with a total fibre length of 55 packets. With a link capacity of 10Gb/s and assuming 1000 byte packets as in [98], this translates to 8.8km of fibre.

**Figure 4.4. Throughput as a function of the number of flows for various values of the offered load to the system.**

A further analysis in [98] is of the throughput of a node as a function of the number of flows for various values of the offered load in the system. Fixing the buffer size to 10 packets (thus, in reality, sufficient fibre to hold 55 packets in a travelling buffer) and increasing the offered load, the through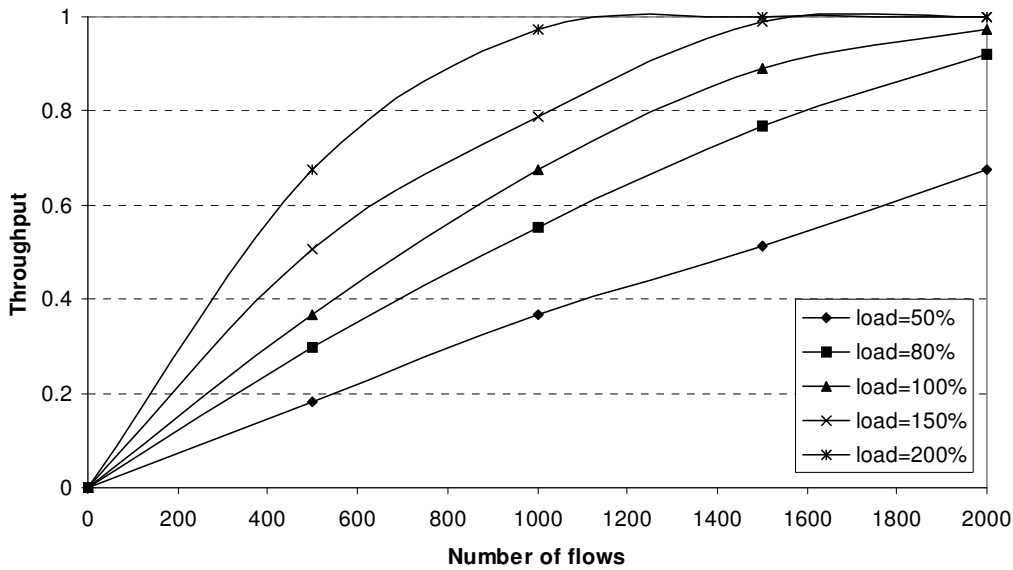put increases as the offered load increases beyond 100%. This shows that even when a network is under-provisioned, small buffers can achieve reasonable throughput. The results in Figure 4.4 are comparable to those in [98] even though TCP dynamics were not taken into account beyond the contribution of the multiple TCP flows and the heavy-tailed nature of the flows.

## 4.4 Conclusions

The results shown in this chapter show that if the metric used to analyse buffer performance is the throughput of the network, that quite small buffers can be sufficient: in accordance to the results in [98] where TCP dynamics were also taken into account, it has been shown that buffer sizes of 10 packets can provide acceptable throughput (effectively a bit less than 10km of fibre, although this depends on the packet length). It is assumed that the results are comparable to those in [98] despite a significantly

different approach because the buffer dimensioning should in fact not depend too much on the TCP dynamics, as, in fact, proposed in [98].

The question becomes which metric to use for buffer dimensioning. In a network where capacity is definitely simpler to realise and cheaper than optical buffering, it would seem as if dimensioning for link utilisation is not really the issue. On the other hand, dimensioning for a reduced packet loss as described in the previous chapter seems to make sense as the results shown are for links that are not congested, as would be the case for an over-provisioned network. What has become clear from researching dimensioning issues of the cross-connects, however, is that the effects of TCP cannot be ignored. *The network has to be designed according to the most important application of the network*. This might not imply sizing the buffers according to the saw tooth action of the buffer control algorithm of TCP, but it seems as if it at least implies that the heavy-tailed traffic characteristics of TCP should to a certain degree be taken into account when analysing the traffic flows through the network.

**CHAPTER 5 AN OPTICAL THRESHOLD FUNCTION BASED ON POLARISATION ROTATION IN A SINGLE SEMICONDUCTOR OPTICAL AMPLIFIER**

## 5.1 Introduction

Optical threshold functions are a basic building block for optical signal processing as they provide an all-optical way of implementing simple decisions in various applications. In [53] an optical threshold function is described where a laser diode was subjected to external feedback and light injection.  This setup suffered from instability due to a free space optics implementation and frequency dependence. In [14] a fibre optic approach based on coupled ring lasers is introduced. The threshold function can be extended to form an arbiter using a laser neural network, used for all-optical buffering in [100][99]. One disadvantage of this coupled ring laser design is that it uses two active elements, semiconductor optical amplifiers (SOAs), hence increasing the footprint of the setup and its power consumption. Another limitation is that the injected optical power must be sufficient (e.g. 8.2dBm as described in [100]) to suppress one lasing mode before the other can start lasing.

In this chapter we demonstrate a novel threshold function that relies on a single SOA, and switching between the two states requires smaller optical powers, resulting in application flexibility.  The threshold function uses the principle of nonlinear polarization rotation in an SOA that results from the device birefringence due to the difference between the amplifier TE and TM mode effective indices [101]. The advantage of using this effect in an SOA is that a small index difference can cause a large relative phase shift. TE and TM modes show different gain response because they couple to different hole reservoirs [66]. As the optical power in the SOA increases, the saturation-induced phase difference alters the intensity of the light that is output from the SOA.

This chapter is based on the results in [99]:

## 5.2 Operating Principle

When an optical signal propagates through a semiconductor optical amplifier, the TE and TM components propagate independently, although the two modes are indirectly coupled through the carriers in the SOA. As in [66] we use that the TE and TM polarizations couple the electrons in the conduction band with two distinct reservoirs of holes.
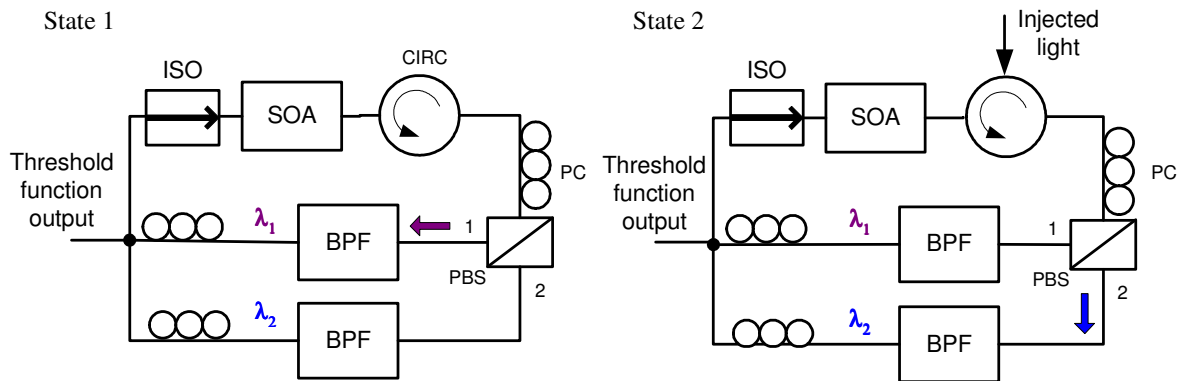


**Figure 5.1 Experimental setup of the threshold function. PC: polarization controller, SOA: semiconductor optical amplifier, CIRC: circulator, BPF: band pass filter, PBS: polarization beam splitter, ISO: isolator.**
**State 1: the system is adjusted to allow most of the light to exit from port 1 of the PBS so that $\lambda_1$ is lasing. State 2: Externally injected light will result in polarization rotation due to birefringence, and $\lambda_2$ will start to lase.**

Figure 5.1 shows the experimental setup that is based on the principle that the TE and TM modes can be treated independently in a coupled ring laser that is built using an SOA. The two ring lasers are coupled through the SOA, so that a single gain element is shared by both lasers. The two laser cavities are then separated through the polarization beam splitter (PBS), and the resulting TE and TM modes pass through band pass filters with different wavelengths to facilitate distinction between the two modes. The two modes are coupled together again with a 2×2 coupler that provides the output of the threshold function as well as completing the ring laser through an isolator.

The system operates as follows. The two coupled ring lasers are separated by the PBS so that one laser works with the TE mode, and the other with the TM mode, as output by the two PBS ports. Optical band pass filters are placed in each cavity and act as wavelength selective elements so that each cavity lases at a different wavelength. Three polarization controllers are placed in the cavities. The role of the first polarization controller is to align the SOA output light with the PBS and thus to separate the two cavities. The role of the other two polarization controllers is to align the polarization of the SOA input light with the SOA layers. This determines the working point of the system.

The system can have two states. In state 1, the cavity operating at wavelength $\lambda_1$ (cavity 1) is lasing while the cavity operating at $\lambda_2$ (cavity 2) is suppressed. In this case the polarization controllers are aligned such that maximum feedback is achieved for cavity 1 and that the feedback for cavity 2 is very small (although still slightly above threshold). If additional light is injected via the circulator, the control light introduces additional polarization rotation in the SOA, causing the feedback in cavity 1 to reduce and the feedback in cavity 2 to increase. If the power in cavity 1 has dropped sufficiently below threshold, cavity 1 switches off and cavity 2 switches on. This situation remains until injection of the external light has stopped.

## 5.3 Nonlinear Polarization Rotation

The model for the threshold function is based on the SOA model introduced in [66]. This model is based on the fact that purely TE and TM polarized modes propagate independently through the SOA. The modes are indirectly coupled via the carriers. The change in phase, $\theta$, between the TE and the TM modes due to the polarization rotation results in a change in photon numbers associated with the TE and the TM modes. The phase difference is given by:

$$\theta = \phi^{TE} - \phi^{TM} = \frac{1}{2}(\frac{\alpha^{TE}\Gamma^{TE}g^{TE}}{v_g^{TE}} - \frac{\alpha^{TM}\Gamma^{TM}g^{TM}}{v_g^{TM}})L$$

(1)

Where the linearized gain $g^{TE/TM}$ for each mode is given by:

$$g^{TE} = \frac{\xi^{TE}(2n_x + n_y - N_0)}{1 + \varepsilon(S^{TE} + S_{inj}^{TE})}$$

$$g^{TM} = \frac{\xi^{TM}(2n_y + n_x - N_0)}{1 + \varepsilon(S^{TM} + S_{inj}^{TM})}$$

(2)

Where $S_{inj} = S_{inj}^{TE} + S_{inj}^{TM}$ because the injected light consist of both a TE and a TM component, $n_x$ and $n_y$ refer to the hole reservoirs associated with the TE and TM modes respectively, $\xi^{TE/TM}$ are the gain coefficients for each mode, $L$ is the SOA length, $\Gamma^{TE/TM}$ are the confinement factors for both modes and $N_0$ is the carrier number at transparency. The rate equations for $n_x$ and $n_y$ are given by:

$$\frac{\partial n_x}{\partial t} = -\frac{n_x - \overline{n_x}}{T} - g^{TE}\Gamma^{TE}S^{TE} - g^{TE}\Gamma^{TE}S_{inj}^{TE}$$

$$\frac{\partial n_y}{\partial t} = -\frac{n_y - \overline{n_y}}{T} - g^{TM}\Gamma^{TM}S^{TM} - g^{TM}\Gamma^{TM}S_{inj}^{TM}$$

(3)

$\overline{n}_x$ and $\overline{n}_y$ are the respective equilibrium values given by:

$$\overline{n}_x = \frac{\overline{n}f}{1 + f}$$

$$\overline{n}_y = \frac{\overline{n}}{1 + f}$$

(4)

Where

$$\overline{n} = \frac{I}{e}T$$

(5)

In equation (5), $I$ is the injection current, $e$ is the elementary charge unit and $T$ is the electron-hole recombination time. In the case of an isotropic bulk, the transitions will be symmetric. But for a bulk medium experiencing tensile strain, one of the two modes may be favoured. (Other causes of polarisation dependence, such as waveguide asymmetry and anisotropic gain in quantum wells [102], are beyond the scope of this analysis.) The population imbalance factor, $f$, is used to model this type of asymmetry. Due to tensile strain the mixture of light and heavy holes in the bulk medium [102] can be such that TM transitions are favoured over TE transitions [66]. Finally, the rate-equations for photon numbers of the TE and TM modes are:

$$\frac{\partial S^{TE}}{\partial t} = (\Gamma^{TE} g^{TE} - \alpha_{cav}^{TE} \cos(\theta + \delta^{TE})) S^{TE}$$

$$\frac{\partial S^{TM}}{\partial t} = (\Gamma^{TM} g^{TM} - \alpha_{cav}^{TM} \sin(\theta + \delta^{TM})) S^{TM}$$

$$(6)$$

Equation (6) includes the loss for both TE and TM components in the cavities of the ring lasers, $\alpha_{cav}^{TE}$ and $\alpha_{cav}^{TM}$, as well as the phase for both components, $\delta^{TE}$ and $\delta^{TM}$ (determined by the polarization controllers as shown in Figure 5.1).

The photon number $S^{TE/TM}$, and the output optical power from the threshold function, $P^{TE/TM}$, are related through the following equation:

$$S^{TE/TM} = \frac{P^{TE/TM}}{\hbar \omega} \frac{L}{v_g}$$

$$(7)$$

Here $v_g$ is the group velocity of the light in the SOA, $\omega$ is the frequency of the light and $\hbar$ is Planck's constant (we use $\hbar \omega = 0.8$ eV).

The values for the parameters used in the simulations can be found in Table 5.1.

| Symbol | Parameter | Value |
|---|---|---|
| $\alpha^{TE}$, $\alpha^{TM}$ | Phase modulation coefficients | 5, 5 |
| $\Gamma^{TE}$, $\Gamma^{TM}$ | Confinement factor | 0.2, 0.14 |
| $v_g$ | Group velocity | 100 µm/ps |
| $L$ | SOA length | 800µm |
| $\xi^{TE}$ | TE Gain coefficient | $7.0\times10\text{-}9$ ps$^{-1}$ |
| $\xi^{TM}$ | TM Gain coefficient | $6.4\times10\text{-}9$ ps$^{-1}$ |
| $N_0$ | Optical transition state number | $10^8$ |
| $T$ | Electron-hole recombination time | 500 ps |
| $f$ | Hole population imbalance factor | 0.5 |
| $I$ | Electric current | 160 mA |
| $e$ | Electric charge unit | $1.6\times10^{-19}$C |
| $\tau_e$ | Carrier lifetime | 1 ns |
| $\alpha_{cav}^{TE}, \alpha_{cav}^{TM}$ | Cavity losses for the ring laser | 0.9 |
| $\varepsilon$ | Gain saturation | $10^{-7}$ |

**Table 5.1. Parameter Definitions**

## 5.4 Experiment and Results

In the setup shown in Figure 5.1, a commercially available bulk SOA with an 800µm active region was used. The filters used were Fabry-Perot filters with a 3 dB bandwidth of 0.2nm, and they were set to the following wavelengths: $\lambda_1$ = 1552.55 and $\lambda_2$ = 1543.55 nm. In this SOA the gain difference between the two wavelengths used is less than 2dB. At the bias current used, the polarization gain difference is negligible. The band pass filters ensure that the two ring lasers operate at two distinct wavelengths. For the demonstration, the threshold function was set to lase at $\lambda_1$. When the external optical signal was injected into the SOA, polarization rotation resulted in a phase change between the TE and the TM modes, causing the transmittance through the PBS in cavity 1 to reduce and in cavity 2 to increase. This results in a reduced carrier number in cavity 1 and an increased carrier number in cavity 2.
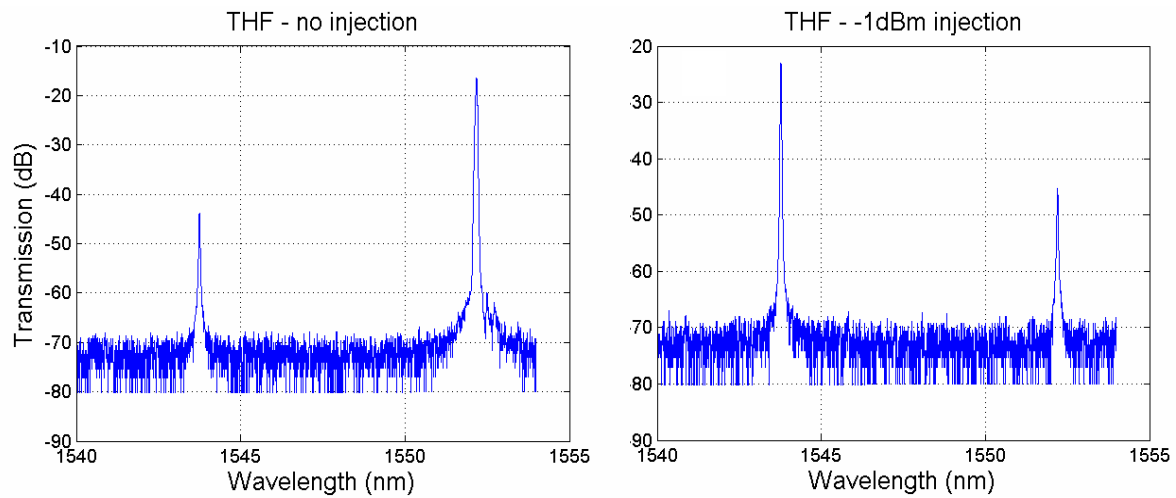
**Figure 5.2 Spectra of the two states of the threshold function. a) $\lambda_1$ = 1552.55nm is dominant until b) -1dBm of external optical power is injected, after which $\lambda_2$ = 1543.55nm becomes the dominant wavelength. In each case a contrast ratio of approximately 20dB can be achieved.**

The optical spectra are shown in Figure 5.2. It is visible that if no external light is injected in the threshold function, cavity 1 dominates over cavity 2. If. -1 dBm of external light ($\lambda$= 1555.7 nm) is injected into the laser, the system changes state and cavity 2 dominates over cavity 1. The contrast ratio between both states is approximately 20 dB.

Figure 5.2 shows the optical power in both cavities directly before switching and after switching with a small control signal. Figure 5.3 shows the experimental results where the injected control signal is increased gradually until it results in gain quenching of the two threshold function wavelengths. In Figure 5.3 it can be seen that the cavity that is not dominant after switching is suppressed to below lasing threshold due to the gain quenching caused by the increasing injected control signal. This results in an extinction ratio between 15 and 20dB.
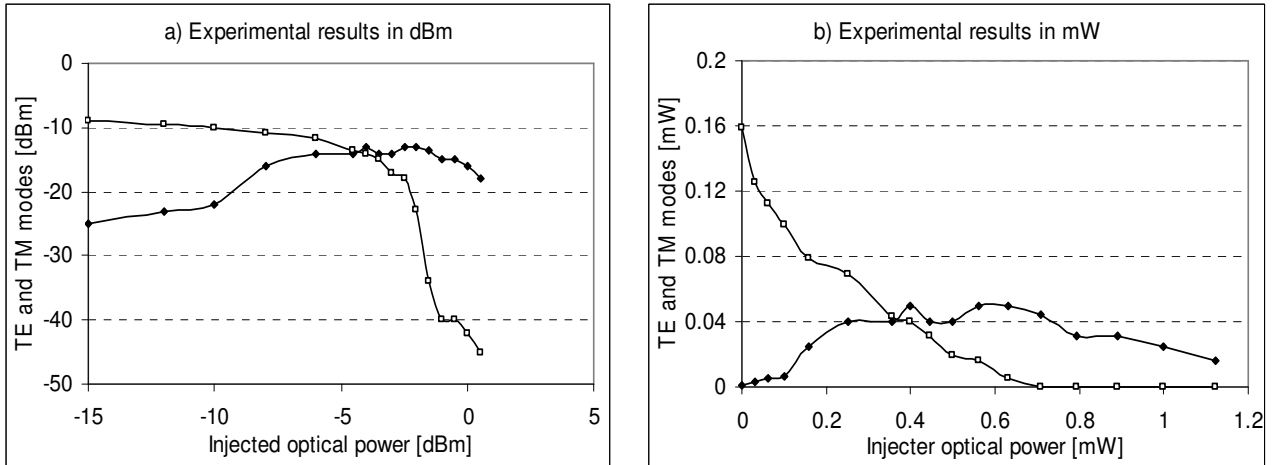
**Figure 5.3 Measured results shown in dBm and mW. Here switching is shown from the TM mode to the TE mode, with an extinction ratio between 15 and 20dB. Switching is achieved with an injected optical power of approximately -4dBm.**

## 5.5 Theoretical analysis

Solving equations (1) to (7) using the parameters as described in Table 5.1 yields results as shown in Figure 5.4. Differences between the analytical and measured results are possibly due to the phases in equation (6) that are unknown and need to be estimated, loss factors in the experimental setup such as connector and transmission loss to the measurement equipment, and loss and polarization change of the injected light. Errors inherent to the numerical solution of nonlinear equations that have multiple solutions can also play a role. Another factor influencing the measured results is the change in polarization over time, and may be compensated for by using polarization maintaining fibre in the experimental setup.

It was clear from both the experiments and the analysis that the system is very sensitive to any changes in parameters, especially the phase, $\delta^{TE}$ and $\delta^{TM}$, as shown in equation (6). The results shown in Figure 5.4 were obtained using phases $\delta^{TE} = \delta^{TM} = 1.1\pi$ obtained through trial and error.
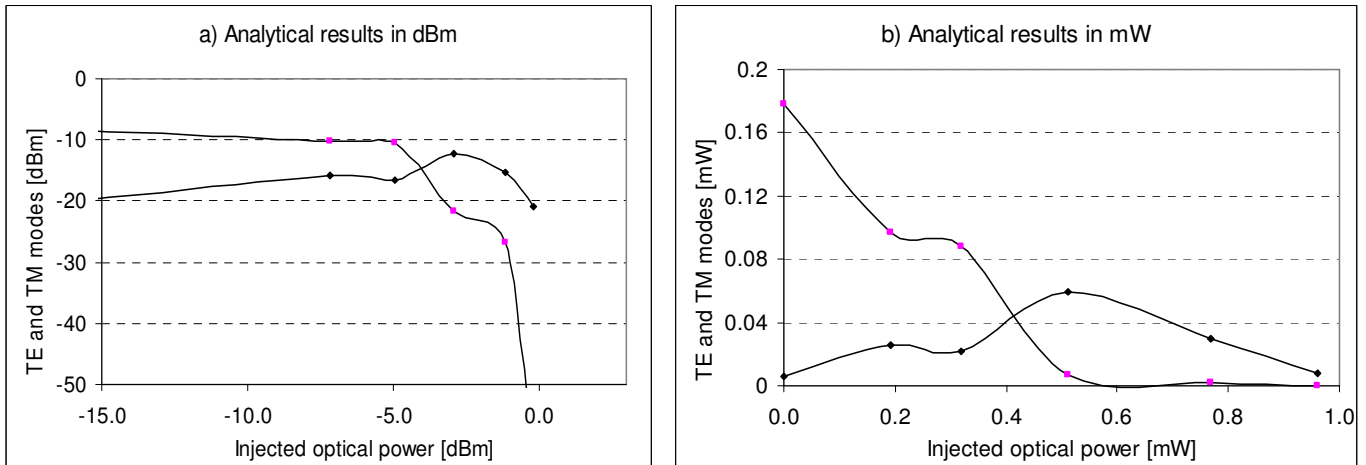
**Figure 5.4 Analytical results are similar to the measured results shown in Figure 5.3. These results were obtained using $\delta^{TE} = \delta^{TM} = 1.1\pi$, taking into account the loss of the injected light before reaching the threshold function, assuming the injected light consists of 90% TE and 10% TM modes, and assuming a cavity loss of 0.9.**

## 5.6 Conclusions

In this chapter a novel optical threshold function that can be used in optical signal processing has been proposed. It functions due to an induced modification of the birefringence of a semiconductor optical amplifier caused by an externally injected optical control signal. The major advantage of the configuration is that a single active element is used.

An important advantage of implementing an all-optical threshold function using polarization rotation in a SOA is that it does not require a significant rotation to affect a change in output. The reason for this is that the laser threshold curve is very steep which means that a small change in polarization will lead to a large difference in output optical power. The measured contrast ratio between the output states was in the order of 20 dB. It is possible to switch the threshold function with a control signal of less than 0dBm, which is significantly lower than 8dBm, as described for the threshold function used in [66]. As the injected power increases, the two signals in the threshold function are quenched due to the injected light.

The measured results were supported by the simulation results that are based on the SOA rate equations. The model used is based on the fact that the TE and TM components of the light correspond to the two principle axes of the SOA, and that the two modes are indirectly coupled through the carriers. Differences between the measured results and the simulated results are mainly due the change of polarization in the experimental setup over time and the phases of the TE and TM mode photon numbers which are determined by the polarization controllers in the setup shown in Figure 5.1 and are estimated in the analysis; these phases are important as the setup is very sensitive to any variations.

# CHAPTER 6 MULTIPLE RECIRCULATIONS THROUGH A CROSSPOINT SWITCH FABRIC FOR RECIRCULATING OPTICAL BUFFERING

## 6.1 Introduction

Contention resolution in optical switching can be addressed using both fibre delay lines (FDLs) and the wavelength domain [4]. FDLs can be implemented in either travelling (input or output buffering) or recirculating configurations [52]. Recirculating buffers require less physical fibre, and also provide flexibility in that shorter delay lines can be used and packets can be accessed upon each recirculation through the switch fabric. The main drawbacks of recirculating buffering using an electro-optic switch are the loss resulting from traversing the switch fabric multiple times, accumulated ASE due to the resulting amplification requirement, and switch crosstalk that accumulates with multiple traversals of the signal. Loss is solved using in-loop optical amplifiers or a switch with gain, the ASE can largely be filtered out (although it can play a role with a very high number of recirculations), but it is more difficult to get rid of crosstalk.

The CrossPoint optical switch was developed keeping in mind the requirements of speed, crosstalk and scalability for optical packet-switching applications. Furthermore, low insertion loss, low path-dependent loss and low polarisation dependent loss were also considered, along with the possibility of large-scale monolithic integration. The polarisation dependence of the CrossPoint switch is due to the polarisation dependence of the coupling and of the optical gain [105]. For this reason, polarisation controllers were required in the experimental setup. This characteristic can be improved upon in future as it has been demonstrated that vertical couplers can be made polarisation independent [106] and that polarisation-independent gain structures are possible for SOAs [107].

This chapter is based on the results in [104]:

In order to develop a large switch fabric, it is important to keep the signal paths passive so that the signal can pass through a switch unit when it is in the OFF-state. Based on InGaAsP-InP active vertical coupled (AVC) structures, the CrossPoint optical switch consists of two waveguide layers. Two active vertical couplers are formed at each cross-point of the switch by having an active waveguide stacked on top of both input and output passive waveguides. This is shown in Figure 6.1. The switching mechanism of the CrossPoint is carrier-induced refractive index and gain changes in the AVCs [105]. A total internal reflection mirror vertically penetrates the active waveguide layer to deflect the optical signal for 90° from the input AVC to the output AVC. The injection of carriers into the active layer turns the device into the ON state. In the ON state, the effective refractive index of the active upper layer is reduced by the presence of injected carriers to equal that of the lower waveguide thereby allowing coupling. The injected carriers in the active layer also provide gain for the signal resulting in a high ON/OFF contrast, with an ON-OFF extinction ratio as high as 70dB being demonstrated. Lossless switching with optical gain of up to 5dB is achieved across the matrix.
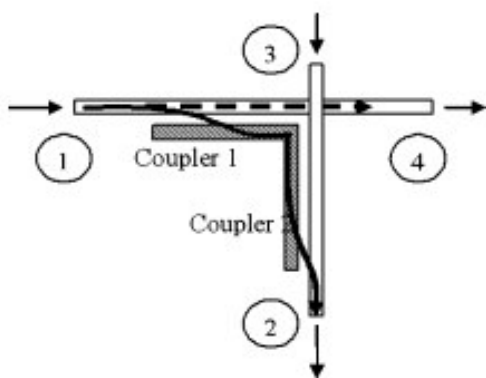


**Figure 6.1. Optical switch unit employing an active switching mechanism (shaded) and passive waveguides. Solid line: signal path in the ON-state, and dashed lines: signal paths in the OFF-state. From [105]**

4×4 CrossPoint switch fabrics have been demonstrated so far, but are scalable without the inherent losses associated with broadcast and select schemes . It has also been shown that the CrossPoint switch output power can be dynamically controlled on a packet to packet basis for a large input power range [106], optical gain differences of less than 3dB are attainable between the shortest and longest switch paths [109], and multicasting without optical split loss is possible [110].

In the CrossPoint switch, ultra-low OFF state crosstalk is achieved through the highly absorptive state of the active waveguide, together with the weakened coupling so that the stray signal is attenuated [111]. Crosstalk as low as –60 dB has routinely been demonstrated. Due to this low crosstalk, together with ultra-fast switching speed as shown in Figure 6.2, the CrossPoint switch provides an excellent electro-optic switch fabric to be investigated in the implementation of packet switched cross-connects for optical networks.

When a single optical input is present at any of the 4 input ports, under zero current injection to all switch cells, the measured background signal leakage levels at all outputs are lower than -60dB. This is a conservative value, as in most cases the power levels are below the power meter sensitivity.

When a switch cell is turned on, the fibre-fibre transmission between the input and the intended output is approximately -16 dB. This gives an extinction ratio of > 44 dB when compared with the -60dB background level. Again in fact the extinction ratio is much higher, as the actual background level is lower. Data measured directly from chips (not fibre coupled devices) suggest an extinction ratio of >60dB. Furthermore, under this condition, no obvious increase in the background signal leakage levels at other (unintended) outputs is observed, that is, no obvious increase in crosstalk levels.
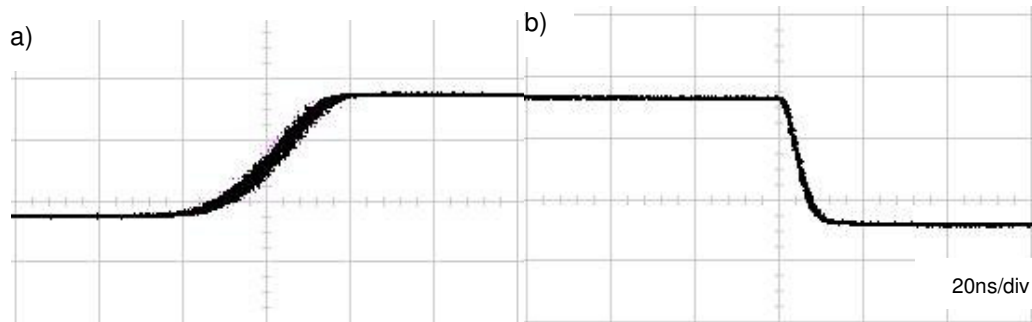
**Figure 6.2 a) Typical rise time of the CrossPoint switch module is in the order of 35ns. b) Typical downtime of the CrossPoint is less than 10ns. Both are dominated by limited speed of the driver electronics as the switch chip has switching time in the order of a few nanoseconds [105].**

## 6.2 Crosstalk in the CrossPoint Switch: Switch Scalability, Cascadability and Recirculating Buffers

The main reason for the low crosstalk in the CrossPoint, which is the key difference between the CrossPoint and other devices, is that the vertical coupler active layer has very high absorption when there is no current. A weak coupling (or leakage) into the active layer still exists, but any light that leaks into the active layer is nearly completely absorbed, because the quantum wells have an absorption co-efficient in the order of $10^3$ - $10^4$ /cm. This is not the case for other coupler-based switches that rely solely on destructive interference between optical modes to realise low crosstalk. Using interference is limited as both modes require exactly the same amplitude: if they differ by only 0.1%, the crosstalk is >-30dB.

In this section this important characteristic of the CrossPoint switch is analysed with regards to the crosstalk-limited scalability and crosstalk-limited cascadability of the switch. The specific implementation of a low crosstalk switch is also theoretically analysed for a recirculating buffer. That is because a recirculating buffer (a flexible, minimum-fibre buffering solution) is not feasible unless a switch with low crosstalk is

used, and it is for this reason that the CrossPoint switch, specifically, has been examined in this thesis.

### 6.2.1 Scalability

If the switch crosstalk in dB is *10log(x)*, assuming a worst case scenario with the most waveguide crossings (the longest path) and with all inputs populated with the same input power (ignoring secondary crosstalk factors which are very small), the output optical signal to noise ratio can be approximated by:

$$\frac{1-(N-1)x}{(N-1)x}$$

(1)

for an N×N switch. This is assuming negligible attenuation between switch cells within the switch. To obtain a BER of $10^{-12}$, a typical optical signal to noise ratio, OSNR, dependent on the optical bandwidth and bandwidth of the receiver and taking into account impairments in optical transmission systems, of around 20dB is required [1]. Using equation (1) this translates to a limitation of a 2×2 switch with crosstalk of -20dB, a 100×100 switch for -40dB crosstalk, and a 9900×9900 switch for -60dB which is the measured crosstalk for the CrossPoint switch. So it can be seen that based on crosstalk alone, the scalability is not really limited.

Rather, the scalability will be limited by path dependent loss and the ASE of the switch cell itself. The switch cell can be seen as an SOA with a certain noise figure. Before the signal reaches the switch cell it passes several passive cross points. This will result in a loss of around 0.5dB/cross point which in turn will result in a marked difference in path dependent loss when the switch is scaled up. If the switch cell has gain, path dependent loss can be compensated for to some extent, but the SNR at the output will still be different for different paths as they experience different attenuations. The analysis of this is rather complicated though as the noise figure of

each cell would have to be taken into account at different injection levels for the equalisation of path dependent loss.

### 6.2.2 Cascadability

If M number of N×N switches are cascaded, the output signal to noise ratio is given by:

$$\frac{[1-(N-1)x]^M}{(N-1)x\sum_{j=0}^{M-1}[1-(N-1)x]^j}$$

(2)

which provides the results as shown in Figure 6.3. This assumes that attenuation between cascaded switches is compensated for by EDFAs. An OSNR above 20dB which is required to achieve a BER of $10^{-12}$ can be achieved quite easily for the low crosstalk levels characteristic of the CrossPoint switch, and only provides severe limitations when switch crosstalk is as high as -20dB.
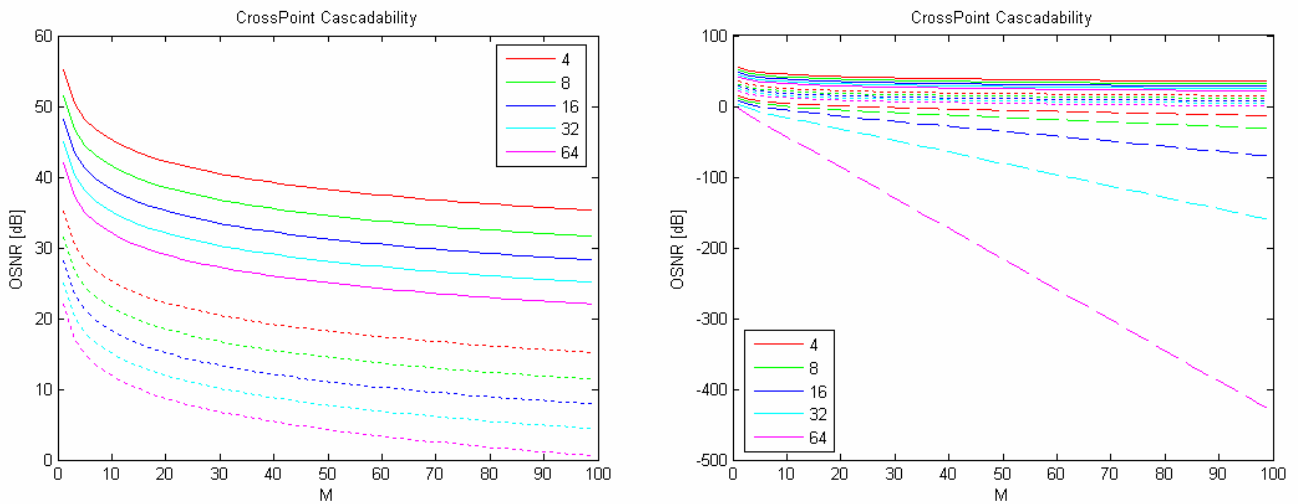


**Figure 6.3 Solid line: -60dB crosstalk, Dotted line: -40dB crosstalk, Dashed line: -20dB crosstalk. M: number of cascaded switches. Different switch sizes, N×N, were investigated, with N shown in the legend.**

### 6.2.3 Recirculating Buffering

Because of the ultra-low crosstalk of the CrossPoint switch, it is an ideal switch to consider for the implementation of a recirculating buffer used for contention resolution, as this regime is most adversely affected by switch crosstalk as packets have to traverse the switch fabric multiple times [112]. Figure 6.4 shows the influence of crosstalk on the signal quality for multiple recirculations. Figure 6.5 shows that a switch crosstalk as low as -50dB is required for a low BER when multiple recirculations are required.
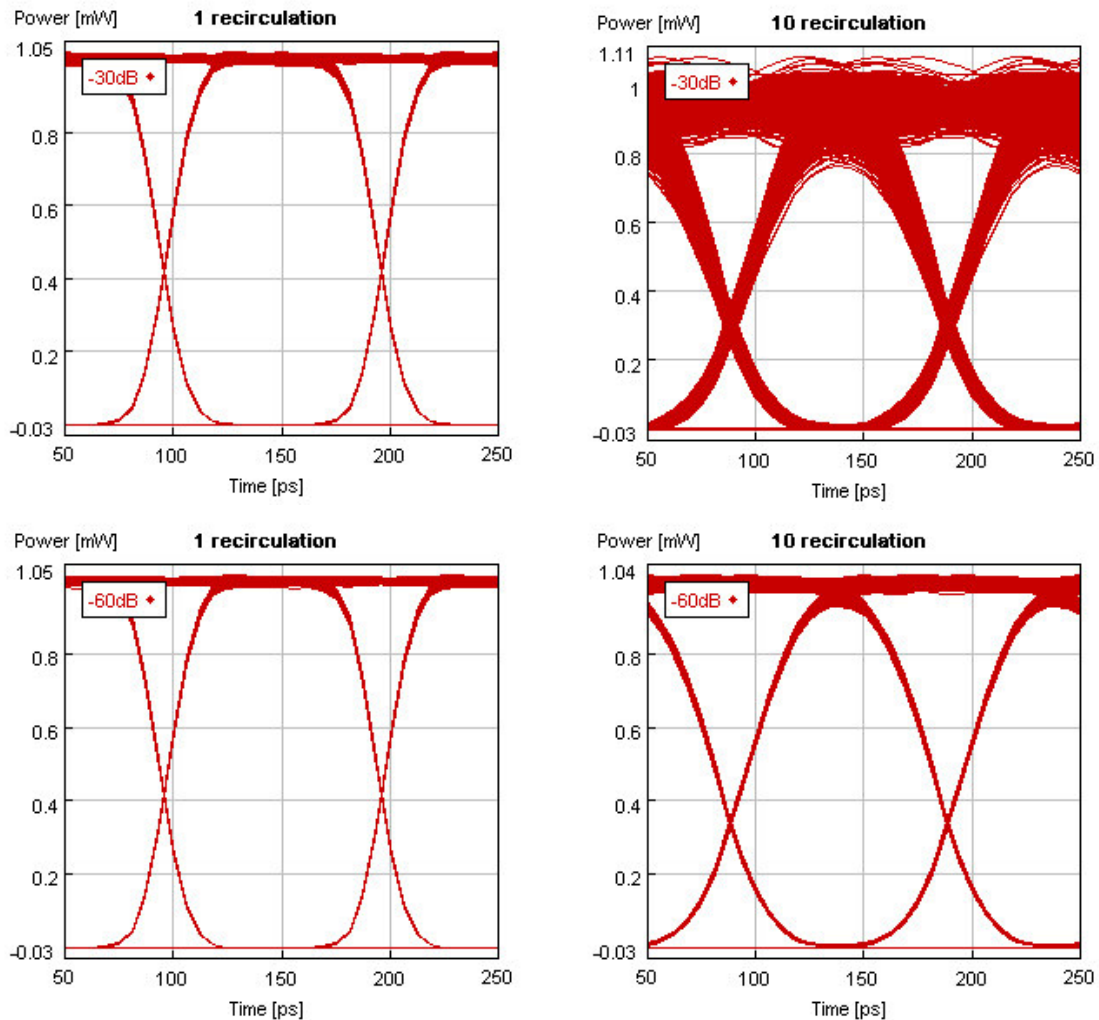
**Figure 6.4 The significant difference in signal quality with increasing number of recirculations can be seen here for a switch with crosstalk of -30dB (top) and -60dB (bottom) for a single recirculation (left) and 10 recirculations (right).**
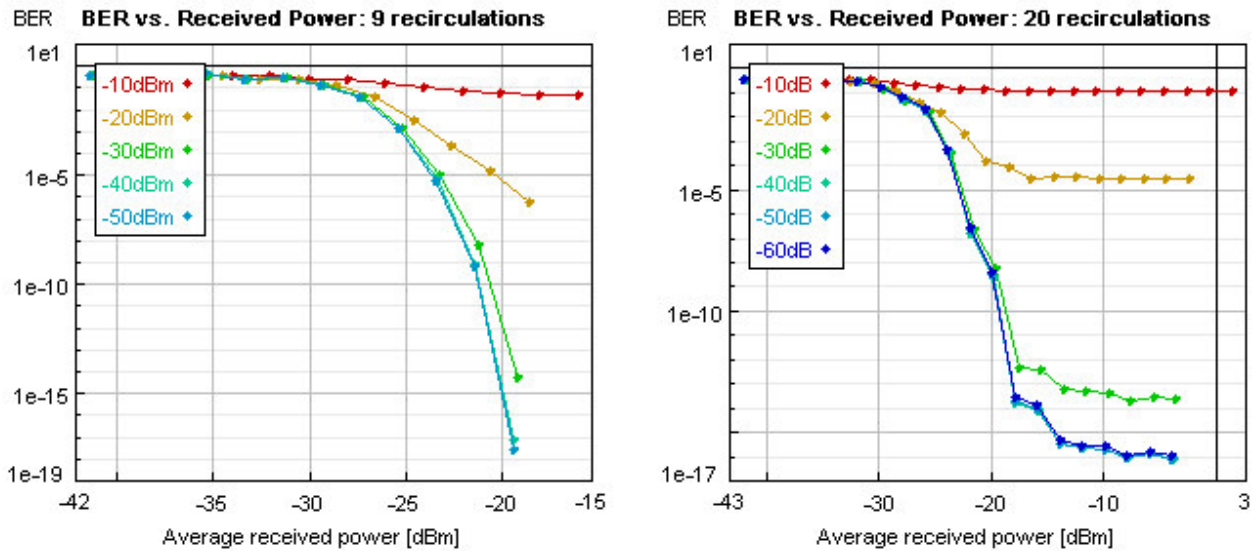


**Figure 6.5 BER vs. received power is shown for varying switch crosstalk values. It can be seen that increasing the number of recirculations from 9 (shown above left, corresponding to the number of recirculations measured experimentally) to 20 or 30 (shown right) has a significant influence on the attainable BER when the switch crosstalk is more than -30dB.**
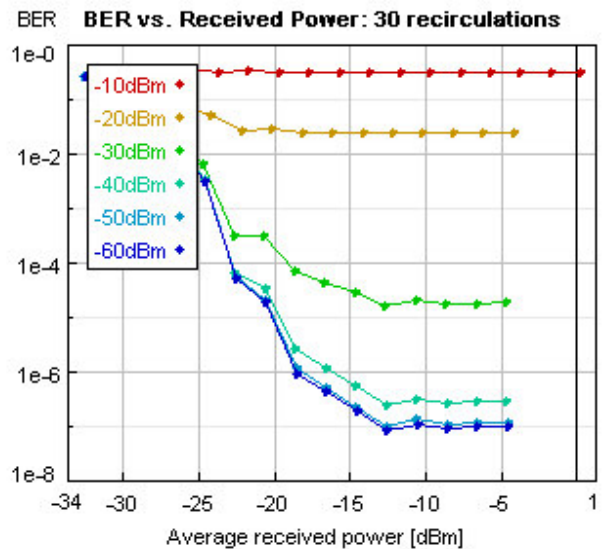


## 6.3 Experiment and Results

Figure 6.6 shows the experimental setup of a recirculating buffer using part of a 4×4 packaged and pigtailed CrossPoint switch device. A 125m FDL is used, and the total

buffer time is 793ns including the lengths of the EDFA, bandpass filter, and polarisation controller. The EDFA is necessary because the CrossPoint switch still has a fibre to fibre transmission loss of around 20dB despite a small on-chip signal gain.

The input packets (with power level of 0 dBm) arrive every 793ns fitting the delay length, and the payload is 60ns of $2^7$-1 PRBS data (using a longer sequence length may result in more degradation with very many recirculations due to the increased possibility of longer strings of 1's and 0's; this is however insignificant because of the short lengths of the packets that were switched) . The payload length is defined to keep a 1:5 switching duty cycle for the CrossPoint in order to avoid excessive thermal strain to the device. The buffered packet is switched into the FDL using switch C1. The recirculations through the buffer are handled by switch D1. The buffered signal is output by switch D2, and the unbuffered packets are switched by C3.
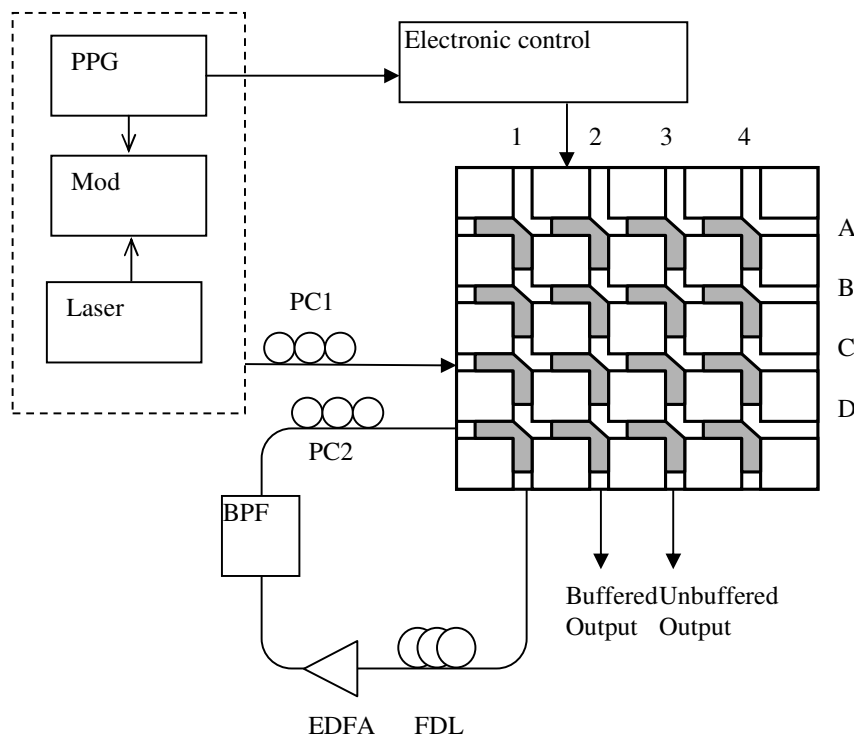


**Figure 6.6   Experimental setup. PC: polarisation controller, BPF: bandpass filter, EDFA: Erbium-doped fibre amplifier, FDL: fibre delay line, PPG: pulse pattern generator. λ=1550nm.**

After the designated number of circulations performed by switch D1, the buffered packet is switched to the output by switch D2, as shown in Figure 6.7 b) in the case of 10 recirculations. The input packets that are not buffered are switched to an alternative output directly by switch C3, and are shown in Figure 6.7 c). The output OSNR for the unbuffered signal is in the order of ~ 35dB (measured with an optical spectrum analyser with 0.1nm optical bandwidth). Figure 6.7 a) shows a close up of the buffered packet when it is output from the CrossPoint switch, and the pattern is clear with very little distortion or signal degradation. The extinction ratio of the back-to-back signal is larger than 12dB, and for the switched signal is about 10dB.

a)



500ps/div

b)



2µs/div

c)



2µs/div
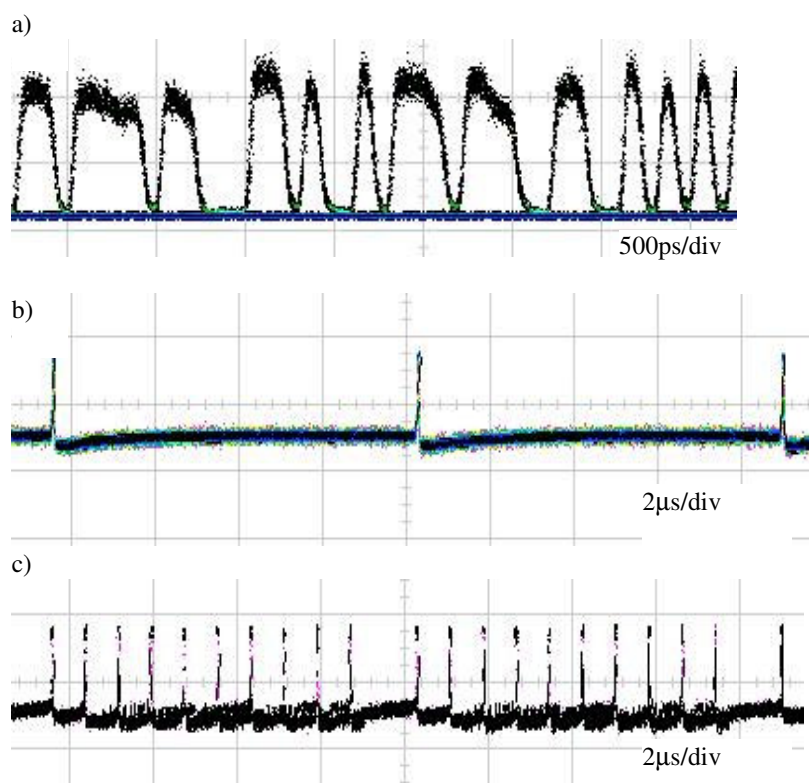
**Figure 6.7 a) A close up of the 10Gbit/s $2^7$-1 payload after 10 recirculations. The pattern is clear with little signal quality degradation. b) Packets are buffered 10 times, so there are 10 793ns time slots in between output packets from the CrossPoint switch, (8.7µs between payloads). c) 10 unbuffered packets are directly switched to an alternative output.**

The eye diagram Q factor after recirculation is estimated and the bit error rate is derived using $BER = \frac{1}{2} erfc(\frac{Q}{\sqrt{2}})$. It can be seen from Figure 6.8 that the penalty after the first recirculation of a packet is approximately 6dB. It is however interesting to note that increasing the number of recirculations does not result in a proportional penalty increase, as 9 recirculations introduce only 3dB further penalty over a single recirculation. The power penalty is due to both the amplified spontaneous emission (ASE) from the EDFA and the pattern effect of the switch. Figure 6.8 also shows that the quality of the unbuffered packets output from C3 that are switched to the output immediately without travelling through the FDL have a low BER, comparable to the buffered packets. Thus signal integrity is maintained whether the packets are buffered or not.



**Figure 6.8 BER performance of the output from the CrossPoint switch. Both the recirculated output (buffered output from D2) and the unbuffered switch output (from C3) are evaluated. BER values are derived from the Q factor. Inset: the output packet eye diagram back-to-back and after 9 recirculations.**

## 6.4 Decimal Optical Buffering

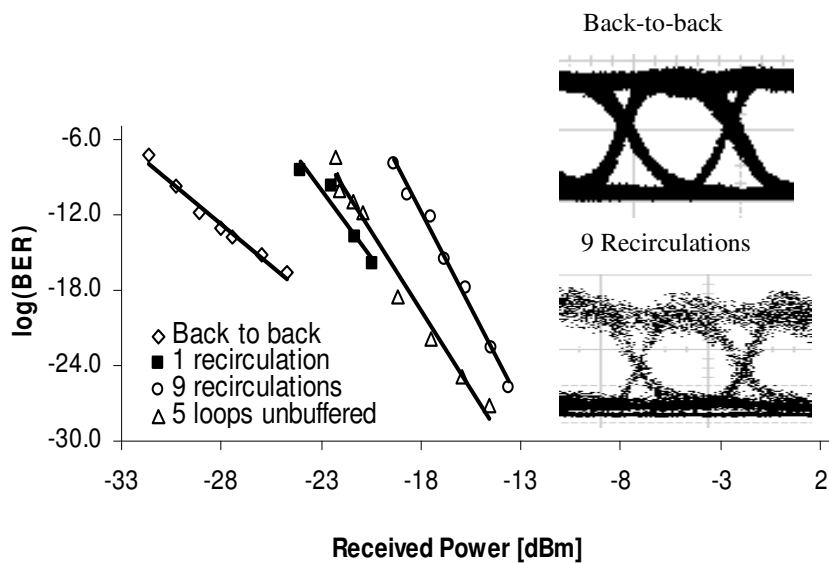In this chapter up to 9 recirculations with low loss were demonstrated. This is the number of recirculations required for a decimal optical buffer as shown in Figure 6.9. The packets input to the buffer from port A4 and output from D4. The other three input and output pairs of the OXS are connected via different fibre delay lines. By selecting the switch cells, the input packets will be guided from the input port into the loops, transmitted in the loops, switched from one loop to another, or guided out from the buffer. Assuming the delays of the three loops are $d_1$, $d_2$ and $d_3$ respectively, and the corresponding numbers of recirculation are $n_1$, $n_2$, and $n_3$. The total delay $T$ of the buffer can be given by

$$T = n_3 d_3 + n_2 d_2 + n_1 d_1$$

(3)

where $d_3 = 10 \times d_2 = 100 \times d_1$ and $n_i = i$ ($i$=1, 2, 3). In this way, a decimal optical buffer is achieved: for instance, if the delays $d_1$, $d_2$ and $d_3$ are set to be 1ns, 10ns and 100ns respectively (corresponding to a fibre of about 20cm, 2m and 200m), the buffer depths can be varied with 1ns steps from 1ns to 999ns with the circulation number, $n_i$, limited to 9. Thus fine granularity and a large variable delay can be achieved simultaneously in this simple scheme. Sufficiently large delay is effective for resolving packet contention, while the fine granularity of the delay allows more efficient statistical sharing of the channel bandwidth among packets belonging to different source and destination pairs.
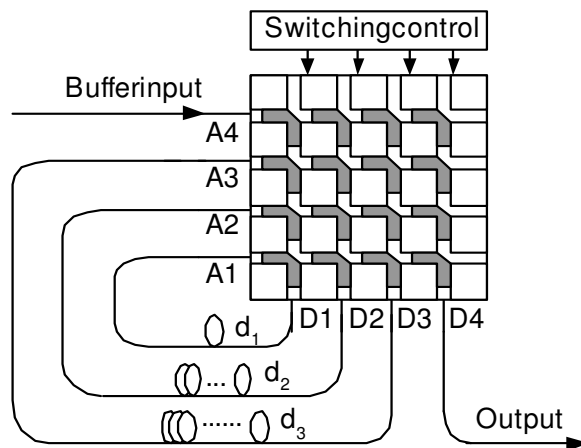
**Figure 6.9 Conceptual diagram of the decimal optical buffer: 3 of the switch input and output ports are used for the buffer.**

To realize the same buffering function by another buffering scheme, either a large number of switches or a large amount of fibre for the delay lines is required. In this proposed scheme only one individual switch element and a small number of fibres are used, hence the router management would be simpler, easier and more stable. When a packet has entered a long fibre delay line, it cannot be switched out but can emerge only at the end of the fibre. However because of the flexibility and fast switching speed of the CrossPoint switch it is feasible to reconfigure the switching cell and retrieve the packet from the buffer. Such delay variability is essential in time-critical applications where packets of information can be released from the buffer as required.

## 6.5 Conclusions

Multiple recirculations through an optical buffer using an AVC based CrossPoint switch matrix has been demonstrated. A 60ns 10Gbit/s payload was used, and signal integrity was maintained with a small power penalty for an increasing number of recirculations. A decimal optical buffering system has also been described that required 9 recirculations through the fibre delay lines of the buffer.

While no crosstalk is observable in the multiple recirculation experiment although other packets are arriving and being switched simultaneously as the recirculation

buffering is taking place, there seem to be two main contributors to the deterioration in the output eye quality. The first main contributor is OSNR deterioration due to amplified spontaneous emission. Because the main source of attenuation in the loop is the switch itself, and as its output OSNR is sufficiently high (35dB), the main OSNR deterioration is due to the EDFA, which after a single pass is measured to have an output OSNR of ~25dB. A second main factor is the pattern effect in the switch. On average, the initial input power of the optical signals to the CrossPoint switch is in the order of 0dBm. Because an EDFA with a fixed gain greater than the switch insertion loss is used without an in-loop adjustable attenuator, the loop gain is not balanced to unity, therefore it is likely that after a number of circulations the input power to the switch is only limited by the EDFA output saturation power, which may have exceeded saturation levels of the switch despite input coupling loss to the switch. The performance can therefore be improved by carefully balancing the loop gain to unity, and, in the future, by realising CrossPoint switch devices with net fibre to fibre gain.

# CHAPTER 7 OPTICAL CROSSPOINT SWITCH: FURTHER IMPLEMENTATION FLEXIBILITY AND TRANSMISSION IMPROVEMENT

## 7.1 Introduction

This chapter provides experimental results that demonstrate the implementation flexibility of the CrossPoint switch. The results underline the importance of being able to use a switch with crosstalk as low as that of the CrossPoint, and the possibility of using a flexible recirculating buffering scheme. Time-slot interchange is demonstrated for a 10Gbit/s packet payload using the fully packaged 4×4 CrossPoint switch matrix. The experiments illustrate that the CrossPoint is an ideal electro-optic switch with which to implement time slot interchange using a feedback architecture to achieve arbitrary time slot permutation due to its ultra-low crosstalk.

An opto-electronic control system is demonstrated that is used to detect the arrival of asynchronous packets at the optical switch input, process the headers of the packets, and control switching according to the header content for both fixed and variable length packets. Furthermore, contention resolution is demonstrated in the optical CrossPoint switch by detecting packets at the input ports and controlling the switch operation accordingly. By incorporating this control system into the CrossPoint switch it is possible to route contending packets to a recirculating fibre delay line and control the switch output in a flexible manner for any type of traffic depending on the applied switching algorithm. The operation of the contention resolution is shown with 155Mbit/s headers and 10Gbit/s payloads transmitted on a single wavelength with a guard time of 12.8 ns between header and payload.

Finally, it is shown that the signal quality of buffered packets can be significantly improved by using DPSK modulation of the payload. This is due to the alleviation of

---

This chapter is based on the results in [113],[114],[115]

the patterning effect of the CrossPoint that degrades the signal quality and limits the cascadability of the switch. In devices where gain is provided by a semiconductor active layer a pattern effect is present due to the carrier saturation during '1' codes and the subsequent recovery of '0' codes. When the code lengths are comparable to the carrier lifetime, this will result in the modulation of subsequent code amplitudes by preceding codes. This patterning effect is aggravated by factors such as refractive index modulation (due to the same carrier dynamic process because any gain change is accompanied by refractive index change). It is possible to mitigate these effects, for example with solutions employing quantum dots [64], but a simple application that reduces the effects is using DPSK modulation.

## 7.2 Time-slot Interchange [113]

In time-division multiplexed systems the time slot of the data determines its routing. This makes time slot interchangers an important method of switching in the time domain. A time slot interchanger (TSI) is a device which can rearrange the order of the time slots in a traffic stream [1]. Furthermore, TSIs are used to reduce the blocking probability of TDM switches [116], and a significant reduction in network blocking probability has been shown using TSIs to provide flexibility in allocating routes [117].

Time slot interchanging has been demonstrated all-optically for both packet interleaving [118] and bit interleaving [119], but all-optical technology is still very limited and complex, and electro-optic approaches provide significantly more flexibility and ease of implementation. In Thompson et al. [120] LiNbO$_3$ directional couplers are used together with delay lines to realise a TSI with recirculating delay lines. In Ramanan et al. [121] this principle is expanded on, with the focus on designing an algorithm that is able to achieve arbitrary time slot permutations while keeping the number of switch elements to a minimum. Both of these recirculating delay line implementations, however, suffer from uneven attenuation and poor crosstalk performance due to the signal traversing the switch fabric multiple times. In an effort to solve this signal degradation, a method implementing feed-forward delay

lines was used that resulted in the use of double the number of switches as in the feedback configurations [122]. But despite the feed-forward configuration, the crosstalk in the LiNbO$_3$ switches is reported to be so high (in the order of -20 – -35dB), that configurations implementing dilation were investigated in Hunter et al. [123], thus increasing the number of switches required for time slot interchanging even more.

In this chapter, a time slot interchanging experiment for a 10Gbit/s packet payload is reported using the fully packaged 4×4 CrossPoint switch matrix. This is carried out in two steps. In the first step signal delay using a programmable recirculating buffer with the CrossPoint device as the core is demonstrated and signal qualities assessed. Then this delay is used to realise time slot interchanging between consecutive packages. These experiments illustrate in principle that the CrossPoint is the ideal electro-optic switch with which to implement time slot interchange using a feedback architecture to achieve arbitrary time slot permutation. 4×4 CrossPoint switch fabrics have been fabricated so far with optical gain differences of less than 3dB attainable between the shortest and longest switch paths [109], so that the attenuation is not as uneven as was shown in [120] and [121]. Furthermore, the major limitation in all the LiNbO$_3$-based TSIs described in [120] [121] [122] [123] was crosstalk, and in the CrossPoint switch, ultra-low OFF state crosstalk is achieved through the highly absorptive state of the active waveguide and the weakened coupling so that the stray signal is attenuated [111].

## 7.2.1 CrossPoint Time Slot Interchanger
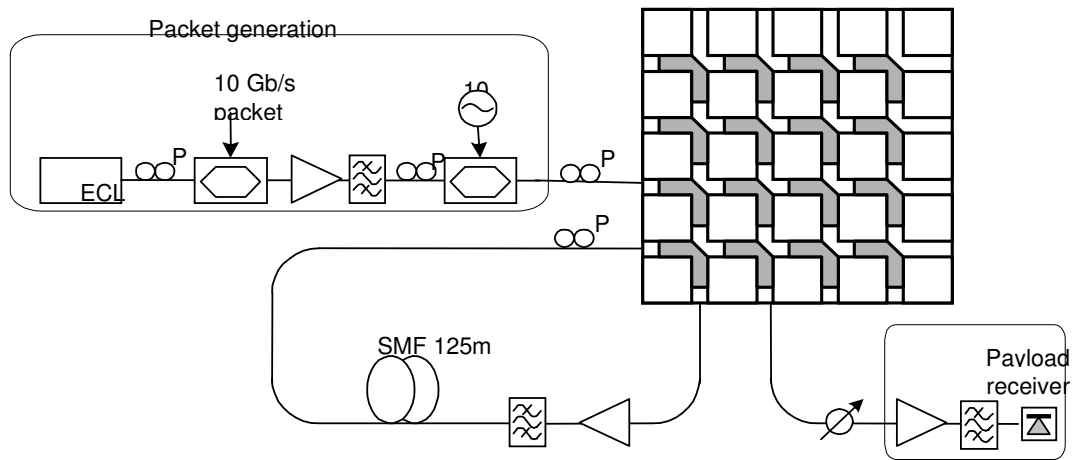


**Figure 7.1 Experimental setup. ECL: external cavity laser, PC: polarisation controller. λ=1550nm.**

Figure 7.1 shows the setup for the time slot interchange experiment. The TSI is realised using a recirculating buffer configuration, the feasibility of which was demonstrated in the previous chapter. The use of a single FDL was shown in Chapter 6 but because the CrossPoint is scalable, the contention resolution of an $n \times n$ switch can be achieved with a recirculating buffer of depth $m$ when an $(n+m) \times (n+m)$ CrossPoint is used.

In a similar configuration to the one used in Chapter 6 where a single time slot delay is implemented to demonstrate the principle of time slot interchange, the packets to be delayed are switched into the FDL using switch C1. The recirculation through the buffer is handled by switch D1. The delayed packets are output by switch D2, and the packets that are not delayed are switched by C2.

Figures 7.2 a)-e) show the 4 input packets used. In order to identify them easily, the following bit patterns were selected: Packet 1: 60ns all 1's, Packet 2: PRBS, Packet 3: 20ns 1's, 20ns 0's, and 20ns 1's (i.e. a 101 shape), Packet 4: 40ns 1's, 20ns 0's (i.e. a 110 shape). In the experiment, the order of the packets was interchanged as follows, by delaying every second packet arriving at the input to the CrossPoint switch:

**Input order:** **Packet 1 – Packet 2 – Packet 3 – Packet 4**

**Output order:** **Packet 2 – Packet 1 – Packet 4 – Packet 3**

Figure 7.2 f) shows the new order of the packets leaving the TSI. The eye diagram Q factor after the TSI is evaluated and the corresponding bit error rate is derived using standard error function calculations. The BER performance is shown in Figure 7.3 where the BER values are plotted against the average received power. The output OSNR of the signal is in the order of ~ 35dB (measured with an optical spectrum analyzer with 0.1nm optical bandwidth). The extinction ratio of the back-to-back signal is larger than 12dB and for the switched signal is about 10dB. (The average 2dB penalty differs from the 6dB penalty shown in the recirculating experiment because every packet is not buffered. The results of different experiments also differ slightly due to the polarisation dependence of the components.)
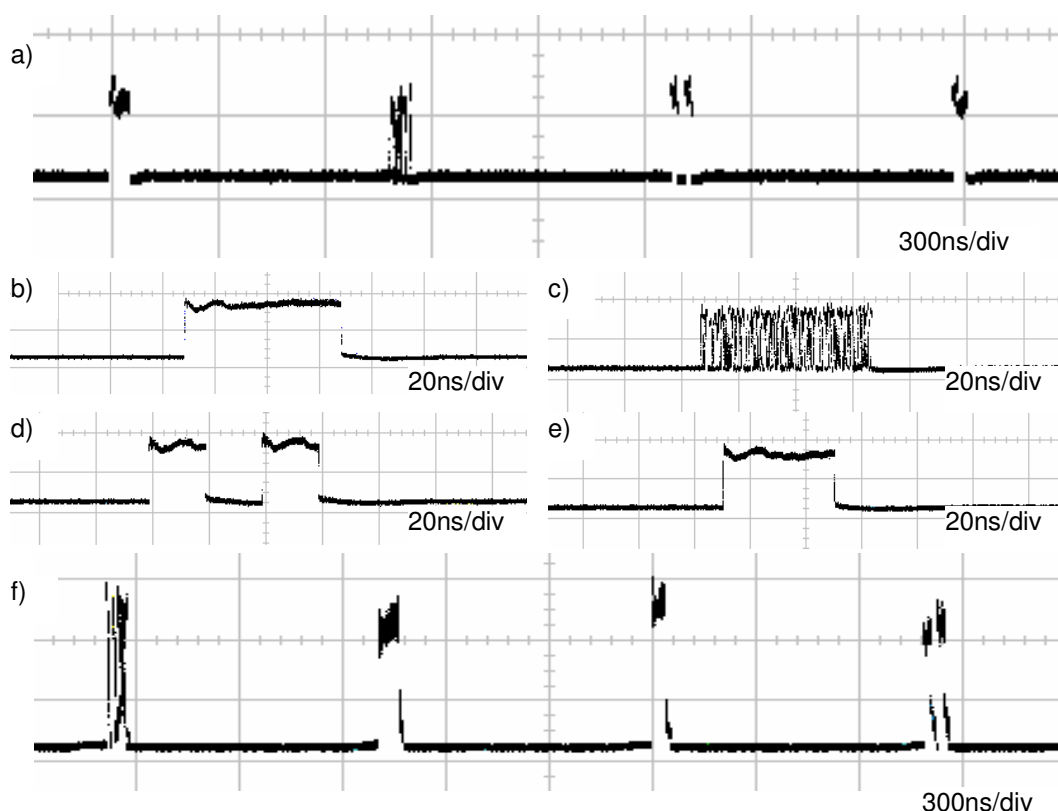
**Figure 7.2 a) Original order of input packets. Packets are numbered left to right as shown in the figure, and can be discerned by their unique shapes as shown in b) – e) respectively: Packet 1: 1's, Packet 2: PRBS, Packet 3: "101" shape, Packet 4: "110" shape. f) The output of the time slot interchanger, with the packets in the following order from left to right: Packet 2, Packet 1, Packet 4, Packet 3. The 60ns payloads are spaced 793ns apart.**

While the results shown here demonstrate the time slot interchange between adjacent packets, it is obviously possible to interchange packets separated up to 10 time slots apart in the setup. For N time slots that need to be interchanged, a maximum of N FDLs are required if a single packet uses the delay of a FDL. Each of these FDLs in turn only need to be a single time slot in length as the fibre can be reused upon recirculations thus minimizing the physical amount of fibre required. In this case an (N+1)×(N+1) switch is required. Alternatively, if the number of switch ports is limited, it is also possible to share a FDL amongst various packets because the FDLs are not FIFO delays as is the case in a feed-forward buffer.
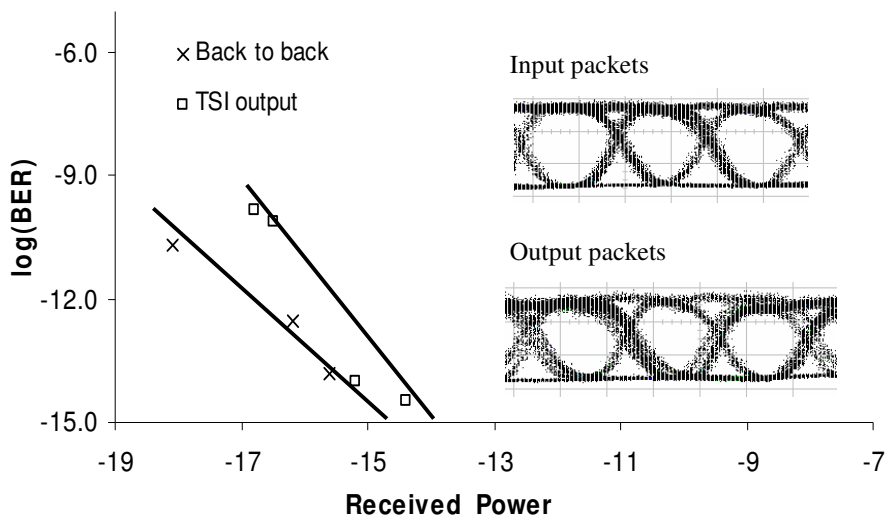


**Figure 7.3 BER performance of the output from the time slot interchanger. BER values are derived from the measured Q factor. The insets show the input packet eye diagram, and the output packet eye diagram.**

### 7.2.2 Discussion of the Timeslot Interchanger

Multiple recirculations through an optical buffer using an AVC based CrossPoint switch matrix have been demonstrated. A 60ns 10Gbit/s payload was used and signal integrity was maintained with a small power penalty for increasing numbers of recirculations. Up to 10 recirculations or a total delay of 7.93 µs has been realised as shown in the previous chapter. This optical delay was then used to implement time slot interchange of packets successfully. Because the switch is scalable, the electronic control is easily programmable and the switch is fast reconfigurable, the time slot interchange capabilities of the CrossPoint implementation can be very flexible.

In the algorithms discussed in [121] and [123], either feed-forward architectures or feedback architectures with a single recirculation are described. The result of this was both a large number of 2×2 switches required ($2\log_2 N-1$ and $2\log_2 MN^2-1$ respectively, where N is the number of time slots accommodated, and M refers to the number of ports) and a large amount of fibre for the delay lines (one FDL per switch in the TSI

configuration, with lengths varying from 1 time slot to N/2 time slots).
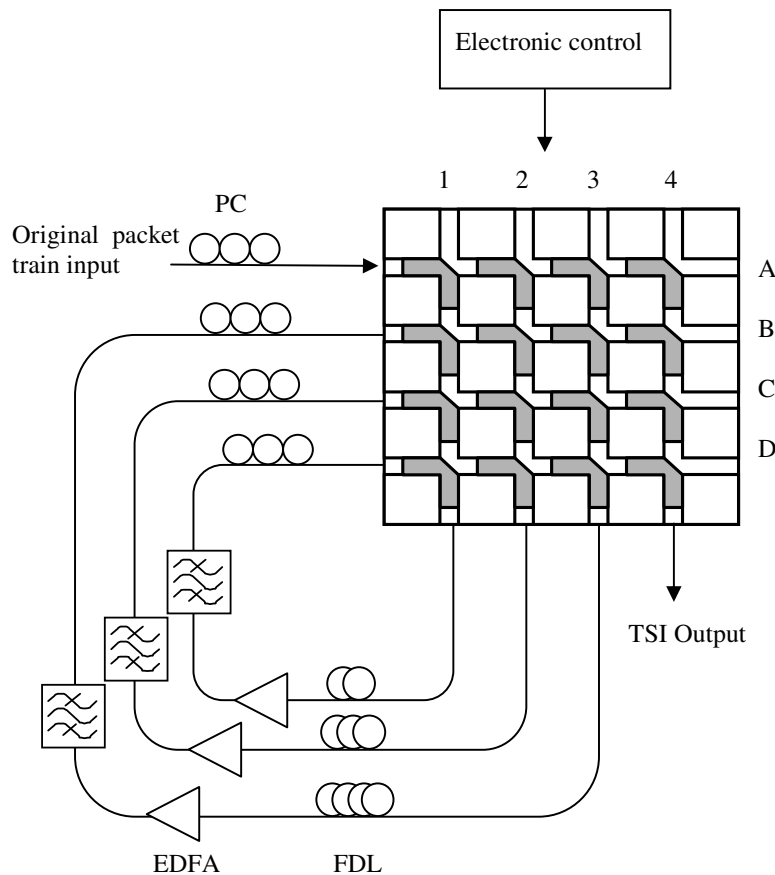


**Figure 7.4 Possible TSI configuration implemented with a 4×4 CrossPoint switch and using a buffer depth of 3. Multiple FDLs with varying delay lengths facilitate the granularity required to implement time slot interchange with the minimum number of switches and FDLs, resulting in minimal packet train total delay.**

Because of the scalability of the CrossPoint together with its control flexibility, it is feasible to consider configurations implementing not only 2×2 switches, thus minimizing the number of individual switch elements. Furthermore, utilizing recirculating buffers not only minimizes the amount of fibre required due to the reuse of the same fibre, but also provides substantial implementation flexibility in terms of the algorithm used to achieve arbitrary permutation because of the reduced achievable delay granularity. By using single time slot recirculating FDLs, packets can be delayed and inserted in the packet train arbitrarily, effectively reducing the total delay from 2N-3 [121] or 3N/2-1 [123] to a realistically achievable delay of only N (because the total

train is not delayed more than the delay required to place the required output packet at the start of the train). This concept is illustrated in Figure 7.4.

## 7.3 Header Recognition and Contention Resolution [114]

In this section the flexibility of the CrossPoint is demonstrated with the implementation of an electronic control interface and various applications using recirculating delay lines and exploiting the CrossPoint's low crosstalk characteristics: header processing in order to dynamically control the switching operation, contention resolution that makes use of the reconfigurable header processor and a recirculating delay line, and the switching of both fixed and variable length packets in slotted and unslotted operation.

### 7.3.1 Unslotted Operation with Variable Length Packets
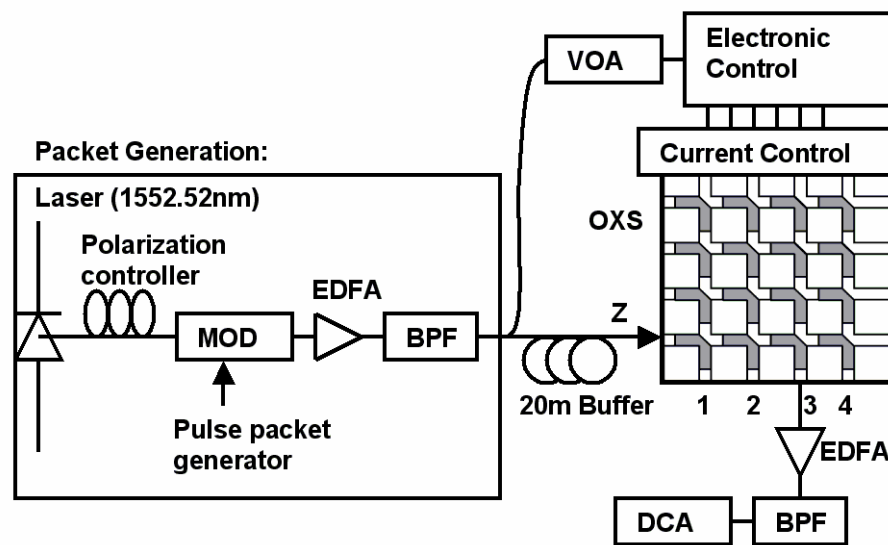


**Figure 7.5 Header recognition and switch control is sufficiently flexible to accommodate fixed or variable length packets, and slotted or unslotted operation. VOA: variable optical attenuator, DCA: digital communications analyzer, MOD: modulator, BPF: band pass filter, EDFA: erbium doped fibre amplifier.**

In order to detect packets arriving in unslotted communication that have a variable length it is necessary to process each packet header upon arrival. The electronic control

interface to the CrossPoint switch is based on a Xilinx (XC 2C 32 VQ44) Coolrunner II Complex Programmable Logic Device (CPLD) that interfaces with the input block of the node via four PINFET optical receiver modules with a sensitivity of –37dBm that support a maximum data rate of 350Mb/s. Control signals are then sent via the SMA connectors to the CrossPoint current control to open the required switch cells. Optical power is tapped off from the input. While the header processing is being done the whole packet is buffered by 20m of fibre before entering the OXS to ensure that the correct switch cell is fully opened when the packet arrives at the switch cell. The system is used to process the 155Mb/s headers and switch the header and 10Gb/s payloads as shown in Figure 7.5. Because the control detects packets as they arrive, asynchronous operation is supported. The packet header contains information about the packet length as well as the output port that the packet must be routed to.
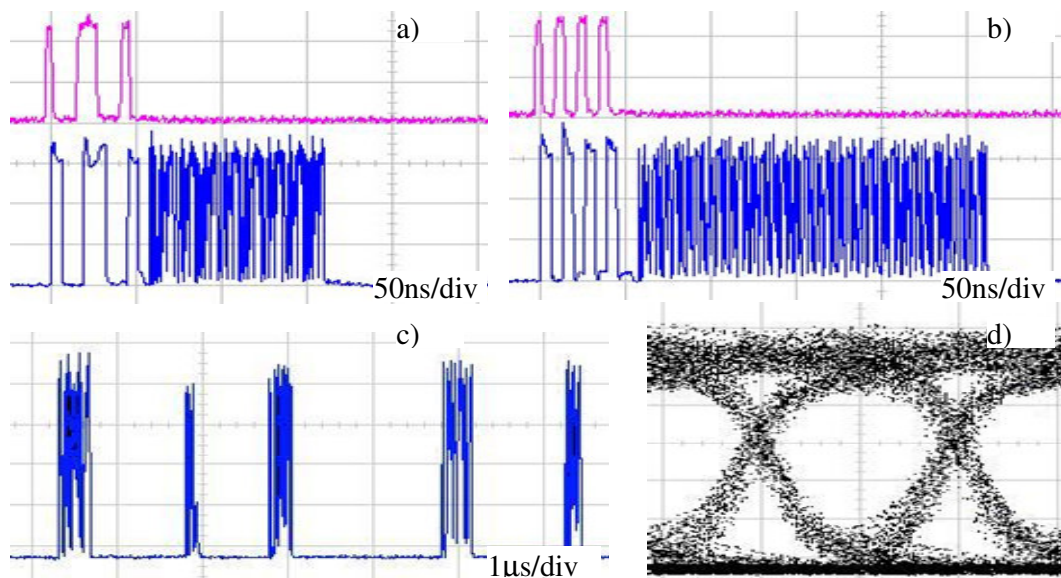


**Figure 7.6 a) and b) show different variable length packets together with the output of the header recognition at the top of the figures, c) shows a packet train of asynchronous variable length packets that are switched to different switch outputs, and d) shows a clear and open eye diagram at one of the switch outputs.**

Figure 7.6 shows close-ups of two of the different packets, a train of asynchronous packets that enter the node, as well as the eye diagram of the correctly switched packets on one of the output ports which is open and clear. For this experiment the

CrossPoint was operated as a 1×2 switch, with the specified output varying for different packets. Correct operation was verified by checking the resulting control signal to the specific CrossPoint switch (switches Z2 and Z3 as shown in Figure 7.5).

### 7.3.2 Contention Resolution

If two packets on the same wavelength arrive at the CrossPoint on different input ports at the same time and are destined for the same output port, the contention needs to be detected and resolved accordingly. Using the flexible electronic control interface this is shown with the CrossPoint using fixed length packets in this experiment: the 10Gbit/s 102.4ns $2^7$-1 PRBS payload is separated from the 155Mbit/s header by a 12.8ns guard time as shown in Figure 7.7a). To demonstrate the contention resolution one stream of packets was generated and sent in every second timeslot, a timeslot being 1.107μs as shown in Figure 7.7b). This spacing is in order to keep a 1:5 switching duty cycle for the CrossPoint to avoid excessive thermal strain to the device.
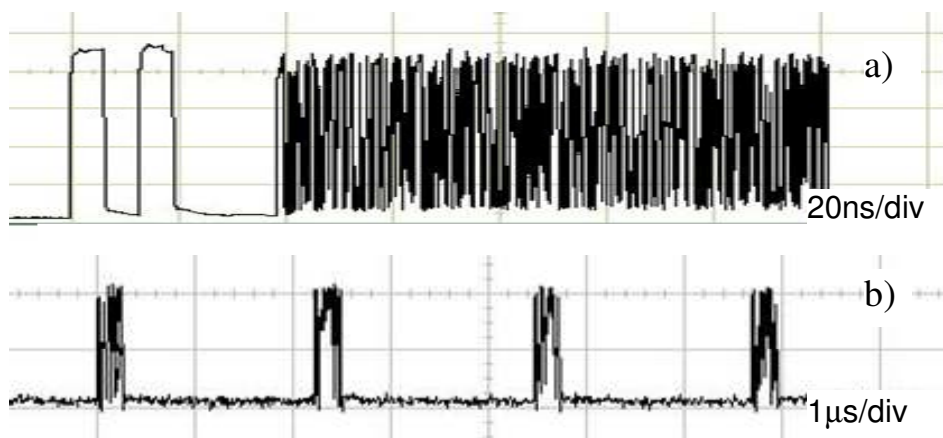


**Figure 7.7 a) Fixed length packets with 155Mb/s 4-bit headers and 102.4ns 10Gb/s payloads are transmitted every second timeslot, b) which are 1.107μs long. Fixed length synchronous packets were used to demonstrate contention resolution.**

The experimental setup is shown in Figure 7.8. The laser transmits a continuous 1552.52nm wave that is modulated with a Mach-Zehnder modulator. The optical signal is amplified and filtered. A band pass filter is used to remove the amplified spontaneous emission (ASE) noise from the EDFA. This packet stream is then split

with a 50:50 coupler to create two identical input streams at input 1 and input 2 of the switch. Optical power is tapped from both these streams and the header is processed by the CPLD. While the processing is being done, the packets are buffered for 100ns: the time it takes for the processing and complete opening of the correct switch cell.
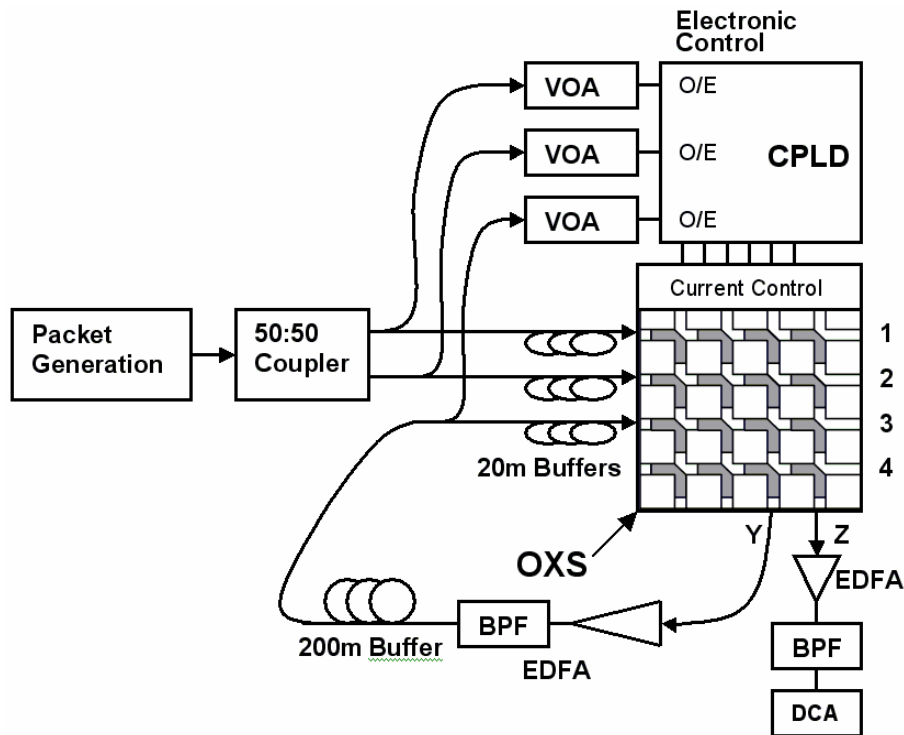


**Figure 7.8 Contention resolution experimental setup. A 200m fiber delay line provides a delay of 1.107μs together with the length of the filter and the EDFA. Buffered and unbuffered packets are output at port Z.**

Contention is detected since both packets are destined for output Z and arrive at the same time. Switch cell Z1 and Y2 are opened in the first time slot to switch the packet from input 1 to the correct output and the packet from input 2 to the buffer at output Y. The buffer delays this packet for one timeslot length, 1.107μs. At the beginning of the second timeslot, no packets are present on input 1 and 2, there is only one packet in the buffer. An open timeslot is therefore detected for output Z. While the header is being processed, the packet is again buffered for 100ns. Switch cell Z3 is opened to switch the packet from the buffer to output Z. In the third timeslot, this process is repeated.

The whole packet is being switched, header and payload, to ensure that the information in the header is not lost. The information in the header is needed when the packet needs to be processed again for example when the packet is in the buffer. The final output also includes both the header and payload.

Figure 7.9 shows the output sequence as well as the switching window sent to switch cell Z3. Packets from input 1 are present at every even timeslot and packets from input 2 are present at every odd timeslot resulting in packets at every timeslot at the output. The packets from input 1 are at higher optical power than the packets from input 2 due to the gain imbalance in the node. Packets arrive at the switch on input 1 at –2.72dBm and on input 2 at –2.28dBm. Switch cell Z1 has a loss of about 23.47dB. Packets from input one exit the switch at a power level of –27.89dBm and are amplified by a fixed gain of approximately 15dB to a power level of –11.05dBm at the DCA. The packets from input 2 lose about 25.39dB due to switch cell Y2. These packets arrive at the switch again after traveling through the buffer on input port 3 with an optical power level of –4.12dBm. Switch cell Z3 has a loss of 25.72dB resulting in these packets having optical power of only –15.20dBm at the DCA. The difference in power levels of about 4dB is visible in Figure 7.9.



1µs/div
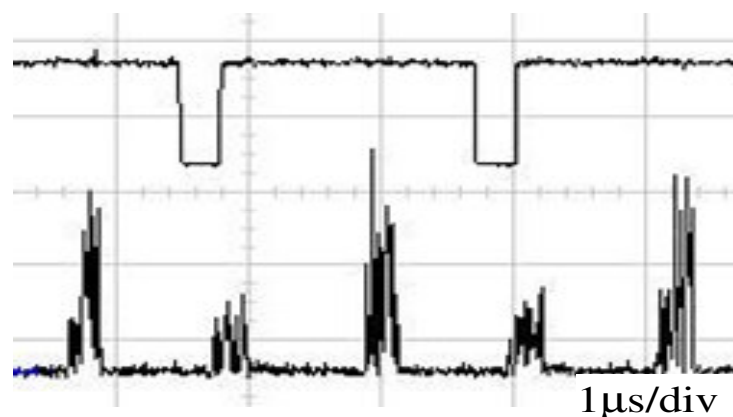
**Figure 7.9 The output from the contention resolution, including unbuffered packets and attenuated buffered packets. At the top the switching window sent to the switch cell Z3 is shown.**

## 7.4 Using DPSK to Improve Signal Quality after Buffering [115]

All the results shown thus far suffer from a pattern effect due to the semiconductor nature of the CrossPoint switch. In this section it is shown that the patterning-induced degradation in this kind of optical buffer can be alleviated by using a DPSK (Differential Phase Shift Keying) format payload. The advantage of DPSK over OOK modulated signals is that DPSK requires a 3-dB lower optical signal to noise ratio to achieve a given BER when a balanced receiver is used. The nonlinear tolerance is also higher, and an increased robustness to narrow optical filtering and fluctuations in signal level at the receiver decision circuit has been demonstrated [125]. The experimental results show that the DPSK payload can outperform the OOK payload by 3.2 dB after 9 recirculating loops in the buffer.

### *7.4.1 DPSK Experimental Setup and Results*
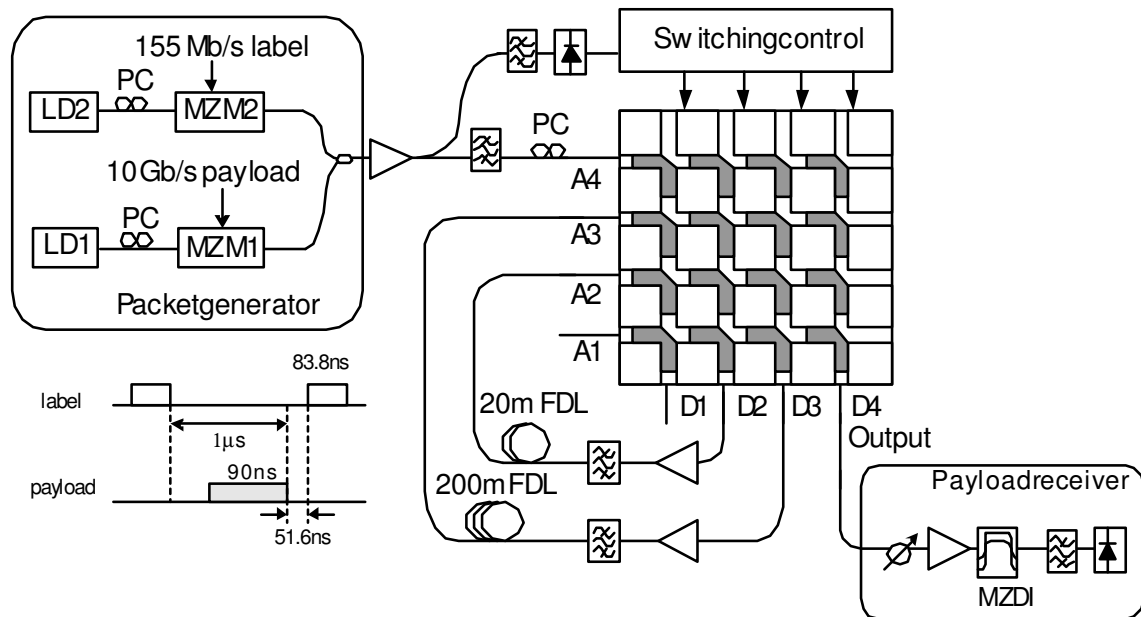


**Figure 7.10 Experimental setup. MZM: Mach-Zender modulator, LD: laser diode, FDL: fibre delay line, PC: polarisation controller, MZDI: Mach-Zehnder delay interferometer.**

The experimental setup is shown in Figure 7.10. The payload source is an external tuneable laser at 1550nm. The 10 Gb/s PRBS $2^{15}-1$ signal is generated with an external Mach-Zehnder modulator (MZM). Depending on the bias of the modulator, either a

NRZ OOK signal (biased at the half maximum) or a DPSK signal (biased at the null of its transmission) can be generated. The synchronous 155 Mb/s label signal is generated by another laser and combined to the payload by a 3-dB coupler, thus realising an optical packet in a wavelength labelling scheme.

To perform the switching function, a fraction of the input packet is tapped for opto-electronic label processing. The remaining part of the packet is firstly label-erased by an optical band-pass filter and then input to the OXS. The input optical power is 2dBm. The output DPSK payload passes through a fibre-based stabilised Mach-Zehnder delay interferometer (MZDI) for the phase demodulation, and then detected by a pre-amplified 10GHz receiver.
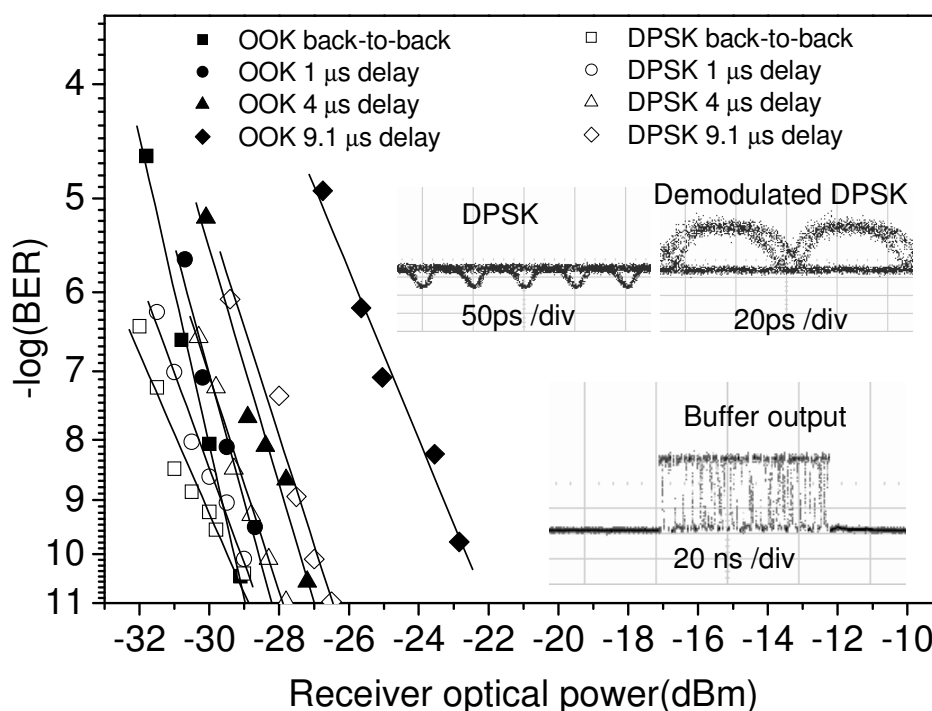


**Figure 7.11 Measured BER curves for the back-to-back case and output from the buffer for the OOK signal and DPSK signal. Insets: DPSK before and after the demodulator and the packet output from the buffer.**

Figure 7.11 shows the measured BER curves for the OOK signal and DPSK signal for the back-to-back case and after optical buffering. The inset figure in Figure 7.11

shows the eye-diagram for the DPSK signal before and after the demodulator. It can be seen from Figure 7.11 that the penalty for the OOK after 9.1 μs is approximately 6.5dB. The power penalty is due to both the spontaneous emission from the EDFA and the pattern effect of the switch. However, for the DPSK signal, the receiver penalty for 9.1 μs switching is only 3.3 dB. Figure 7.12 (a) to (d) show close-ups of the received packet after several recirculations within the OXS loop. Obviously the OOK signal shows a strong pattern effect after more recirculation loops. For the long continuous 'one's, the first bit of 'one' would have an overshoot and the power will gradually reduce for the subsequent 'one's. The pattern effect also appears as the overshoot of a logic 'one' after continuous 'zero's. The more switching loops, the worse the pattern effect. So the pattern effect is the main limiting factor for cascaded operation of the OXS when an OOK payload is deployed. In comparison, the DPSK signal maintains a very clear pattern after multiple loops, with very little distortion or signal degradation. The penalty is mainly induced by the noise accumulation. Therefore it is clear that DPSK has a large advantage over OOK to improve the cascadability of the OXS.



**Figure 7.12 Measured pattern for (a) 4 loops of OOK, (b) 9 loops of OOK, (c) 4 loops of DPSK, (d) 9 loops of DPSK. A clear reduction in the pattern effect of the switch is visible when DPSK modulation is used.**

## 7.5 Conclusions

The CrossPoint switch's ultra-low crosstalk and control versatility enable it to be used for various applications. In this chapter the first de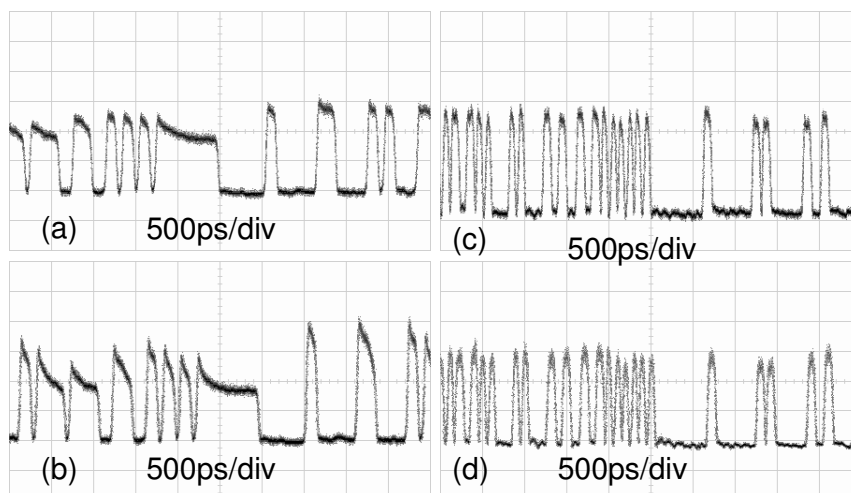monstrations of these applications were described, all of which exploit the flexibility of recirculating buffers. Firstly it was shown that time slot interchange is possible using the CrossPoint switch by implementing delay lines. Arbitrary time slot permutations can be achieved by scaling or cascading CrossPoints, and the TSI application can be simplified using the CrossPoint because multiple recirculations through a single switch fabric is possible due to the very low crosstalk of the switch. A maximum switch size of N+1 is required, with the maximum number of FDLs required being N.

The successful header recognition of incoming packets has been demonstrated, resulting in correct switch configuration for both synchronous and asynchronous operation, and for both fixed and variable length packets. The successful implementation of contention resolution using packet detection has also been shown utilising header processing, fast reconfigurable control of the CrossPoint switch and a recirculating fibre delay line. The contention resolution was demonstrated here for synchronous fixed length packets, but the handling of asynchronous variable length packets can easily be extended to include buffering by using multiple recirculations through varying lengths of fibres as described in the previous chapter [124].

The main causes of signal degradation in the implementations described in this and the previous chapter are the ASE from the EDFAs, the varying gain of different signal paths due to the limitations of available equipment, and to some extent the pattern effect of the individual switch cells. A significant improvement would be attained by eliminatting the fiber-to-fiber transmission loss of the Crosspoint switch and thus removing EDFAs from the configuration, which is being addressed by a new design of the CrossPoint switch device. Another solution is to use DPSK modulation of the payload instead of OOK. In this chapter a variable-delay optical buffer utilizing a 4×4 CrossPoint switch matrix for a 10 Gb/s DPSK payload and a 155 Mb/s NRZ label has

been demonstrated. The results show that using a DPSK payload can result in a 3.2dB sensitivity improvement over using an OOK payload. This is due to the alleviation of the patterning-induced degradation of the signal which is present when OOK is used. DPSK is a promising modulation format to overcome nonlinear impairments and to extend the number of hops in all-optical packet switched network as the pattern effect is the major limitation for the cascadability of this switch.

# CHAPTER 8 CONCLUSIONS

Various buffering configurations for packet switches have been proposed, many of them incorporating FDLs for buffering in travelling, recirculating, or combination architectures [126],[127]. For most of these, the routing or switching function is performed passively with an arrayed waveguide grating (AWG) due to its small size, low loss and good crosstalk [4],[53],[128]. This implies that the intelligence required for the decision, i.e. the signal processing, is performed prior to the signal reaching the buffer, as it already needs to be on the correct wavelength. Alternatively, it is shown that electronic control is used to control the wavelength via tuneable wavelength converters [50],[9]. In fact, with electronic control, optical packet switches have the flexibility even to handle variable length packets and traffic shaping [129]. Chapters 6 and 7 of this thesis describe a recirculating buffer implementation using a CrossPoint switch that is able to provide fast switching and does not result in significant crosstalk as is the case with, for example, $LiNbO_3$ switches. Despite the flexibility provided by electronic control, it does still result in an O/E/O conversion bottleneck.

In terms of all-optical implementations, many recirculating buffer experiments have been shown that demonstrate solely the buffering, without considering any switching or routing [130],[67],[44],[40], thus only taking into consideration the physical characteristics of the optical buffer, and not implementing a buffering system in a packet switch. The all-optical contention resolution implementations described in Chapters 2 – 4 in this thesis take into consideration the entire switching and contention resolution functionality as is required by an all-optical packet-switched cross-connect. *The significance of the all-optical buffer implementation as described in Chapters 2 – 4 is that it demonstrates contention resolution of packets, utilising only optical signal processing.*

Apart from the problem of optical buffering, another significant challenge in all-optical cross-connects is the use of optical signal processing. Optical threshold functions are an essential building block in realising all-optical cross-connects as they provide the decision-making functionality that enables all-optical wavelength routing in an all-optical cross-connect. In the all-optical recirculating buffering experiment described in Liu et al. [65] a threshold function based on two coupled ring lasers was used. The two disadvantages of this method are that two active elements (SOAs) are required, and that the optical switching power required is in the order of 8dBm. In Chapter 5 an alternative threshold function design is investigated based on polarisation rotation. Supported by the SOA rate equations, the results show that it is possible to realise a threshold function with a single SOA that can be switched with an optical control signal in the order of 0dBm, with a typical extinction ratio between 15 and 20dBm.

Chapter 3 describes how all-optical buffering is limited with the use of bulky fibre delay lines, the feasibility of which is only slightly improved with the use of the wavelength dimension by incorporating tuneable wavelength converters in the switch fabric and in the shared buffers. The buffer algorithms can also be improved to optimise the use and improve the simplicity of an all-optical implementation, but ultimately the physical implementation of large all-optical buffers seems infeasible if photonic integration is required. Apart from changing the network architecture to minimise the required buffering with a philosophy such as burst switching, various other solutions have also been proposed including a combination of optical and electrical buffers [133], optical shift memories [134], and semiconductor quantum dot waveguides [68].

The initial performance metric used in Chapter 3 was the packet loss ratio, with the goal being to achieve a BER of $10^{-9}$ as is required of an optical transmission system. Using a self-similar traffic model, which is a realistic representation of the burstiness of Internet traffic, it was shown that extremely large buffers are required. If, however, this type of traffic model is used in order to provide realistic results, it becomes

necessary to regard the implementation of an optical cross-connect in a realistic network: a network where 95% of the traffic comes from TCP sources, and whose design is thus necessarily affected by the interdependence of the protocol and the hardware. Furthermore, taking TCP into account when analysing the buffer requirements of a node in the core network, minimising the packet loss ratio by increasing the buffer size increases latency, which is a more important problem for the relevant applications. In order to minimise latency, the throughput of the links must be as high as possible, and this results in a different requirement for buffer dimensioning. Within this framework, it is shown in Chapter 4 that a feasibly small optical buffer is required depending on how the packets are defined (length and speed).

If the loss of packets is to be limited, the number of recirculations possible with a system as described in Chapter 3 may not provide a viable solution if several recirculations are required in a fibre delay line. Experiments as described in Sakamoto et al. [40] provide some answers to how several recirculations may be achieved. In Sakamoto et al. [40] a variable optical delay is described based on wavelength conversions in highly nonlinear fibre (HNLF) parametric wavelength converters, upon each recirculation. In this way, a decision is made on when to let the packet exit the buffer, depending on the wavelength. The initial wavelength thus determines the circulation number. It is shown that by addressing issues such as spectral broadening and wavelength conversion efficiency, up to 100 recirculations are possible. Another alternative technology to be considered is slow light: light that has ultraslow group velocities in ultra cold atomic gas, hot atomic vapours, as well as in solids [131]. This is caused by electromagnetically induced transparency (EIT) that results in the dispersion characteristics of the material being altered. Ku et al. [67] describe an application of slow light to realise a variable optical buffer in a semiconductor material by controlling the dispersion through an external control light source. In this demonstration, a slow down factor of $10^4$ was achieved in semiconductor quantum dot structures. Also in Yang et al. [132], the principle of slow light is used to simulate variable optical delays consisting of single- and multi-stage selective all-optical

variable delay buffers. Slow light does have some implementation limitations however. The slow light bandwidth limits the minimum duration of an optical pulse that can be delayed without distortion, thus limiting the maximum data rate of the optical system [135]. Slow light buffers may not be suitable for contention resolution due to the limitations in capacity, but may be more suitable for applications of small, compact all-optical buffering [136].

# REFERENCES

[1] R. Ramaswami, K.N. Sivarajan, "Optical Networks: A Practical Perspective", 2nd edition, ISBN 1-55860-655-6, Morgan Kaufman Publishers, San Francisco, USA, 2002.

[2] J.M. Yates, M.P. Rumsewicz, J.P.R. Lacey, "Wavelength Converters in Dynamically Reconfigurable WDM Networks*", Communications Surveys*, pp.2-15, 1999.

[3] K. Fukuchi, T. Kasamatsu, M. Morie, R. Ohhira, T. Ito, K. Sekiya, et al. "10.92-Tb/s (273×40-Gb/s) triple-band/ultra-dense WDM optical-repeatered transmission experiment", *Proceedings of OFC* , Vol.4, pp. PD24-1 - PD24-3, 17-22 March 2001

[4] D. K. Hunter, M. C. Chia and I. Andonovic, "Buffering in Optical Packet Switches", *IEEE Journal of Lightwave Technology*, Vol. 16, pp.2081-2094, December 1998.

[5] G. Charlet, E. Corbel, J. Lazaro, A. Klekamp, R. Dischler, P. Tran, "WDM transmission at 6-Tbit/s capacity over transatlantic distance, using 42.7-Gb/s differential phase-shift keying without pulse carver", *IEEE Journal of Lightwave Technology*, Vol. 23, pp. 104 – 107, January 2005.

[6] M.J. O'Mahoney, D. Simeonidou, D.K Hunter, A. Tzanakaki, "The application of optical packet switching in future optical communication networks", *IEEE Communications Magazine*, Vol. 39, pp.128-135, March 2001.

[7] C. Qiao and M. Yoo, "Optical Burst Switching (OBS)- A New Paradigm for an Optical Internet," *Journal of High Speed Networks*, Vol. 8, pp. 69-84, January 1999.

[8] T. Battestilli, H. Perros, "An introduction to optical burst switching", *IEEE Communications Magazine*, Vol. 41, pp. S10 - S15, August 2003.

[9] A.M.J. Koonen, J.J. Vegas Olmos, I. Tafur Monroy, J.G.J. Jennen, C. Peucheret, E. van Breusegem, "Optical packet routing using orthogonal labeling – results from the FP5 STOLAS project," *Proceedings of ECOC*, Mo.4.4.1., Glasgow, 2005.

[10] F. Ramos, E. Kehayas, J. M. Martinez, R. Clavero, J. Marti, L. Stampoulidis, et al. "IST-LASAGNE: Towards All-Optical Label Swapping Employing Optical Logic Gates and Optical Flip-Flops", *IEEE Journal of Lightwave Technology*, Vol. 23, No. 10, pp. 2993-3011, October 2005.

[11] G.I. Papadimitriou, C. Papazoglou, A.S. Pomportsis, "Optical switching: switch fabrics, techniques, and architectures", *IEEE Journal of Lightwave Technology*, Vol. 21, pp.384-405, February 2003.

[12] M.J. Connelly, "*Semiconductor Optical Amplifiers*", Kluwer Academic Publishers, Dordrecht, The Netherlands, 2002.

[13] M. C. Chia, D. K. Hunter, I. Andonovic, P. Ball, I. Wright, "Optical packet switches: a comparison of designs", *Proceedings of ICON*, 2000, pp. 365 – 369.

[14] M.T. Hill, E.E.E. Frietman, H. de Waardt, G.D. Khoe, H.J.S. Dorren, "All fibre optic neural network using coupled SOA based ring lasers", *IEEE Transactions in Neural Networks*, Vol. 13, pp. 1504-1513, November 2002.

[15] D.J. Blumenthal, P.R. Prucnal, J.R. Sauer, "Photonic Packet Switches: Architectures and Experimental Implementations", *Proceedings of the IEEE*, Vol. 82, pp. 1650-1668, November 1994.

[16] B. Hoanca, S. Dubovitsky, D.X. Zhu, A.A. Sawchuk, W.H. Steier, P.D. Dapkus, "All-Optical Routing Using Wavelength Recognizing Switches", *IEEE Journal of Lightwave Technology*, Vol. 16, No. 12, December 1998.

[17] O. Boyraz, J.W. Lou, K.H. Ahn, Y. Lian, T.J. Xia, Y.-H. Kao, et al. "Demonstration and Performance Analysis for the Off-Ramp Portion of am All-Optical Access Node", *IEEE Journal of Lightwave Technology*, Vol. 17, No. 6, June 1999.

[18] P.R. Prucnal, "Optically Processed Self-Routing, Synchronisation, and Contention Resolution for 1-D and 2-D Photonic Switching Architectures", *IEEE Journal of Quantum Electronics*, Vol. 29, No. 2, February 1993.

[19] T.J. Xia, K.H. Liang, J.W. Lou, O. Boyraz, Y.-H. Kao, X.D. Cao, et al. "All-Optical Packet-Drop Demonstration Using 100-Gb/s Words by Integrating Fibre-Based Components", *IEEE Photonics Technology Letters*, Vol. 10, No. 1, January 1998.

[20] K.-H. Park, T. Mizumoto, A. Matsuura, Y. Naito, "All-Optical Address Extraction for Optical Routing", *IEEE Journal of Lightwave Technology*, Vol. 16, No. 7, July 1998.

[21] K.-H. Park, T. Mizumoto, "A Packet Header Recognition Assigning the Position of a Signal in the Time Axis and its Application to All-Optical Self-Routing", *IEEE Journal of Lightwave Technology*, Vol. 19, No. 8, August 2001.

[22] S.A. Hamilton, B.S. Robinson, "40-Gb/s All-optical Packet Synchronisation and Address Comparison for OTDM Networks", *IEEE Photonics Technology Letters*, Vol. 14, No. 2, February 2002.

[23] D. Cotter, J.K. Lucek, M. Shabeer, K. Smith, D.C. Rogers, D. Nesset and P. Gunning, "Self-routing of 100 Gbit/s packets using 6-bit keyword address recognition", *Electronics Letters*, Vol. 31, pp. 2201-2202, Dec. 1995.

[24] I. Glesk, J.P. Solokoff and P.R. Prucnal, "All-optical address recognition and self-routing in a 250-Gbit/s packet switched network", *Electronics Letters*, Vol. 30, pp. 1322-1323, 1994.

[25] I. Glesk, K.I. Kang, P.R. Prucnal, "Ultrafast photonic packet switching with optical control", *Optics Express*, Vol. 1, No. 5, 1 September 1997.

[26] J. P. Sokoloff, P. R. Prucnal, I. Glesk, M. Kane, "A terahertz optical asymmetric demultiplexer (TOAD)," *IEEE Photonics Technology Letters*, Vol. 5, pp. 787 – 790, July 1993.

[27] I. Glesk, K.I. Kang, and P.R. Prucnal, "Demonstration of Ultrafast all-optical packet routing", *Electronics Letters*, Vol. 33, pp. 794-795, April 1997.

[28] M. T. Hill, A. Srivatsa, N. Calabretta, Y. Liu, H. de Waardt, G.D. Khoe, H.J.S. Dorren, "1×2 optical packet switch using all-optical header processing", *Electronic Letters*, Vol. 37, pp. 774-775, 2001.

[29] A. Srivatsa, H. de Waardt, M.T. Hill, G.D. Khoe, H.J.S. Dorren, "All-optical serial header processing based on two-pulse correlation", *Electronics Letters*, Vol. 37 No 4, pp. 234-235, 15 Feb. 2001.

[30] N. Calabretta, Y. Liu, H. de Waardt, M.T. Hill, G.D. Khoe, H.J.S. Dorren, "Multiple-output all-optical header processing technique based on two-pulse correlation principle", *Electronics Letters*, Vol. 37 No. 20, pp. 1238 – 1240, 27 Sep. 2001.

[31] Y. Liu, M.T. Hill, H. de Waardt, and H.J.S. Dorren, "All-Optical Switching of Packets for All-Optical Buffering Purposes", *Proceedings of ECOC*, Amsterdam, Netherlands, October 2001.

[32] M. Eiselt, W. Pieper, H.G. Weber, "SLALOM: Semiconductor Laser Amplifier in Loop Mirror", *IEEE Journal of Lightwave Technology*, Vol. 13, pp. 2099-2112, October 1995.

[33] A.E. Willner, D. Gurkan, A.B. Sahin, J.E. McGeehan, M.C. Hauer, "All-optical address recognition for optically-assisted routing in next-generation optical networks", IEEE Communications Magazine, Vol. 41, Issue 5, pp. S38 - S44 May 2003.

[34] K. Kitayama, "Code division multiplexing lightwave networks based upon optical code conversion", IEEE Journal on Selected Areas in Communications, Vol. 16, Issue 7, pp. 1309 – 1319, September 1998.

[35] M.C. Cardakli, S. Lee, A.E. Willner, V. Grubsky, D. Starodubov, J. Feinberg, "Reconfigurable optical packet header recognition and routing using time-to-wavelength mapping and tunable fiber Bragg gratings for correlation decoding", IEEE Photonics Technology Letters, Vol. 12, Issue 5, pp. 552 – 554, May 2000.

[36] L.F.K. Lui, Lixin Xu, Kwan Lau, P.K.A. Wai, H.V. Tam, M.S. Demokan, "All-optical packet switching with all-optical header processing and 2R regeneration", in Procedings of Conference on Lasers and Electro-Optics, 2005. (CLEO). Vol. 1, 22-27 May 2005 pp. 719 - 721

[37] J.P. Wang, B.S. Robinson, S.A. Hamilton, E.P. Ippen, "Demonstration of 40-Gb/s Packet Routing Using All-Optical Header Processing", IEEE Photonics Technology Letters, Vol. 18, Issue 21, pp. 2275 – 2277, November 1, 2006.

[38] W. D. Zhong and R. S. Tucker, "Wavelength routing-based photonic packet buffers and their applications in photonic packet switching systems," *IEEE Journal of Lightwave Technology*, Vol. 16, pp. 1737–1745, October 1998.

[39] A. Agarwal, L. Wang, Y. Su, P. Kumar, "All-Optical Loadable and Erasable Storage Buffer Based on Parametric Nonlinearity in Fiber", *IEEE Journal of Lightwave Technology*, Vol. 23, pp. 2229-2238, July 2005.

[40] T. Sakamoto, A. Okada, O. Moriwaki, M. Matsuoka, K. Kikuchi, "Performance analysis of variable optical delay circuit using highly nonlinear fibre parametric wavelength converters", *IEEE Journal of Lightwave Technology*, Vol. 22, pp.874 – 881, March 2004.

[41] S.L. Danielsen, B. Mikkelsen, C. Joergensen, T. Durhuus, K.E. Stubkjaer, "10Gb/s operation of a multiwavelength buffer architecture employing a monolithically integrated all-optical interferometric Michelson wavelength converter", *IEEE Photonics Technology Letters*, Vol. 8, pp.434-436, 1996.

[42] Y. Liu, M.T. Hill, N. Calabretta, H. de Waardt, G.D. Khoe, H.J.S. Dorren, "Three-state all-optical memory based on coupled ring lasers", *IEEE Photonics Technology Letters*, Vol. 15, pp. 1461-1463, October 2003.

[43] S. Lee, K. Sriram, H. Kim, J. Song, "Contention-Based Limited Deflection Routing Protocol in Optical Burst-Switched Networks", *IEEE Journal on Selected Areas in Communications*, Vol. 23, Issue 8, pp.1596 – 1611, August 2005.

[44] Y.Liu, M.T. Hill, E. Tangdiongga, H. de Waardt, N. Calabretta, G.D. Khoe, H.J.S. Dorren, "Wavelength conversion using nonlinear polarisation rotation in a single semiconductor optical amplifier", *IEEE Photonics Technology Letters*, pp. 90-92, January 2003.

[45] T. Durhuus, B. Mikkelsen, C. Joergensen, S.L. Danielsen, K.E. Stubkjaer, "All-optical wavelength conversion by semiconductor optical amplifiers", *IEEE Journal of Lightwave Technology*, Vol. 14, pp. 942-954, June 1996.

[46] D. Nesset, T. Kelly, and D. Marcenac, "All-optical wavelength conversion using SOA nonlinearities," *IEEE Communications Magazine*, Vol. 36, pp. 56–61, December 1998.

[47] H. Kawaguchi, "Bistable laserdiodes and their applications: State of the art", *IEEE Journal on Selected Topics in Quantum Electronics*, Vol. 3, pp.1254-1270, October 1997.

[48] T. Sakamoto, K. Noguchi, R. Sato, A. Okada, Y. Sakai, M. Masuoka, "Variable optical delay circuit using wavelength converters", *Electronics Letters*, Vol. 37, 29 March 2001.

[49] Carena, M.D. Vaughn, R. Gaudino, M. Shell and D.J. Blumenthal, "OPERA: An optical packet experimental routing architecture with label swapping capability", *IEEE Journal of Lightwave Technology*, Vol.16, pp.2135-2145, December 1998.

[50] C. Guillemot, M. Renaud, P. Gambini, C. Janz, I. Andonovic, R. Bauknecht, et al., "Transparent Optical Packet Switching: The European ACTS KEOPS Project Approach", *IEEE Journal of Lightwave Technology*, Vol.16, pp. 2117-2134, Dec. 1998.

[51] D.K. Hunter, H.M. Nizam, M.C. Chia, I.Andonovic, K.M. Guild, A. Tzanakaki, et al., "WASPNET, A wavelength switched packet network", *IEEE Communications Magazine*, pp. 120-128, March 1999.

[52] W.D. Zhong and R.S. Tucker, "A new wavelength routed photonic packet buffer combining traveling delay lines with delay-line loops", *IEEE Journal of Lightwave Technology*, Vol. 19, pp. 1085-1092, Aug. 2001.

[53] E.C. Mos, J.J.L. Hoppenbrouwers, M.T. Hill, M.W. Blüm, J.J.H.B. Schleipen, H. de Waardt, "Optical neuron by use of a laser diode with injection seeding and external optical feedback", *IEEE Transactions on Neural Networks*, Vol. 11, pp. 988-996, July 2000.

[54] R. Geldenhuys, Y. Liu, N. Calabretta, M. T. Hill, F.M.Huijskens, G. D. Khoe, H.J.S. Dorren, "All-Optical Signal Processing for Optical Packet Switching", Invited paper, *Journal of Optical Networking*, Vol. 3, No. 12, pp. 854-865, December 2004.

[55] D. J. Blumenthal, J.E. Bowers, L. Rau, H.F. Chou, S. Rangarajan, W. Wang, et al., "Optical signal processing for optical packet switching networks," *IEEE Optical Communications*, Vol. 41, pp. S23-S29, Feb. 2003.

[56] M.C. Cardakli, S. Lee, A.E. Willner, V. Grubsky, D. Starodubov, and J. Feinberg, "Reconfigurable optical packet header recognition and routing using time-to-wavelength mapping and tunable fibre Bragg gratings for correlation decoding", *IEEE Photonics Technology Letters*, Vol. 12, pp. 552-554 2000.

[57] D. Nesset, M.C. Tatham, L.D. Westbrook, and D. Cotter, "Degenerate wavelength operation of an ultrafast all-optical AND gate using four-wave mixing in a semiconductor laser amplifier", *Electronics Letters*, Vol. 30, 1pp. 938-1939, 1994.

[58] D.K. Hunter, W.D. Cornwell, T.H. Gilfedder, A. Franzen and I. Andonovic, "SLOB, A switch with large optical buffers for packet switching", *IEEE Journal of Lightwave Technology*, Vol. 16, pp. 1725-1736, Oct. 1998.

[59] H.J.S. Dorren, M.T. Hill, Y. Liu, N. Calabretta, A. Srivatsa, F.M. Huijskens, et al., "Optical Packet Switching and Buffering by using all-Optical Signal Processing Methods", *IEEE Journal of Lightwave Technology*, Vol. 21, pp. 2-12, Jan. 2003.

[60] N. Calabretta, H. de Waardt, G.D.Khoe, H.J.S. Dorren, "Ultrafast Asynchronous Multioutput All-Optical Header Processor", *IEEE Photonics Technology Letters*, Vol. 16, April 2004.

[61] N. Calabretta, Y. Liu, F. M. Huijskens, M. T. Hill, H. de Waardt, G. D. Khoe and H. J. S. Dorren, "Optical Signal Processing based on Self-induced Polarisation Rotation in a Semiconductor Optical Amplifier", *IEEE Journal of Lightwave Technology*, Vol. 22, pp. 372-381 February 2004.

[62] Masashi Usami, Munefumi Tsurusawa, and Yuichi Matsushima, "Mechanism for reducing recovery time of optical nonlinearity in semiconductor laser amplifier" *Applied Physics Letters*, Vol. 72, pp. 2657-2659, May 25, 1998.

[63] R.J. Manning, D.A.O. Davies, J.K. Lucek, "Recovery rates in semiconductor laser amplifiers: optical and electrical bias dependencies", *Electronics Letters*, Vol. 30, pp. 1233 - 123521 July 1994.

[64] T. Akiyama, N. Hatori, Y. Nakata, H. Ebe, and M. Sugawara, "Pattern-effect-free semiconductor optical amplifier achieved using quantum dots", *Electronics Letters*, Vol. 38, pp.1139-1140, September 2002.

[65] Y.Liu, M.T.Hill, R.Geldenhuys, N.Calabretta, H.de Waardt, G.D.Khoe, H.J.S.Dorren, "Demonstration of a variable optical delay for a recirculating buffer by using all-optical signal processing", *IEEE Photonics Technology Letters*, 1748 – 1750, Vol. 16, July 2004.

[66] H.J.S.Dorren, D.Lenstra, Y.Liu, M.T.Hill, G.D. Khoe, "Nonlinear polarisation rotation in semiconductor optical amplifiers: theory and application to all-optical flip-flop memories", *IEEE Journal of Quantum Electronics*, Vol. 39, pp. 141-148, January 2003.

[67] P.C. Ku, C.J. Chang-Hasnain, S.L. Chuang, "Variable semiconductor all-optical buffer", *Electronics Letters*, Vol. 38, pp.1581 – 1583, 21 Nov. 2002 .

[68] P.Ku, C. Chang-Hasnain, J. Kim, S. Chuang, "Semiconductor all-optical buffers using quantum dots in resonator structures", OFC 2003 23-28 March 2003 pp.76 - 78 Vol.1

[69] M. Takenaka and Y. Nakano, "Realisation of all-optical flip-flop using directionally coupled bistable laser diode," IEEE Photonics Technology Letters, Vol. 16, pp. 45–47, 2004.

[70] R. Geldenhuys, Y. Liu, M.T. Hill, G.D. Khoe, F.W. Leuscher, H.J.S. Dorren, "Architectures and Buffering for All-Optical Packet-Switched Cross-Connects", *Photonic Network Communications*, Issue 11:1, pp. 65-75, January 2006.

[71] H. Zang, J.P. Jue, B. Mukherjee, "Capacity allocation and contention resolution in a photonic slot routing all-optical WDM mesh network", *IEEE Journal of Lightwave Technology*, Vol. 18, pp.1728-1741, December 2000.

[72] F. Callegati; W. Cerroni; G. Corazza; C. Develder; M. Pickavet; P. Demeester, "Scheduling Algorithms for a Slotted Packet Switch with either Fixed or Variable Length Packets" *Photonic Network Communications*, Vol.8, pp.163-176, September 2004.

[73] L. Tancevski, S. Yegnanarayanan, G. Castanon, L. Tamil, F. Masetti, T. McDermott, "Optical Routing of Asynchronous, Variable Length Packets", *IEEE Journal on Selected Areas in Communications*, Vol. 47, pp. 1593-1603, October 1999.

[74] F. Callegati, "Approximate Modeling of Optical Buffers for Variable Length Packets", Photonic Network Communications, Vol. 3, pp. 383-390, Oct. 2001.

[75] V. Paxson and S. Floyd, "Wide Area Traffic: The Failure of Poisson Modeling", *IEEE/ACM Transactions on Networking*, Vol. 3, pp. 226-244, June 1995.

[76] M.E. Crovella and A. Bestavros, "Self-Similarity In World Wide Web Traffic: Evidence And Possible Causes", *IEEE/ACM Transactions on Networking*, Vol. 5, December 1997.

[77] W. Willinger, M.S. Taqqu, R. Sherman, D.V. Wilson, "Self-Similarity through high-variability: statistical analysis of Ethernet LAN traffic at the source level", *IEEE/ACM Transactions on Networking*, Vol. 5, pp. 71-86, February 1997.

[78] J.J. He, D. Simeonidou, S. Chaudhry, "Contention resolution in optical packet-switching networks: under long-range dependent traffic", in *Proceedings of OFC, 2000*, Vol. 3 pp. 295 –297.

[79] C. Develder, M. Pickavet, P. Demeester, "Choosing an appropriate buffer strategy for an optical packet switch with a feed-back FDL buffer", in *Proceedings of ECOC, 2002*, Vol. 3, pp. 8.5.4.

[80] Fei Xue, Ben Yoo, "Self-similar traffic shaping at the edge router in optical packet-switched networks", in *Proceedings of ICC, 2002*, Vol. 4, pp.2449 –2453.

[81] K. Park, G. Kim, and M. E. Crovella, "On the Effect of Traffic Self-Similarity on Network Performance," *CSD-TR 97-024*, Dept. of Computer Sciences, Purdue University, July 1997.

[82] Sikdar, B.; Chandrayana, K.; Vastola, K.S.; Kalyanaraman, S., "Queue management algorithms and network traffic self-similarity", *High Performance Switching and Routing. Workshop on Merging Optical and IP Technologies*, pp. 319 –323, 26-29 May 2002.

[83] R. Langenhorst, M. Eiselt, W. Pieper, G. Grosskopf, R. Ludwig, L. Kueller, et al., "Fibre Loop Optical Buffer", *IEEE Journal of Lightwave Technology*, Vol. 14, pp. 324-335, March 1996.

[84] S.L. Danielsen, C. Joergensen, B. Mikkelsen, K.E. Stubkjaer, "Analysis of a WDM packet switch with Improved Performance Under Bursty Traffic Conditions Due to Tuneable Wavelength Converters", *IEEE Journal of Lightwave Technology*, Vol. 16, pp. 729-735, May 1998.

[85] C.S Chang, D.S. Lee and Y.S. Jou, "Load balanced Birkhoff-von Neumann switches, part I: one-stage buffering," *Computer Communications*, Vol. 25, pp. 611-622, 2002.

[86] M.J. Karol, M.G. Hluchyj, "Input versus output queueing on a space-division packet switch", *IEEE Transactions on Communications*, Vol. 35, pp.1347-1356, December 1987.

[87] L. Tancevski, L. Tamil, F. Callegati, "Nondegenerate buffers: an approach for building large optical memories", *IEEE Photonics Technology Letters*, Vol. 11, August 1999.

[88] Sung-Ho Jin, Jae-Hong Yi, Dong-il Kim, "Performance analysis of ATM switch queue under self-similar traffic", *5th IEEE International Conference on High Speed Networks and Multimedia Communications*, pp. 213-217, 3-5 July 2002

[89] B. Tsybakov, N.D.Georganas, "On self-similar traffic in ATM queues: definitions, overflow probability bound, and cell delay distribution", *IEEE/ACM Transactions on Networking*, Vol. 5, pp.397-409, June 1997.

[90] S. Fong, S. Singh, "Performance evaluation of shared-buffer ATM switches under self-similar traffic", in *Proceedings of IPCCC, 1997*, pp. 252-258.

[91] S. Yao, B. Mukherjee, S.J.B. Yoo, S. Dixit, "A unified study of contention-resolution schemes in optical packet-switched networks", *IEEE Journal of Lightwave Technology*, Vol. 21, pp. 672 –683, March 2003.

[92] T. V. Lakshman and U. Madhow, "The performance of TCP/IP for networks with high bandwidth-delay products and random loss," *IEEE/ACM Transactions on Networking*, Vol. 5, pp. 336–350, June 1997.

[93] D. Munoz, S. Villarreal, F. Houmayoun, K. Basu, "Heavy tail jitter in mobile packet networks", in *Proceedings of VTC 2001*, Vol. 3, pp. 2224 – 2228, 6-9 May 2001.

[94] R.P. Singh, Sang-Hoon Lee, Chong-Kwoon Kim, "Jitter and clock recovery for periodic traffic in broadband packet networks", *IEEE Transactions on Communications*, Vol. 42, pp. 2189 – 2196, May 1994.

[95] G. Appenzeller, I. Keslassy, N. McKeown, "Sizing Router Buffers", *ACM SIGCOMM 2004*, Portland, August 2004.

[96] L. Malynowsky, "Get smart with packet switching", Telephony Online, 11 December 2000, http://telephonyonline.com/mag/telecom_smart_packet_switching/ (accessed 2007-01-07).

[97] N. Beheshti, Y. Ganjali, R. Rajaduray, D. Blumenthal, N. McKeown, "Buffer sizing in all-optical packet switches", *In Proceedings of OFC/NFOEC*, Anaheim, CA, 5-10 March 2006, pp.1-3.

[98] M. Enachescu, Y. Ganjali, A. Goel, N. McKeown, T. Roughgarden "Routers with very small buffers", In *Proceedings of the IEEE INFOCOM'06*, Barcelona, Spain, April 2006.

[99] R. Geldenhuys, Y. Liu, J.J. Vegas Olmos, F.W. Leuschner, G.D. Khoe, H.J.S. Dorren, "An optical threshold function based on polarisation rotation in a single semiconductor optical amplifier", submitted *Optics Express* January 2007.

[100] Y. Liu, M.T. Hill, H. de Waardt, G. D. Khoe, and H.J.S. Dorren, "All-optical buffering using laser neural networks", *IEEE Photonics Technology Letters*, Vol. 15, pp. 596-598, April 2003.

[101] H. Soto, D. Erasme, and G. Guekos, "Cross-polarization modulation in semiconductor optical amplifiers", *IEEE Photonics Technology Letters*, Vol. 11, pp. 970-972, August 1999.

[102] T.D. Visser, D. Lenstra, H. Blok, A. Fasolino, "Propagation of Polarized Waves in Semiconductor Laser Amplifiers", *Proceedings of SPIE*, Issue 3283, No.2, pp. 675-682, January 1998.

[103] Y. Takahashi, A. Neogi, H. Kawaguchi, "Polarization dependent nonlinear gain in semiconductor optical amplifiers," *IEEE Journal of Quantum Electronics*, Vol. 34, pp. 1660–1672, September 1998.

[104] R. Geldenhuys, Z. Wang, N. Chi, I. Tafur Monroy, A.M.J. Koonen, H.J.S. Dorren, F. W. Leuschner, G. D. Khoe, S. Yu, "Multiple Recirculations Through a Crosspoint Switch Fabric for Recirculating Optical Buffering", *Electronics Letters* Vol. 41, Issue 20, pp. 1136-1138, 29 September 2005.

[105] R. Varrazza, I.B. Djordjevic, S. Yu; "Active vertical-coupler-based optical crosspoint switch matrix for optical packet-switching applications", *IEEE Journal of Lightwave Technology*, Vol. 22, pp.2034 – 2042, September 2004.

[106] R. J. Deri, F. G. Patterson, and S. P. Dijaili, "Birefringence compensation for polarization-independent directional coupler wavelength filters," *IEEE Photonics Technology Letters*, Vol. 7, pp. 376–378, Apr. 1995.

[107] T. Ito, N. Yoshimoto, K. Magari, and H. Sugiura, "Wide-band polarization-independent tensile-strained InGaAs MQW-SOA gate," *IEEE Photonics Technology Letters*, Vol. 10, pp. 657–659, May 1998.

[108] A. Wonfor, S. Yu, R.V. Penty, I.H. White, "Constant Output Power Control in an Optical CrossPoint Switch Allowing Enhanced Noise Performance Operation", in *Proceedings of ECOC 2001*, pp. 136-137.

[109] R. Varrazza, S.C. Lee, S. Yu, "A fully packaged optical CrossPoint packet switch matrix and its application demonstrations", in *Proceedings of SPIE*, Vol. 5624, pp.482-492, 2005.

[110] S.C. Lee, R. Varrazza, O. Ansell, S. Yu, "Highly flexible 4×4 optical CrossPoint packet switch matrix for optical multicast operations", *IEEE Photonics Technology Letters*, Vol.17, pp. 911-913, 2005.

[111] S. Yu, M. Owen, R. Varrazza, R.V. Penty, I.H. White, "Demonstration of high-speed optical packet routing using vertical coupler CrossPoint space switch array", *Electronics Letters*, Vol. 36, pp. 556-558, March 2000.

[112] W. Pieper, M. Eiselt, G. Grosskopf, R. Langenhorst, A. Ehrhardt, H.G. Weber, "Investigation of crosstalk interference in a fibre loop optical buffer", *Electronics Letters*, Vol. 30, pp.435 – 436, 3 March 1994.

[113] R. Geldenhuys , Z. Wang, N. Chi, I. Tafur Monroy, A. M. J. Koonen, H. J. S. Dorren, F. W. Leuschner, G. D. Khoe, S. Yu , "Time Slot Interchanging using the CrossPoint Switch and a Recirculating Buffer", *IEEE Microwave and Optical Technology Letters*, Vol. 48 No. 5, pp.897-900, May 2006.

[114] J.S. van der Merwe, R. Geldenhuys , K. Thakulsukanant, et al., "Resolving Contention in an Optical Packet Switching Network by using the Active Vertical-Coupler-Based Optical Crosspoint Switch, a Delay Buffer and Electronic Header Processing", in *Proceedings of ECOC 2006*.

[115] N. Chi, R. Geldenhuys, J.J. Vegas Olmos et al., "Alleviation of the Pattern Effect in a Crosspoint-Switch Based Optical Buffer by Using a DPSK Payload", in *Proceedings of APOC 2006*.

[116] E. Karasan, E. Ayanoglu, "Performance of WDM Transport Networks", *IEEE Journal on Selected Areas in Communications*, Vol.16, pp. 1081-1096, 1998.

[117] J.Yates, J.Lacey, D.Everitt, "Blocking in multiwavelength TDM networks", *Telecommunications Systems*, Vol. 12, pp. 1-19, 1999.

[118] J.Yao, P.Barnsley, N.Walker, M.O'Mahony, "Time slot interchanging using semiconductor laser amplifiers", *Electronics Letters*, Vol.29, pp. 1053-1054, 1993.

[119] M.C. Cardakli, D. Gurkan, S.A. Havstad, A.E.Willner, K.R. Parameswaran, M.M. Fejer, I. Brener, "Tunable All-Optical Time slot-Interchange and Wavelength Conversion Using Difference-Frequency-Generation and Optical Buffers", *IEEE Photonics Technology Letters*, Vol.14, pp. 200-202, February 2002.

[120] R.A. Thompson, P.P. Giordano, "An Experimental Photonic Time slot Interchanger Using Optical fibres as Re-entrant Delay-Line Memories", *IEEE Journal of Lightwave Technology*, Vol.LT-5, pp.154-162, 1987.

[121] S.V. Ramanan, H.F. Jordan, J.R. Sauer, "A New Time Domain, Multistage Permutation Algorithm", *Transactions on Information Theory*, Vol.36, pp. 171-173, 1990.

[122] D.K. Hunter, I. Andonovic, P.E. Barnsley, "Demonstration of optical time slot interchanging through 2×2 crosspoints and feedforward delay lines", *Electronics Letters*, Vol.30, pp. 875-876, 1994.

[123] D.K. Hunter, D.G. Smith, "New Architectures for Optical TDM Switching", *IEEE Journal of Lightwave Technology*, Vol.11, pp.495-511, 1993.

[124] Z. Wang, N. Chi, S. Yu, "Time-Slot Assignment Using Optical Buffer With a Large Variable Delay Range Based on AVC Crosspoint Switch", *IEEE Journal of Lightwave Technology*, Vol. 24, pp. 2994 – 3001, Aug. 2006.

[125] A.H.Gnauck, P.J.Winzer, "Optical phase-shift-keyed transmission", *IEEE Journal of Lightwave Technology*, Vol. 23, pp. 115 – 130, Jan. 2005.

[126] D. Fiems, K. Laevens, H. Bruneel, "Performance analysis of an all-optical packet buffer", in *Proceedings of Conference on Optical Network Design and Modeling*, February 7-9, 2005 pp.221 – 226.

[127] H. Yang, S.J.B. Yoo, "Combined Input and Output All-Optical Variable Buffered Switch Architecture for Future Optical Routers", *IEEE Photonics Technology Letters*, Vol. 17, pp.1292 – 1294, June 2005.

[128] K.M. Guild, M.J. O'Mahony, "Routing and buffering architecture in all-optical switching node", *Electronics Letters*, Vol. 35, pp.161 – 162, 21 January 1999.

[129] F. Xue, Z. Pan, H. Yang, J. Yang, J. Cao, K. Okamoto, et al. "Design and experimental demonstration of a variable-length optical packet routing system with unified contention resolution", *IEEE Journal of Lightwave Technology*, Vol. 22, pp. 2570 – 2581, November2004.

[130] L. Wang, A. Agarwal, Y. Su, P. Kumar, "All-optical picosecond-pulse packet buffer based on four-wave mixing loading and intracavity soliton control", *IEEE Journal of Quantum Electronics*, Vol.38, pp. 614-619, June 2002.

[131] A. Turukhin, V.S. Sudarshanam, M.S. Shahriar, J.A. Musser, P.R. Hemmer, "First observation of ultraslow group velocity of light in a solid", in *Proceedings of Quantum Electronics and Laser Science Conference, 2001*. QELS '01. Technical Digest. Summaries of Papers Presented at the 6-11 May 2001 pp.6 – 7

[132] H. Yang, S.J.B. Yoo, "A new optical switching fabric architecture incorporating rapidly switching all-optical variable delay buffers", in *Proceedings of OFC 2004*, Vol. 2, 23-27 February 2004, pp. 334 – 336.

[133] L.Wosinska, J.Haralson, L.Thylén, J.Öberg B.Hessmo, "Benefit of Implementing Novel Optical Buffers in an Asynchronous Photonic Packet Switch", in *Proceedings of ECOC 2004*.

[134] S. Zhang, Z. Li, Y. Liu, R. Geldenhuys, H. Ju, M.T. Hill, D. Lenstra, G.D. Khoe and H.J.S. Dorren, "Optical shift register based on an optical flip-flop with a single active element", in *Proceedings of IEEE/LEOS Benelux*, 2-3 December 2004, Ghent, Belgium.

[135] Zhaoming Zhu, A.M.C. Dawes, D.J. Gauthier, "Slow Light via Stimulated Brillouin Scattering in Optical Fibers", *Digest of the LEOS Summer Topical Meetings, 2006* pp.38 – 39 17-19 July 2006.

[136] R.S. Tucker, Pei-Cheng Ku, C.J. Chang-Hasnain, "Slow-light optical buffers: capabilities and fundamental limitations", *IEEE Journal of Lightwave Technology*, Vol. 23, Issue 12, pp. 4046 – 4066, December 2005.

# LIST OF ABBREVIATIONS

| | |
|---|---|
| ASE | Amplified Spontaneous Emission |
| ATM | Asynchronous Transfer Mode |
| AVC | Active Vertical Coupler |
| AWG | Arrayed Waveguide Grating |
| BLD | Bistable Laser Diodes |
| BPF | Band Pass Filter |
| CCW | Counter clockwise |
| CW | Clockwise |
| DFP | Dual Feedback Laser |
| DPSK | Differential Phase Shift keying |
| DWIL | Dual Wavelength Injection Locking |
| E/O | Electrical to Optical Conversion |
| EDFA | Erbuim-Doped Fibre Amplifier |
| EIT | Electromagnetically Induced Transparency |
| FBG | Fibre Bragg Grating |
| FDL | Fibre Delay Line |
| FIFO | First In First Out |
| FLP | Fixed Length Packet |
| FP-LD | Fabry-Perot Laser Diode |
| HNLF | Highly Nonlinear Fibre |
| HOL | Head of Line Blocking |
| HPP | Header Pre-Processor |
| IP | Internet Protocol |
| LNN | Laser Neural Network |
| LNN | Laser Neural Network |
| MEMS | Microelectromechanical Systems |
| NRZ | Non Return to Zero |

| | |
|---|---|
| O/E | Optical to Electrical Conversion |
| O/E/O | Optical to Electrical to Optical Conversion |
| OC | Optical Circulator |
| OOK | On-off Keying |
| OTF | Optical Threshold Function |
| OTF | Optical Threshold Function |
| OXC | Optical Cross-Connect |
| PBS | Polarisation Beam Splitter |
| PC | Polarisation Controller |
| PDL | Polarisation Dependent Loss |
| PLR | Packet Loss Ratio |
| RAM | Random Access Memory |
| SLALOM | Semiconductor Laser Amplifier in a Loop Mirror |
| SOA | Semiconductor Optical Amplifier |
| SVLP | Slotted Variable Length Packet |
| TCP | Transmission Control Protocol |
| TDM | Time Division Multiplexing |
| TE | Transverse Electrical |
| TF | Tuneable Filter |
| TM | Transverse Magnetic |
| TOAD | Terahertz Optical Asymmetric Demultiplexer |
| WDM | Wavelength Division Multiplexing |
| WRN | Wavelength Routing Network |
| XGM | Cross Gain Modulation |
| XPT | CrossPoint |

## LIST OF PUBLICATIONS

Journal papers

1. <u>R. Geldenhuys</u>, Y. Liu, J.J. Vegas Olmos, F.W. Leuschner, G.D. Khoe, H.J.S. Dorren, "An optical threshold function based on polarisation rotation in a single semiconductor optical amplifier", submitted Optics Express January 2007.

2. <u>R. Geldenhuys</u>, N. Chi, I. Tafur Monroy, A.M.J. Koonen, H.J.S. Dorren, F.W. Leuschner, G.D. Khoe, S. Yu, and Z. Wang, "Multiple recirculations through Crosspoint switch fabric for recirculating optical buffering", Electronics Letters, Vol. 41 Issue 20, p. 1136-1138   29 September 2005.

3. <u>R. Geldenhuys</u> , Z. Wang, N. Chi, I. Tafur Monroy, A. M. J. Koonen, H. J. S. Dorren, F. W. Leuschner, G. D. Khoe, S. Yu , "Time Slot Interchanging using the CrossPoint Switch and a Recirculating Buffer", Microwave and Optical Technology Letters, Vol. 48 No. 5, pp.897-900, May 2006.

4. <u>R. Geldenhuys</u>, Y. Liu, M.T. Hill, G.D. Khoe, F.W. Leuscher, H.J.S. Dorren, "Architectures and Buffering for All-Optical Packet-Switched Cross-Connects", Photonic Network Communications, Issue 11:1, January 2006.

5. <u>R. Geldenhuys</u>, Y. Liu, N. Calabretta, M. T. Hill, F.M.Huijskens, G. D. Khoe, H.J.S. Dorren, "All-Optical Signal Processing for Optical Packet Switching", Invited paper, Journal of Optical Networking Vol. 3, No. 12, pp. 854-865, December 2004.

6. Y.Liu, M.T.Hill, <u>R.Geldenhuys</u>, N.Calabretta, H.de Waardt, G.D.Khoe, H.J.S.Dorren, "Demonstration of a variable optical delay for a recirculating buffer by using all-optical signal processing", IEEE Photonics Technology Letters, 1748 – 1750, Vol. 16, July 2004.

Conference papers

1. J.S. van der Merwe, <u>R. Geldenhuys</u> , K. Thakulsukanant, N. Chi, Z. Wang, S. Yu, "Resolving Contention in an Optical Packet Switching Network by using the Active Vertical-Coupler-Based Optical Crosspoint Switch, a Delay Buffer and Electronic Header Processing", European Conference on Optical Communication ECOC 2006, Cannes, France, 24-28 September 2006.

2. N. Chi, <u>R. Geldenhuys</u>, J.J. Vegas Olmos, Z. Wang, J.S.van der Merwe, K. Thakulsukanant, S. Yu, "Alleviation of the Pattern Effect in a Crosspoint-Switch Based Optical Buffer by Using a DPSK Payload", Asia Pacific Optical Conference APOC 2006, Gwangju, South Korea, 3-7 September 2006.

3. <u>R. Geldenhuys</u>, N. Chi, Z. Wang, I. Tafur Monroy, T. Koonen, H. J. S. Dorren, F. W. Leuschner, G. D. Khoe, S. Yu, "Multiple Packet Recirculation in an Optical Buffer using a CrossPoint Switch" , LEOS conference, 23-27 October 2005, Sydney, Australia.

4. J.J. Vegas Olmos, I. Tafur Monroy, J.P. Turkiewicz, M. Garcia Larrode, <u>R. Geldenhuys</u>, A.M.J. Koonen, "An all-optical time-serial label and payload separator generating a synchronisation pulse," European Conference on Optical Communication (ECOC), 26-28 Sept. 2005. Glasgow, Scotland.

5. Y. Liu, M.T. Hill, N. Calabretta, E. Tangdiongga, <u>R. Geldenhuys</u>, S. Zhang, Z. Li, H. De Waardt, G.D. Khoe and H.J.S. Dorren, "All-optical signal processing for optical packet switching networks" invited paper, SPIE Optics & Photonics 2005 Symposium, 31 July-4 August 2005 in San Diego, CA, USA.

6. S. Zhang, Z. Li, Y. Liu, <u>R. Geldenhuys</u>, H. Ju, M.T. Hill, D. Lenstra, G.D. Khoe and H.J.S. Dorren, "Optical shift register based on an optical flip-flop with a single active element", proc. 9th Annual Symposium of the IEEE/LEOS Benelux Chapter, 2-3 December 2004; IEEE, Gent, Belgium, 2004, pp. 67-70.

7. H.J.S. Dorren, M.T. Hill, Y. Liu, N. Calabretta, <u>R. Geldenhuys</u> and G.D. Khoe, "All-optical header processing and optical buffering for optical packet switching networks", Invited paper, Asia-Pacific Optical Communications Conference, APOC, 7–11 November 2004, Beijing, China.

8. <u>Ronelle Geldenhuys</u>, Jesús Paúl Tomillo, Ton Koonen and Idelfonso Tafur Monroy, "Optical Feedback Buffering Strategies", OpNeTec 2004, Pisa Italy, 15 – 17 October 2004.

9. Y.Liu, M.T.Hill, <u>R.Geldenhuys</u>, N.Calabretta, H. de Waardt, G.D.Khoe, H.J.S. Dorren, "Demonstration of an all-optical variable delay for recirculating buffers", proc. ECOC 2004. 4, TH2.6.4, 5-9 September 2004; ECOC, Stockholm, Sweden, 2004, pp. 892-893.

10. H.J.S.Dorren, D.Lenstra, H.Ju, X.Yang, E.Tangdiongga, S.Zhang, M.T.Hill, A.K.Mishra, Y.Liu, <u>R.Geldenhuys</u>, "All-optical logic based on ultra-fast nonlinearities in a semiconductor optical amplifier", (Invited) proc. MOC 2004. H-1, 1-3 September 2004; Friedrich-Schiller-University, Jena, Germany, 2004, pp. 1-4.

11. <u>R. Geldenhuys</u>, Y. Liu, G. D. Khoe, F. W. Leuschner, H. J. S. Dorren, "Overflow Buffering in an All-Optical Packet-Switched Cross-Connect" IEEE Africon, Gabarone Botswana, 15-17 September 2004.

12. H.J.S.Dorren, <u>R.Geldenhuys</u>, D.Lenstra, G.D.Khoe, X.Yang, E.Tangdiongga, S.Zhang, Z.Li, M.T.Hill, H.Ju, A.K.Mishra, Y.Liu, "All-optical signal processing based on ultrafast nonlinearities in semiconductor optical amplifiers", (Invited) proc. SSDM 2004, 15-17 September 2004, Tokyo, Japan, 2004, pp. 920-921.

13. H.J.S. Dorren, H. Ju, X. Yang, E. Tangdiongga, S. Zhang, Z. Li, M.T. Hill, A. Mishra, Y. Liu, <u>R. Geldenhuys</u>, D. Lenstra, G.D. Khoe, "All-optical logic based on ultra-fast nonlinearities in a semiconductor optical amplifier" Invited paper, submitted 10th Microoptics Conference, 1-3 September, 2004, Jena, Germany.

14. <u>R. Geldenhuys</u>, Y. Liu, H.J.S. Dorren, N. Calabretta, G.D. Khoe, F.W. Leuschner, "Selecting Fibre Delay Line Distributions for Travelling Buffers in an All-Optical Packet Switched Cross-Connect", Canadian Conference on Electrical and Computer Engineering, IEEE CCECE 2003, 4-7 May 2003, Montréal, Canada.

15. H.J.S. Dorren, Y. Liu, M.T. Hill, E. Tangdiongga, N. Calabretta, H. de Waardt, X. Yang, <u>R. Geldenhuys</u>, D. Lenstra and G.D. Khoe, "All-optical signal processing based on nonlinear polarisation rotation in a semiconductor optical amplifier", Invited Paper ICOCN 2002, Singapore.

## ACKNOWLEDGEMENTS

## CURRICULUM VITAE

Ronelle Geldenhuys was born in Bellville, South Africa, in 1975. She completed her bachelor's degree in electronic engineering at the University of Pretoria in 1996, and her master's degree in the Management of Technology at the same university in 1998. During 1999 she worked for the telecommunications company Telkom in South Africa, researching fibre channel storage area networks. She has been a senior lecturer at the University of Pretoria since 2000 where she has taught under-graduate and post-graduate optical communication, and led several final year project students in the field of electro-optics.

Since 2002 she has been working towards a PhD at the Eindhoven University of Technology in the field of optical contention resolution and optical signal processing.